

**A disrupted parvalbumin network state impairs maternal
behavior in a mouse model of Rett Syndrome**

A Dissertation Presented by

Alexa Hope Pagliaro

Submitted to

The Cold Spring Harbor School of Biological Sciences

In Partial Fulfillment of the Requirements for the

Degree of Doctor of Philosophy

in

Biological Sciences

Cold Spring Harbor Laboratory

April 2023

Table of Contents

<i>Acknowledgements</i>	6
<i>List of Figures</i>	9
<i>List of Tables</i>	11
<i>List of Abbreviations</i>	12
<i>Author Contributions</i>	13
<i>Summary</i>	14
Chapter 1: Introduction	16
1.1 An Introduction to Neuroplasticity	16
1.2 Inhibitory Control of Neuroplasticity	17
1.3 Parvalbumin Interneurons as Critical Period Regulators	19
1.3.1 Properties of Parvalbumin Interneurons.....	19
1.3.2 Parvalbumin Neurons and Perineuronal Nets.....	21
1.4 Maternal Retrieval Behavior	23
1.5 Maternal Experience-Induced Plasticity in the Auditory Cortex	24
1.6 Rett Syndrome – Genetic Underpinnings and Clinical Presentation	26
1.6.1 Genetic Underpinnings.....	26
1.6.2 Clinical Presentation	28
1.6.3 Mouse Model of Rett Syndrome.....	29
1.6.4 Parvalbumin Network Abnormalities in the Rett Syndrome Mouse Model	30

1.7 Research Aims.....	32
 <i>Chapter 2: ACtx PV Activity Does Not Regulate Retrieval Behavior on a Moment-to-</i>	
<i>Moment Basis</i>	34
2.1 PVMHET Surrogates Fail to Learn Maternal Pup Retrieval.....	34
2.2 Evidence of ACtx PV Plasticity in Wild Type, but not PVMHET, Surrogates in Response to Pup USVs.....	37
2.3 Low Frequency ACtx PV Fluctuations are Absent in PVMHET Surrogates	40
2.4 ACtx PV Activity Reflects Sensory and Behavioral Events in Wild Type, but not PVMHET, Surrogates	45
2.5 ACtx PV Activity Does Not Regulate Retrieval on a Moment-to-Moment Basis.	46
2.6 Discussion.....	53
2.6.1 Technical Considerations for Fiber Photometry Studies.....	53
2.6.2 Auditory Cortex as a Higher-Order Processing Area	54
2.6.3 Circuit Interactions for Retrieval Behavior – Within and Beyond Auditory Cortex	58
 <i>Chapter 3: ACtx PV Fluctuations May Reflect a PV Network Configuration that Favors</i>	
<i>Plasticity</i>	60
3.1 Wild Type ACtx PV Fluctuations Occur Independently of Context.....	60
3.2 ACtx PV Activity and ACtx Acetylcholine Release are Highly Correlated with Pupil Diameter	63
3.3 Discussion.....	68

3.3.1 What do we Mean by a PV Network State?	68
3.3.2 A Possible Relationship Between ACtx PV Activity and Attention	69
3.3.3 A Correlation that Persists in PVMHETs.....	71
<i>Chapter 4: Manipulation of the ACtx PV Network to Rescue Retrieval Performance in PVMHETs</i>	73
4.1 Chronic, but not Acute, ACtx PV Inhibition Improves Retrieval Behavior in PVMHETs	73
4.2 Chronic ACtx PV Inhibition in PVMHETs Disassembles PNNs	80
4.3 Chronic ACtx PV Inhibition Increases Low Frequency Fluctuations in PVMHETs	82
4.4 Discussion	84
4.4.1 A Time Course for PV Network Reconfiguration	84
4.4.2 Technical Limitations.....	85
4.4.3 Enzymatic Dissolution of PNNs in PVMHETs.....	86
<i>Chapter 5: Materials and Methods</i>	90
5.1 Experimental Subjects	90
5.1.1 Genotyping Procedures	91
5.2 Maternal Pup Retrieval Behavior	92
5.2.1 Ultrasound Recording during Pup Retrieval Behavior	93
5.2.2 Analysis of Maternal Pup Retrieval Behavior	93
5.3 Linear Encoding Model	94

5.4 Surgical Procedures	96
5.4.1 Viral Injections	96
5.4.1.1 Procedures for Fiber Photometry Experiments.....	98
5.4.1.2 Procedures for Chemogenetic Experiments.....	98
5.5 Chemogenetic Manipulation of PV Interneurons.....	99
5.5.1 Acute Chemogenetic Manipulation of PV Interneurons.....	99
5.5.2 Chronic Chemogenetic Manipulation of PV Interneurons.....	100
5.6 Optogenetic Manipulation of PV neurons.....	100
5.6.1 Optogenetic Stimulation Paradigm.....	101
5.7 Electrophysiological Validation of Optogenetic Silencing.....	102
5.7.1 Single Cell Loose-Patch Electrophysiology.....	102
5.7.2 Presentation of Auditory Stimuli.....	103
5.7.3 Optogenetic Inactivation During Electrophysiological Recordings	103
5.8 Fiber Photometry.....	104
5.8.1 Fiber Photometry Acquisition system.....	104
5.8.2 Fiber Photometry Data Analysis.....	105
5.9 Low Frequency Fluctuations in Fiber Photometry Signal.....	106
5.10 Presentation of Ultrasonic Vocalizations	106
5.11 Fiber Photometry and Chondroitinase ABC Removal of PNNs	107
5.12 Pupillometry Setup	108
5.13 Pupil tracking with DeepLabCut	109
5.13.1 Correlation of Pupillometry and PV Interneuron (or Acetylcholine) Activity...	110

5.14 Histology.....	110
5.15 Fluorescence Microscopy.....	112
5.16 Quantification of Perineuronal Nets	112
5.17 Statistical Analysis and Figure Generation.....	113
<i>Chapter 6: Conclusions and Perspectives.....</i>	<i>114</i>
6.1 Where Does the ACtx PV Network Fit into the Overall Execution of Maternal Pup Retrieval Behavior?	115
6.2 How We Think About PV Neurons in Plasticity Periods	118
6.3 Future directions.....	123
<i>Bibliography.....</i>	<i>125</i>

Acknowledgements

First and foremost, I would like to thank my research advisor, Steve Shea, for his support, guidance, and kindness throughout my time in the lab. Thank you for always being the optimistic one, and getting excited about any and all data that I would bring to you, no matter how disappointing I warned you that it would be. The many students that flock to your lab are a testament to your dedication to mentorship, and I personally have greatly appreciated the balance you strike in juggling independence and guidance for your trainees. I would also be remiss to not formally thank you for your contributions to my education outside of the laboratory setting – namely the plethora of 80s and 90s references that you have thrown my way over the years. We'll still call that one a work in progress, but I take solace in the fact that I can equally stump you with some choice Gen Z vernacular.

I would like to take this opportunity to also thank the members of my thesis committee that have helped shape the direction of this work over the years. In particular I would like to express my profound gratitude to John Inglis who has served as my academic mentor since my arrival at CSHL. Thank you, John, for always being there to lend a sympathetic ear, offer sage advice, and be a sounding board for my next steps. I'd also like to thank Tony Zador for generously serving as the Co-Sponsor for my F31 grant, and Florin Albeanu for his additional work as the chair of my committee. Thank you also to David Schneider for so generously taking the time to serve as the external examiner for this thesis.

The administrative support that students of the CSHL SBS receive is unrivalled. Thank you to Alex Gann, Zach Lippman, Monn Monn Myat, Alyson Kass-Eisler, Kim Creteur, and Kim Graham for all that you do behind the scenes to ensure that students don't have to worry about anything but their science. I would also like to take a moment to recognize some of the

institutional support that has made my work possible – particularly the LAR for taking such stellar care of my mice, and the OSP for all of their help with grants administration, especially Catherine Perdikoylis and Renee Cercone. Thank you also to the members of both the WiSE and BEC executive committees that I have had the privilege of working alongside during my time at CSHL.

To the members of the Shea Lab, thank you for the comradery and inspiration in our collective quest to understand social behavior. Thank you to past and present lab members Clancy Kelahan, Roman Dvorkin, Yunyao Xie, Alberto Corona, Luqun Shen, Ally Nowlan, DeeDee Rupert, and Hoda Ansari for all of the training, discussions, and fun times. I especially want to thank Ally and DeeDee for not only welcoming me into their office, but also for taking me under their wing and showing me the ropes when I joined the lab. I also need to give a huge shout out to our lab technician, Jane Choe, who not only procures the best lab snacks, but also keeps the lab running, and whose technical support allows me get my work done.

Although I did not have to travel far to arrive at CSHL, many of my classmates sure did, and I could not be more thankful that they decided to make that journey. I've been lucky enough to have found some of my best friends in my classmates, and it has been a real comfort going through the highs and lows of graduate school together. Special thanks to Amritha, Marie, Jonathan, Mo, and Pickles the Cat for being the best housemates and second family anyone could ask for. I sincerely hope that I can continue my phage legacy from afar as we inevitably disperse to all corners of the globe. To Teri and Asad – I don't know that thank you would be the appropriate word. You've undone my shoe laces and strung them from the ceiling, printed dozens of pictures of my face and hidden them all over our house, and have somehow

coerced me into mopping up your flooded basement on multiple occasions. All I can say is that I'd be happy to do it again.

To all of those that have been on this journey with me since before I arrived at CSHL: thank you for reminding me that life exists outside of the lab, and for supporting me throughout my graduate school career. A special thanks to Tori, George, Joanne, Annabel, Erik, Stela, Val, Julie, and Lauren for all of the laughs and support throughout the years.

Last but certainly not least, I would not be here without the unconditional love and support of my family. Thank you to my parents for your understanding in planning around my oftentimes rigid schedule when it came to mouse work and experimental time points. Thank you for always coming down to help me move, and always sending me back to Long Island loaded up with food and supplies. And thank you to my sister, Zoe. I don't know that the many hours I've spent on Facetime watching your cat perform 'skilled tricks' have significantly contributed to this thesis, but I'm sure that there is something to be said for the mental breaks those calls have provided. Also special thanks to my grandma for sending enough treats for not only me, but for the rest of my class to enjoy. To my entire family: your support and encouragement continue to mean the world to me, so thank you.

List of Figures

Figure 2.1: PVMHET surrogates fail to learn the pup retrieval behavior.....	36
Figure 2.2: Changes in ACtx PV responses to USVs depend upon maternal experience and functional MeCP2.....	39
Figure 2.3: PVMHET surrogates lack low frequency ACtx PV fluctuations.....	42
Figure 2.4: Pup retrieval performance correlation with ACtx PV low frequency fluctuations.....	44
Figure 2.5: ACtx PV activity reflects sensory and behavioral events in PV- <i>Cre</i> , but not PVMHET, surrogates.....	48
Figure 2.6: ACtx PV responses to behavioral events occur independently of auditory stimuli.....	49
Figure 2.7: PVMHET surrogate responses to USV playback in a freely moving context.....	50
Figure 2.8: Sensory and behavioral events are insufficient covariates for a robust linear encoding model.....	51
Figure 2.9: ACtx PV inhibition does not impair retrieval.....	52
Figure 2.10: Surrogates' instantaneous velocity is not correlated with ACtx PV fluctuations.....	57
Figure 3.1: ACtx PV fluctuations occur independently of context.....	62
Figure 3.2: ACtx PV activity is correlated with pupil size	65
Figure 3.3: ACtx PV correlation with pupil is independent of locomotion.....	66
Figure 3.4: ACtx ACh release is correlated with pupil size.....	67
Figure 4.1: Acute optogenetic ACtx PV silencing in PVMHETs does not rescue retrieval performance.....	76

Figure 4.2: Optogenetic construct validation.....77

Figure 4.3: Acute chemogenetic ACtx PV silencing in PVMHETs does not rescue retrieval performance.....78

Figure 4.4: Chronic ACtx PV silencing in PVMHETs rescues retrieval performance.....79

Figure 4.5: Chronic ACtx PV inhibition in PVMHETs leads to disassembly of PNNs.....81

Figure 4.6: Chronic ACtx PV inhibition in PVMHETs modestly restores low frequency fluctuations.....83

Figure 4.7: Enzymatic dissolution of PNNs is not conducive to stable recordings.....89

Figure 6.1: Proposed model for lack of ACtx PV low frequency fluctuations in MeCP2^{het} mice.....122

List of Tables

Table 5.1: Primer sequences used for genotyping mouse lines.....	91
Table 5.2: Linear Encoding Model Covariates.....	95
Table 5.3: Viral Constructs for Injection.....	97

List of Abbreviations

AAV	Adeno-associated virus
ACC	Anterior cingulate cortex
ACh	Acetylcholine
ACtx	Auditory cortex
AMPA	α -amino-3-hydroxy-5-methyl-4-isoxazole propionic acid
ASD	Autism Spectrum Disorder
AUC	Area under the curve
Ca ²⁺	Calcium
CNO	Clozapine-N-oxide
DREADD	Designer receptors exclusively activated by designer drugs
GABA	γ -Aminobutyric acid,
GAD	Glutamate decarboxylase
GCaMP	Genetically encoded calcium indicator
GFP	Green fluorescent protein
GRAB	GPCR (G-protein coupled receptor) Activation Based
hM4Di	Modified form of human M4 muscarinic receptor (inhibitory DREADD)
IP	Intraperitoneal
LC	Locus Coeruleus
LOF	Loss of function
KO	Knockout
MeCP2	Methyl CpG binding protein 2
MeCP2 ^{het}	Heterozygous for MeCP2 LOF allele
MMP	Matrix metalloproteinase
MPOA	Medial preoptic area
P	Postnatal day
PNN	Perineuronal net
PSAM	Pharmacologically selective actuator module
PSEM	Pharmacologically selective effector molecule
PV	Parvalbumin
PVMHET	PV- <i>Cre</i> ^{het} and MeCP2 ^{het} genotype
RTT	Rett Syndrome
SST	Somatostatin
stGtACR2	Soma-targeted <i>Guillardia theta</i> anion-conducting channelrhodopsin
USV	Ultrasonic vocalization
VIP	Vasoactive intestinal peptide
VTA	Ventral tegmental area
WT	Wild type
Zdff	Z-scored change in fluorescence over fluorescence

Author Contributions

I would like to acknowledge and thank those that have directly contributed to this work. The headfixed fiber photometry experiments presented in Figure 2.2 were a collaboration with DeeDee Rupert, and are included in the *BiorRxiv* preprint, Rupert et al., 2023. The linear encoding model presented in Figure 2.8 was a collaboration with Julia Wang, a graduate student in Tatiana Engel's lab. Jane Choe assisted with the tissue processing for PNN immunolabeling that is presented in Figure 4.5. Zara Ward, a summer undergraduate student in the Shea Lab, labeled pup contact events as either overlapping or nonoverlapping events with pup USVs, which is included in Figure 2.6.

Summary

Rett Syndrome is a neurodevelopmental disorder caused by heterozygous loss of function mutations to the gene that encodes methyl CpG-binding protein 2 (MeCP2) – a ubiquitously expressed transcription factor. Amongst other deficits, Rett Syndrome results in a failure of the brain to activate plasticity programs during times that call for experience-dependent learning. The onset of maternal experience is an ideal time to experimentally probe such plasticity mechanisms in adulthood, as this period reflects a time of great learning demands within an ethologically relevant context.

Consistent with an inability to activate plasticity programs, female mice in a Rett Syndrome mouse model (MeCP2^{hets}) fail to learn a maternal behavior that relies on auditory processing of newborn pup vocalizations. Pups emit ultrasonic vocalizations when they are separated from the litter which prompts maternally experienced females to find and retrieve the pups back to the nest. MeCP2^{hets} not only fail to learn this retrieval behavior, but they also exhibit parvalbumin inhibitory interneuron (PV) abnormalities in the auditory cortex (ACtx) during this period of experience-dependent plasticity. Aberrations specific to the PV network are particularly intriguing given this neural subpopulation's well-documented role in regulating critical periods for plasticity.

Previous characterizations of the PV abnormalities in MeCP2^{hets} point towards a hyperactive and hypermature ACtx PV network, likely reflecting insufficient plasticity for the retrieval behavior to be successfully learned. However, technical limitations of these studies have only provided snapshots of the ACtx PV network at timepoints with relevance to the onset of maternal experience; this has impeded our understanding of the real-time ACtx PV network

contributions to retrieval, and the direct behavioral consequences of its dysregulation in MeCP2^{hets}.

To overcome these limitations, we have monitored ACtx PV activity *during* retrieval behavior over the course of the postnatal period. Our results provide hitherto unequalled insight into ACtx PV dynamics in freely behaving animals, and a cell-type specific network underlying adult experience-dependent plasticity. Through these experiments, we uncovered a characteristic low frequency ACtx PV activity pattern in wild type females that was notably absent in MeCP2^{hets}. The low frequency fluctuations reflected both sensory and behavioral information during retrieval assays, but together these events only accounted for a small proportion of the overall signal dynamism. This prompted us to consider that the low frequency fluctuations were more indicative of a plasticity-conducive PV network state, which was supported by the discovery that the ACtx PV activity was tightly coupled with pupil size (an established proxy for attention and arousal). In an effort to induce this ACtx PV network state in MeCP2^{hets}, we showed that chronic, but not acute, chemogenetic ACtx PV inhibition rescued retrieval performance. Not only did this manipulation improve behavior, but it also disassembled perineuronal nets around PV cells (perineuronal nets typically act as blockades to synaptic plasticity), and induced the emergence of modest low frequency ACtx PV fluctuations in MeCP2^{hets}. Taken together, we propose that the low frequency ACtx PV fluctuations are a signature of a PV network state that is prepared to meet plasticity demands in adulthood.

Chapter 1: Introduction

1.1 An Introduction to Neuroplasticity

Neuroplasticity broadly refers to the brain's ability to structurally and functionally reorganize in response to internal or external environmental cues. Although most commonly studied in the contexts of neural development, learning, and injury, neuroplasticity-inducing events are as varied as the molecular, biophysical, and neurochemical processes that work together to facilitate them. Notably, such synaptic remodeling and functional reorganization is not confined to developmental periods, but also persists into adulthood using many of the same mechanisms (Barnes and Finnerty 2010; Hofer et al. 2006; Rupert and Shea 2022). For the purposes of this thesis, we will focus on experience-dependent plasticity in adulthood that occurs during a period of heightened demand for sensory learning.

The concept of a 'critical period' has emerged in the context of sensory neuroplasticity to define a temporal window during which a particular type of environmental trigger is likely to exert its greatest neural influence. There is, however, a subtle nuance with regards to the nomenclature surrounding these windows of heightened plasticity – namely a distinction between a 'sensitive' and a 'critical' period. A sensitive period is generally referred to as any window when sensory experience can exert an unusually strong influence on neural structure and function. A critical period is a more extreme sensitive period - if the appropriate sensory experience is not available during that time, normal circuitry and behavior will never develop (Voss 2013; Knudsen 2004).

A canonical example of this more extreme case stems from foundational work conducted by Hubel & Wiesel. Together, they demonstrated that sensory input in early life

affects the functional organization of the cortex – monocular deprivation dramatically reduces the cortical area typically devoted to the deprived eye while increasing the size of the area receiving inputs from the open eye. The pair subsequently coined a ‘critical period’ during which early visual experience can dramatically reshape neural connectivity and structure in the visual cortex (Wiesel and Hubel 1963; Hubel and Wiesel 1970). This idea has been extended to define critical periods for a variety of sensory systems across many species. Other notable examples include the influence of early whisker stimulation on the development of rat barrel cortex, and early life auditory experience with conspecific birdsong for the development of zebra finch songbirds’ own songs (Erzurumlu and Gaspar 2012; Shoykhet et al. 2005; Lendvai et al. 2000; Eales 1987; Morrison and Nottebohm 1993). Importantly, the underlying neural processes are thought to be the same for critical and sensitive periods, and windows of heightened plasticity in adulthood reactivate the same mechanisms employed during developmental critical periods (Rupert and Shea 2022; Hofer et al. 2006). In both cases, GABAergic inhibitory interneurons play a central role in regulating the opening and closing of these windows of heightened cortical plasticity.

1.2 Inhibitory Control of Neuroplasticity

Broadly speaking, there are two major classes of neurons in the mammalian cortex – glutamatergic excitatory and gamma-aminobutyric acid-containing (GABAergic) inhibitory neurons. Excitatory neurons greatly outnumber their inhibitory counterparts, with GABAergic inhibitory interneurons accounting for only an estimated 10-20% of all cortical neurons (Markram et al. 2004; Petilla Interneuron Nomenclature Group et al. 2008; Tremblay et al. 2016; DeFelipe et al. 2013). Despite this discrepancy in their relative densities, cortical

inhibitory and excitatory drive are largely matched, suggesting a disproportionate influence of inhibitory signaling in shaping overall neural activity patterns (Xue et al. 2014; Vogels et al. 2011; House et al. 2011). Indeed, when it comes to the control of critical periods for plasticity, inhibitory interneurons play a driving role. Critical periods are regulated by changes in GABAergic neurotransmission, and their progression coincides with the maturation of inhibitory circuitry (Fagiolini et al. 2004; Maffei et al. 2010, 2006). In fact, transplantation of immature inhibitory neurons can induce ocular dominance plasticity long after critical period closure, demonstrating the intrinsic power of this GABAergic subpopulation in orchestrating critical period onsets and offsets (Southwell et al. 2010).

In support for the role of inhibition in critical period regulation, experimental manipulations of GABAergic networks have been shown to disrupt their typical progression. For example, mice lacking glutamate decarboxylase (GAD), the rate limiting enzyme for GABA synthesis, are insensitive to monocular deprivation and exhibit abnormal synaptic innervation during development. However, subsequent restoration of GAD function in these mutants fully rescues their capacity for ocular dominance plasticity (Hensch et al. 1998; Chattopadhyaya et al. 2007). Manipulation of GABAergic signaling is also able to control the timing of critical periods. Direct enhancement of GABAergic signaling via diazepam administration (a GABA_A receptor agonist) prematurely opens the window for ocular dominance in young mice, leading to the proposition that a threshold for inhibitory neurotransmission may, once crossed, trigger critical periods (Fagiolini and Hensch 2000). As such, it would appear that increased inhibition and the maturation of inhibitory networks signal the closure of critical periods, and that their delayed maturation may therefore prolong critical period closure. Indeed, reducing intracortical inhibition promotes visual cortex plasticity in

adult rats, and mice in which inhibition remains immature fail to enter critical periods (Harauzov et al. 2010; Fagiolini and Hensch 2000; Deidda et al. 2015). Conversely, heightened inhibitory neurotransmission and network maturity accelerate the onset and signal the closure of critical periods for plasticity (Huang et al. 1999; Hanover et al. 1999; Fagiolini and Hensch 2000; Iwai et al. 2003; Hensch 2005; Di Cristo et al. 2007). Taken together, these results suggest that the maturation of inhibitory networks coincides with the closure of critical period plasticity.

1.3 Parvalbumin Interneurons as Critical Period Regulators

1.3.1 Properties of Parvalbumin Interneurons

Although only comprising 10-20% of all cortical neurons, there is great heterogeneity within the GABAergic population. Indeed, inhibitory neuronal subpopulations have been characterized on the basis of their morphology, connectivity, neuropeptide release, and protein expression (Kawaguchi and Kubota 1997; Markram et al. 2004; DeFelipe 1997; Petilla Interneuron Nomenclature Group et al. 2008; Tremblay et al. 2016; DeFelipe et al. 2013). One particular inhibitory subpopulation, parvalbumin-positive interneurons (PV), has been heavily implicated in the control of critical periods for plasticity. PV neurons are defined by their expression of the calcium-binding protein, parvalbumin, and account for ~ 40% of the total cortical GABAergic population (Rudy et al. 2011; Tamamaki et al. 2003; DeFelipe 1993). They mediate feedforward, lateral, and recurrent inhibition through synaptic connectivity with pyramidal (glutamatergic) neurons, other cortical PV interneurons, and themselves (Callaway 2004; Lu et al. 2007; Kuramoto et al. 2022; Galarreta and Hestrin 1999; Deleuze et al. 2019;

Szegedi et al. 2020). PV innervation of pyramidal neurons is dense and largely non-specific, and PV interneurons have wide-reaching, elaborate dendritic branching (Packer and Yuste 2011; Karnani et al. 2014; Bartholome et al. 2020). Furthermore, PV neurons typically synapse directly either on the soma or the axon initial segment (Kepecs and Fishell 2014). Together, these key features position PV neurons to serve as key integrators and orchestrators of overall cortical activity patterns.

Sometimes referred to as ‘fast spiking’ neurons, electrophysiological studies have demonstrated that PV neurons exhibit high spontaneous and stimulus-induced firing rates (Kawaguchi et al. 1995; Connors and Gutnick 1990). This defining property is largely mediated by their expression of rapidly repolarizing Kv3 potassium channels, and Ca²⁺ permeable AMPA receptors with rapid gating kinetics (Rudy and McBain 2001; Geiger et al. 1997). This temporal precision suggests a role for PV interneurons in inhibitory synapse spike-timing-dependent-plasticity (STDP) which heavily relies on precise coincidence detection of neuronal firing (D’amour and Froemke 2015; Kuhlman et al. 2010). Furthermore, the fast spiking nature of PV cells and their robust reciprocal connectivity may contribute to the generation of cortical gamma rhythms - high frequency (30-80 Hz) periodic signals resulting from synchronous neural activity (Galarreta and Hestrin 1999; Sohal et al. 2009; Cardin et al. 2009; Bartos et al. 2007). Gamma rhythms in particular emerge during periods of heightened arousal and attention, and are hypothesized to enhance sensory and information processing (Sohal et al. 2009; Cardin et al. 2009; Bosman et al. 2012; Kim et al. 2016, 2015; Börgers et al. 2008). The PV network is largely thought to orchestrate gamma rhythms through synchronous PV firing and the resulting large-scale coordination of pyramidal neurons. Indeed, optogenetic activation of PV neurons induces gamma rhythms, and PV inhibition dramatically

suppresses their power (Cardin et al. 2009; Sohal et al. 2009; Etter et al. 2019). Taken together, these results suggest that the unique characteristics of PV neurons render them exceptionally poised to coordinate large neural ensembles and exert influence over cortical states.

1.3.2 Parvalbumin Neurons and Perineuronal Nets

Out of all GABAergic subpopulations, PV inhibitory interneurons have been the most heavily implicated in regulating critical periods for cortical plasticity. More specifically, the development of PV networks drives critical period trajectories. Upon maturation, PV neurons are selectively engulfed by perineuronal nets (PNNs) – sulfated proteoglycan structures in the extracellular matrix that act as a blockade to synaptic plasticity and physically prevent synaptic modifications of PV neurons (Krishnan et al. 2015; Sorg et al. 2016; Sigal et al. 2019; Miyata and Kitagawa 2017; Patrizi et al. 2020). PNNs consist of a hyaluronan backbone that acts as a scaffold for link proteins, chondroitin sulfate (a sulfated glycosaminoglycan), and other anchoring proteins to form a condensed mesh structure capable of latching onto cell membranes (Brückner et al. 1993; Day and Prestwich 2002). The engulfment of PV neurons by PNNs is a hallmark signaling the closure of critical periods for plasticity across sensory systems, and their precocious appearance prematurely terminates these windows (Takesian and Hensch 2013; Pizzorusso et al. 2002; Sorg et al. 2016; Miyata and Kitagawa 2017; Reh et al. 2020; Krishnan et al. 2015; Patrizi et al. 2020). Notably, enzymatic PNN removal reopens critical periods, and a genetic attenuation of PNN formation results in persistent plasticity (Lensjø et al. 2017; Pizzorusso et al. 2002; Gogolla et al. 2009; Happel et al. 2014; Krishnan et al. 2017; Carulli et al. 2010). Taken together, these results reinforce the critical role that PNNs, and the PV neurons that they engulf, play in regulating cortical plasticity.

The vast majority of cortical PNNs selectively engulf PV interneurons in an activity-dependent manner as developmental windows close (Härtig et al. 1992; Pizzorusso et al. 2002; Dityatev et al. 2007; Giamanco and Matthews 2012). Indeed, PV neuronal activity is necessary for PNN formation (Reimers et al. 2007; Favuzzi et al. 2017). It follows that parvalbumin protein expression is correlated with PNN engulfment, given that parvalbumin protein expression intensifies when PV neuronal activity increases (Yamada et al. 2015; Kamphuis et al. 1989; Patz et al. 2004; Cisneros-Franco and de Villers-Sidani 2019; Donato et al. 2013; Rowlands et al. 2018). Given this relationship between PV neuron activity and PNN formation, several studies have attempted to reopen critical periods for plasticity by directly manipulating PV activity. In fact, chemogenetic inhibition of PV neurons has been shown to reopen critical periods in the auditory and visual systems, and improve learning and memory when inhibiting hippocampal PV neurons. Importantly, this plasticity is accompanied by evidence of PNN dissolution (Cisneros-Franco and de Villers-Sidani 2019; Donato et al. 2013; Devienne et al. 2021). Furthermore, chemogenetically inhibited PV neurons, but not their untransduced neighbors, are the ones to show a reduction in PNN presence (Devienne et al. 2021). This suggests that there is PV cell autonomous regulation of PNN formation based on individual neural activity patterns.

While overall PNN deposits accumulate with age, clearly PNN density fluctuates in response to external cues and their resulting influence on PV activity. This is largely possible due to the work of the endogenous matrix metalloproteinase (MMP) enzyme that degrades the PNN backbone structures (Rossier et al. 2015). Intuitively, MMP expression declines following the closure of critical periods, but its persistent presence in the mature brain provides a mechanism by which experience-induced synaptic plasticity may occur (Murase et al. 2017).

However, the direct relationship between PV activity, molecular processes such as MMP activation, and PNN integrity remains unclear and is an active area of investigation.

1.4 Maternal Retrieval Behavior

Maternal pup retrieval is an exceptional system in which to study adult experience-dependent plasticity in an ethologically relevant context. Newborn mouse pups are born blind, deaf, and unable to thermoregulate their core body temperature which renders them particularly vulnerable to environmental insult. Therefore, when pups are displaced from the nest, they produce distress cries in the form of high pitch ultrasonic vocalizations (USVs) that increase in frequency and volume during repeated bouts of isolation (Ehret 2005; Myers et al. 2004). To naive virgin females, USVs are meaningless and the pups are ignored. However, maternally experienced females will come to recognize these USVs and their significance, which prompts them to quickly locate and retrieve the pups back to the warmth and safety of the nest (Ehret 2005; Sewell 1970; Cohen and Mizrahi 2015; Liu et al. 2006; Koch and Ehret 1989; Elyada and Mizrahi 2015; Marlin et al. 2015; Ehret 1987; Liu and Schreiner 2007; Cohen et al. 2011).

It is critical to emphasize that maternal pup retrieval is a *learned behavior* – ideal for use as a sensitive assay to assess adult experience-dependent plasticity. Females that have never given birth (naive virgins) can learn to retrieve pups through “surrogate” maternal experience in the form of co-habitation with a dam and litter (Rosenblatt 1967; Galindo-Leon et al. 2009; Cohen et al. 2011; Cohen and Mizrahi 2015; Stolzenberg and Champagne 2016; Krishnan et al. 2017; Lau et al. 2020; Carcea et al. 2021; Seip and Morrell 2008; Alsina-Llanes et al. 2015; Martín-Sánchez et al. 2015). Not only do surrogates learn to retrieve as well as mothers and significantly better than naive virgins, but they also exhibit forms of the ACtx

plasticity associated with this behavior as the significance of pup USVs is reinforced with experience (Krishnan et al. 2017; Lau et al. 2020; Schiavo et al. 2020; Cohen and Mizrahi 2015). Given that our goal is to dissect plasticity mechanisms, this is particularly advantageous – it allows us to probe relevant circuits in surrogates thereby eliminating the additional confound that maternal hormone fluctuations would introduce in mothers.

1.5 Maternal Experience-Induced Plasticity in the Auditory Cortex

While retrieval behavior stems from the integration of multiple sensory cues (visual, olfactory, auditory), the detection of pup USVs and the ACtx are both critical for this behavior to be successfully learned. Indeed, bilateral ACtx lesions in maternally experienced females impairs retrieval (Marlin et al. 2015; Krishnan et al. 2017). Furthermore, mute mouse pups are not retrieved, and USVs are solely capable of guiding retrieval – pups can be replaced by a loudspeaker playing USVs that mothers will approach in the absence of visual or olfactory cues (Ehret 2005; Sewell 1970). These results demonstrate the critical importance of USVs and their detection in the ACtx for retrieval to be successfully learned.

Maternal experience induces several forms of ACtx plasticity, further implicating a role for the appropriate use of USVs to perform this learned behavior (Liu and Schreiner 2007; Galindo-Leon et al. 2009; Lin et al. 2013; Cohen and Mizrahi 2015; Marlin et al. 2015; Lau et al. 2020). For example, mothers demonstrate improved cortical entrainment and strengthened responses to pup USVs, in addition to recruiting an ACtx cellular population that is highly responsive to this newly relevant social stimulus (Liu and Schreiner 2007; Marlin et al. 2015; Shepard et al. 2015; Tasaka et al. 2018; Liu et al. 2006). Furthermore, there is an increased tendency for correlated neural activity in the ACtx of mothers, suggesting enhanced functional

connectivity that is typically seen in various learning paradigms (Rothschild et al. 2013). Notably, responses to pure tones do not change during this window, indicating plasticity mechanisms at work to accommodate learning specific to maternal care (Galindo-Leon et al. 2009; Shepard et al. 2016). In addition, much of this experience-induced plasticity is transient, evident only in an early postnatal period when they are engaged in maternal retrieval behavior (peak window spanning from P0 through P5) (Tasaka et al. 2018; Krishnan et al. 2017).

Perhaps unsurprisingly, inhibitory plasticity mechanisms in the ACtx coincide with the onset of maternal experience. Indeed, inhibitory networks presumably undergo significant changes following maternal experience as GAD67 (responsible for the rate limiting enzymatic reaction for GABA synthesis) levels increase during this window (Krishnan et al. 2017). Additionally, oxytocin, a hormone heavily implicated in social interactions and maternal behavior, has been shown to enable maternal behavior by balancing ACtx inhibition in new mothers (Marlin et al. 2015). Newly relevant pup odors also increase the sound detectability of fast spiking (putative PV) neurons in the ACtx, and new mothers exhibit selective suppression of spontaneous activity in USV-responsive neurons (Cohen et al. 2011; Lin et al. 2013). A reduction in background noise may improve both the detection and discriminability of USVs which is imperative for successful retrieval performance and pup survival. Notably, PV neurons exhibit suppressed firing in response to pup USVs after maternal experience, and mothers exhibit pup USV-evoked inhibition that is strongest in parts of the ACtx tonotopy corresponding to frequencies lower than pup USVs (Lau et al. 2020; Rupert et al. 2023; Galindo-Leon et al. 2009). The strength of this inhibitory plasticity in lateral frequency bands may improve the detection of pup USVs through enhanced contrast discriminability (Galindo-

Leon et al. 2009). Collectively, these results demonstrate that the window for plasticity induced by maternal experience involves reorganization of inhibitory circuitry in the ACtx.

1.6 Rett Syndrome – Genetic Underpinnings and Clinical Presentation

Due to its importance for the survival of offspring, maternal pup retrieval is an exceptionally robust natural behavior. However, instances where the behavior is impaired allow us to probe the circuit dysregulation manifesting in this behavioral deficit, and by extension, understand the neural circuitry underlying its successful performance. For this reason, this study will employ a mouse model of the neurodevelopmental disorder Rett Syndrome, where maternally experienced females notably fail to learn the pup retrieval behavior.

1.6.1 Genetic Underpinnings

Rett Syndrome (RTT) is a rare neurodevelopmental disorder affecting 1 in 10,000 females caused by sporadic *de novo* mutations to the *Methyl CpG Binding Protein 2 (MeCP2)* gene (Amir et al. 1999; Good et al. 2021). Consistent with the typical high penetrance of monogenic disorders, over 95% of RTT cases are attributed to *MeCP2* mutations, and less than 1% of individuals with an *MeCP2* mutation do not develop RTT (Bienvenu et al. 2000; Percy et al. 2007). The vast majority of *MeCP2* mutations resulting in RTT are missense (point), loss of function mutations that occur in the 3rd or 4th exon, but frameshift and nonsense mutations are also possible within the methyl-binding domain coding region (Amir et al. 1999; Percy et al. 2007).

The *MeCP2* gene is located on the q28 band of the X chromosome, meaning that the disorder is X-linked (Sirianni et al. 1998). Males (XY) with mutations to their single gene copy generally die in infancy or before birth, so surviving RTT patients are typically females (XX) that are heterozygous for the mutated copy of *MeCP2*. However, because of lyonization (the silencing of one X chromosome during embryonic development) in females, female RTT patients exhibit a mosaic expression pattern of the affected allele. While the exact incidence of lyonization remains controversial (not necessarily occurring at a true randomness of 50%), it has been suggested that X inactivation may skew in favor of the non-mutated allele in RTT patients (Braunschweig et al. 2004; Busque et al. 1996; Distèche and Berletch 2015; Pereira and Dória 2021). Nevertheless, this mosaicism leads to variable expressivity of the mutated allele in RTT patients.

MeCP2, the protein product of the *MeCP2* gene, is a ubiquitously expressed transcription factor that binds to methylated cytosine and guanine rich repeat sites upstream of transcription start sites, critically regulating chromatin structure and eventual downstream gene expression. While initially MeCP2 was thought of as solely a transcriptional repressor, it has more recently been shown to also function as a transcriptional activator depending on its engagement with other cofactors and its precise binding site (Horvath and Monteggia 2018; Chahrour et al. 2008; Ibrahim et al. 2021; Boyes and Bird 1991; Nan et al. 1998, 1997; Yasui et al. 2007). This flexibility highlights the powerful influence MeCP2 exerts over gene expression profiles.

Although ubiquitously expressed, MeCP2 plays an exceptionally critical role in normal brain development and function. Indeed, mouse models restricting *MeCP2* mutation to the brain recapitulate the majority of the syndromic phenotypes present in germline *MeCP2*

mutants, and the majority of RTT symptoms are neurological (Chen et al. 2001). Functionally, MeCP2 has been shown to both regulate neuronal gene expression and dendritic arborization, as well as maintain the integrity of synaptic connections. Importantly, it not only plays a role in development, but also in the maintenance of the mature brain; MeCP2 deletion in adult mice quickly recapitulates the RTT phenotypes seen in constitutive germline MeCP2^{hets} (Chen et al. 2001; Li et al. 2013; Baj et al. 2014; Zoghbi 2003; Kishi and Macklis 2004; McGraw et al. 2011; Cheval et al. 2012; Nguyen et al. 2012).

1.6.2 Clinical Presentation

The symptomatic presentation of RTT is marked by normal neurological and physical development in early life, followed by an abrupt regression around 6-18 months. At this time, patients lose previously acquired purposeful motor, cognitive, and language abilities. These deficits will persist throughout life, and patients typically survive until middle age (Kirby et al. 2010; Neul et al. 2014; Chahrour et al. 2008). In addition to motor deficits including spastic ataxic gait, loss of purposeful hand use, and discoordination, patients lose language abilities and exhibit many neurological features that resemble those of Autism Spectrum Disorders (ASD) (Neul et al. 2010; Percy et al. 1988). Despite sharing many of their defining diagnostics (social, sensory processing, and communication deficits), RTT patients are not categorized under the ASD umbrella mainly owing to the defined monogenic determinant of RTT (Percy 2011). Furthermore, RTT patients often present with additional comorbidities including epilepsy, microcephaly, respiratory difficulties, scoliosis, Raynaud's phenomena, and impaired sleep (Gold et al. 2018). Taken together, the RTT diagnostic criteria can be quite extensive, and the variety and severity of phenotypes vary greatly between patients (Pini et al.

2016). Moreover, in individual patients the severity of distinct symptoms is not correlated. A particular patient's symptomology likely reflects the pattern and extent of the mutation's mosaicism, with particularly severe deficits likely pointing to increased mosaic burden in a given affected tissue (Wang et al. 2021; Archer et al. 2007).

1.6.3 Mouse Model of Rett Syndrome

Studies of Rett Syndrome in mice have largely employed two MeCP2 loss of function (LOF) mouse models. The “Bird line” achieves heterozygous MeCP2 LOF through comprehensive deletion of *MeCP2* exons 3 and 4, while the “Jaenisch line” features a frameshift mutation in exon 3 (Guy et al. 2001; Chen et al. 2001). We have strategically chosen to conduct our experiments in the Bird line because of its pure C57BL/6 background - given that the majority of *Cre/lox* lines are also of a C57BL/6 background, we have been able to cross the RTT line with other *Cre/lox* lines for functional imaging and manipulation of targeted neuronal subpopulations within the RTT model.

Symptomology of heterozygous females in the Bird line follows the same progression as that of humans. After an initial normal period of early development, female mice start to show symptoms at around 3 months. At that point, they begin to exhibit subtle RTT signatures such as hindlimb clasping phenotypes. By 9 months, more unambiguous symptoms develop and include respiratory difficulties, gait irregularities, and decreased mobility (Guy et al. 2001; Samaco et al. 2013). Given the mosaic nature of the mutation, gross neural alternations are difficult to consistently characterize at a group level. However, subtle changes in neuronal excitability, overall excitatory/inhibitory balance, synaptic connectivity, and dendritic arborization have been reported, although overall adult neuronal densities appear largely

unaffected (Dani et al. 2005; Taneja et al. 2009; Kishi and Macklis 2004; Na et al. 2013; Metcalf et al. 2006).

RTT model surrogates fail to learn maternal pup retrieval, prompting their use in the current study to investigate the circuit dysregulation underlying this behavioral deficit (Krishnan et al. 2017). This particular impairment is somewhat unsurprising given the functional role of MeCP2 as a transcription factor – changes in gene expression facilitate many components of neural plasticity required for experience-dependent learning. Notably, a conditional knockout (KO) of MeCP2 restricted to ACtx neurons is sufficient to disrupt retrieval in surrogates (Krishnan et al. 2017). This result emphasizes the critical role of MeCP2 in the ACtx specifically for learning the retrieval behavior despite the whole-brain penetrance of the MeCP2 mutation in the RTT model pathology.

1.6.4 Parvalbumin Network Abnormalities in the Rett Syndrome Mouse Model

PV interneurons appear to be particularly susceptible to MeCP2 perturbations, and a key player in the manifestation of RTT phenotypes (Morello et al. 2018). Mice with a MeCP2 KO restricted to PV neurons recapitulate the majority of the sensory, cognitive, and social deficits that characterize RTT, including abolished ocular dominance plasticity in the visual cortex and impaired early learning of maternal retrieval behavior (He et al. 2014; Krishnan et al. 2015; Ito-Ishida et al. 2015; Rupert et al. 2023). Importantly, a regionally specific KO of MeCP2 restricted to ACtx PV cells is sufficient to disrupt retrieval, further implicating the role of PV neurons in the ACtx specifically in this behavior (Rupert et al. 2023). Taken together, these results suggest that PV interneurons appear to be particularly susceptible to MeCP2 perturbations, and that their role is not restricted to development – PV circuitry is also

necessary for adult plasticity. A critical role for the PV network in learning the retrieval behavior is perhaps unsurprising given the well documented role of PV neurons in the regulation and timing of critical periods for plasticity across sensory systems, such as that marked by experience with pups.

Not only do MeCP2^{het} surrogates fail to learn the pup retrieval behavior, but they also exhibit abnormally heightened PV activity in the ACtx following maternal experience. In wild type surrogates, maternal experience triggers a *suppression* of PV auditory responses to pup USVs. In stark contrast, this response is *strengthened* following maternal experience in MeCP2^{het} surrogates, as well as in surrogates with an MeCP2 KO restricted to PV neurons (Lau et al. 2020; Rupert et al. 2023). This is particularly interesting as erroneously elevated PV activity in the hippocampus has been shown to impair learning and memory, and PNN formation is correlated with increased PV activity at a cell autonomous level (Donato et al. 2013; Reimers et al. 2007; Favuzzi et al. 2017; Devienne et al. 2021; Patrizi et al. 2020). As a result of this heightened activity, MeCP2^{het} surrogates also exhibit elevated PV protein expression in ACtx PV neurons, and have significantly more well-developed PNNs surrounding those PV neurons. Nevertheless, Chondroitinase ABC-driven removal of PNNs in the ACtx rescues retrieval behavior in MeCP2^{het} surrogates (Krishnan et al. 2017). The restorative effect of this spatially restricted intervention again emphasizes the role of the PV network in the ACtx specifically in retrieval behavior, and further validates the ACtx as a critical area of interest to probe in the current study. Notably, the heightened ACtx PV expression and presence of PNNs in surrogate MeCP2^{het} is transient - these markers are indistinguishable from wild type after pups are weaned and retrieval behavior becomes unnecessary (Krishnan et al. 2017). Therefore, sensitivity to MeCP2 in PV cells and the role

of PV cells in the expression of syndromic phenotypes may be heightened during periods of plasticity, such as that induced by the onset of maternal experience.

1.7 Research Aims

MeCP2^{het} surrogates have a hyperactive and hypermature ACtx PV network during the perinatal period (Lau et al. 2020; Krishnan et al. 2017). However, this characterization of ACtx PV network abnormalities is based on limited postmortem histology and single unit PV activity in headfixed animals listening to playback of pup USVs. These restrictions have impeded our understanding of the real-time ACtx PV network contributions to retrieval, and the direct behavioral consequences of its dysregulation in MeCP2^{hets}. To address this gap in knowledge, we will overcome prior technical limitations to monitor PV activity *during the retrieval behavior* in both wild type and MeCP2^{het} surrogates. For the first time, this work will reveal the real-time contributions of the ACtx PV network to pup retrieval behavior, and how that activity differs in a RTT model with retrieval deficits. In addition to observing PV activity differences during behavior, we will also directly manipulate the ACtx PV network of MeCP2^{hets} in an effort to rescue retrieval behavior performance. These research aims will broadly test the following hypotheses: 1) the ACtx PV network dynamically regulates retrieval behavior, and network dysregulation in MeCP2^{hets} results in retrieval deficits, and 2) inhibition of hyperactive ACtx PV networks in MeCP2^{hets} will remove PNNs in the ACtx and rescue retrieval behavior.

We will address these and other hypotheses over the course of the following three chapters. In Chapter 2, we will, for the first time, monitor ACtx PV activity *during* pup retrieval and compare activity patterns between wild type and MeCP2^{het} surrogates. In doing so, we will

be testing the hypothesis that ACtx PV activity dynamically regulates the behavior on a moment-to-moment basis, and that aberrations to typical activity patterns impair retrieval in MeCP2^{het} surrogates. In Chapter 3, we explore an alternative hypothesis - ACtx PV activity reflects a network configuration that favors plasticity which is disrupted in MeCP2^{het} surrogates. Finally, in Chapter 4, we will rescue the retrieval deficits seen in MeCP2^{het} surrogates by manipulating the ACtx PV network. Taken together, our results suggest that an ACtx PV network state facilitates successful learning in wild type surrogates. This network configuration is, in part, characterized by a signature pattern of ACtx PV activity that is notably distinct in MeCP2^{het} surrogates that fail to learn the retrieval behavior. However, prolonged ACtx PV inhibition induces the emergence of the plasticity-favorable ACtx PV network configuration in MeCP2^{hets}, and rescues retrieval performance.

Chapter 2: ACtx PV Activity Does Not Regulate Retrieval Behavior on a Moment-to-Moment Basis

The primary goal of this chapter is to monitor ACtx PV activity during retrieval behavior, and compare activity patterns between wild type and MeCP2^{het} surrogates. Given that prior characterizations of the ACtx PV network aberrations in MeCP2^{hets} have only been assessed using histological or headfixed, electrophysiological methods, we sought to understand the network activity *during* the behavior itself and how its dysregulation in MeCP2^{hets} may be affecting retrieval performance (Lau et al. 2020; Krishnan et al. 2017; Rupert et al. 2023). In doing so, we found that MeCP2^{hets} lacked the pronounced low frequency ACtx PV fluctuations that characterize the wild type ACtx PV activity pattern, the absence of which appears to reflect their inability to retrieve pups. Upon further investigation, we discovered that the low frequency fluctuations in wild type surrogates reflected both sensory and behavioral events during retrieval sessions, but that the acute ACtx PV network activity during retrieval was not necessary for successful retrieval to occur.

2.1 PVMHET Surrogates Fail to Learn Maternal Pup Retrieval

In order to monitor and manipulate the ACtx PV population in RTT model surrogates, we employed *Cre/lox* viral strategies. For this to be possible, we first crossed female MeCP2^{hets} (the RTT model) with homozygous PV-*Cre* males to generate a ‘PVMHET’ line. Animals of this line were therefore all PV-*Cre*^{het}, and Mendelian genetics dictates that 50% would have the desired MeCP2^{het} genotype that defines the RTT model (Figure 2.1). Females meeting the criterion of PV-*Cre*^{het} and MeCP2^{het} will be referred to as PVMHETs going forward for

simplicity. In order to confirm that crossing the *PV-Cre* line into the $\text{MeCP2}^{\text{het}}$ line did not have any unintended effect on our behavior of interest, we confirmed that PVMHET surrogates also exhibit retrieval behavior deficits (Figure 2.1).

It is important to note that the female mice used in our studies are aged 8-12 weeks. This optimal window captures females past the age of sexual maturity (around 7 weeks) and are therefore prime for learning maternal behaviors, while using females young enough that advanced progression of RTT symptoms will not physically interfere with their ability to perform such behaviors. Indeed, $\text{MeCP2}^{\text{hets}}$ do not yet exhibit robust motor deficits at this age, and it has been previously shown that maternal retrieval behavior deficits seen in $\text{MeCP2}^{\text{hets}}$ are not attributed to gross motor deficits – there is no significant difference in movement between $\text{MeCP2}^{\text{hets}}$ and wild type littermates during retrieval assays (Samaco et al. 2013; Krishnan et al. 2017).

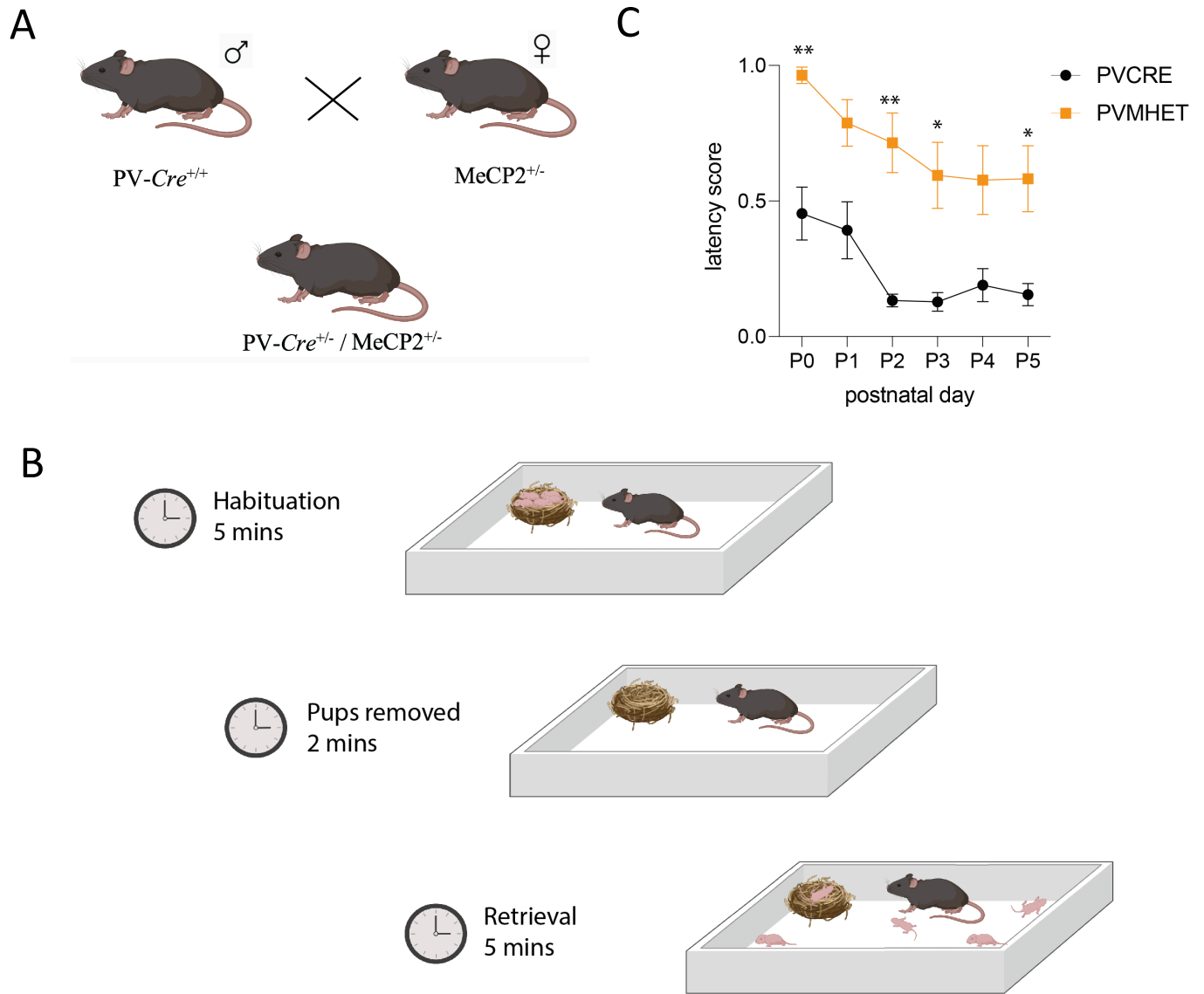


Figure 2.1: PVMHET surrogates fail to learn the pup retrieval behavior. **A)** Generation of the PVMHET line for *Cre/lox*-based PV neural manipulability in the *MeCP2^{het}* background. **B)** Schematic of standard pup retrieval assay. Surrogates are habituated in the home cage with the pups in the nest for 5 minutes. Pups are removed for 2 minutes, and then scattered around the corners of the cage for retrieval. The surrogate is given 5 minutes to retrieve pups. **C)** Average latency score to retrieve pups for *PV-Cre* (N=11) and PVMHET (N=11) surrogates by postnatal day. A score of 1 indicates no retrieval, and lower latency scores indicate a more expedient, successful retrieval. PVMHETs perform significantly worse than *PV-Cre* littermates across postnatal days. A Two-Way ANOVA revealed a significant main effect for postnatal day ($p < 0.0001$) and genotype ($p < 0.0001$), but no significant interaction ($p = 0.5902$). Sidak's post hoc test revealed a significant difference between *PV-Cre* and PVMHET animals for P0 ($p = 0.0019$), P2 ($p = 0.0019$), P3 ($p = 0.0195$), and P5 ($p = 0.0344$). Comparisons on P1 ($p = 0.0537$) and P4 ($p = 0.0860$) did not reach statistical significance.

2.2 Evidence of ACtx PV Plasticity in Wild Type, but not PVMHET, Surrogates in Response to Pup USVs

Our first goal was to monitor the ACtx PV population during free behavior as surrogates engaged in pup retrieval. To accomplish this, we used fiber photometry and *Cre*-dependent GCaMP7s to record PV activity in the left ACtx, given the left hemisphere's well documented sensitivity in recognizing USVs (Ehret 1987; Stiebler et al. 1997; Geissler and Ehret 2004; Marlin et al. 2015). We first implemented our fiber photometry methodology in a headfixed configuration with passive playback of pup USVs, which has proven to be advantageous on multiple fronts. First, it has allowed us to recapitulate previous experimental results that were acquired using single cell loose patch electrophysiology – we can now confirm these results at a population level using an independent technical approach (Lau et al. 2020). Additionally, we used the same surrogates for headfixed and freely behaving studies, which were run in parallel. This experimental design has given us the power to compare ACtx PV network activity across these two contexts, and assess how modulation of ACtx PV responses to USVs upon maternal experience relates to ACtx PV activity during retrieval behavior.

In the headfixed context, we used fiber photometry to monitor bulk PV activity while presenting surrogates a stimulus set comprised of 8 different pup USVs that were recorded in the lab from pups aged postnatal day (P) P0 to P5. We took advantage of the fiber photometry configuration to monitor responses across time as surrogates accrued experience with pups, recording headfixed USV responses at both a naive timepoint prior to pup exposure, and every day from pup P0 – P5. Like previous electrophysiological studies demonstrating that surrogacy inhibits USV-evoked responses in individual ACtx PV neurons, our results show a similar

trend where the onset of maternal experience dampens the overall ACtx PV response magnitude to pup USVs in wild type surrogates (Figure 2.2) (Lau et al. 2020; Rupert et al. 2023). This ACtx PV plasticity is maternal experience-dependent, as females that were not co-housed with a dam and her pups do not exhibit a dampening in response strength over consecutive days of USV presentations (Figure 2.2). Moreover, unlike their wild type (PV-*Cre*) littermates, PVMHET surrogates did not exhibit any evidence of this ACtx PV plasticity - USV-evoked response strength remained consistent across postnatal days in this group (Figure 2.2). Taken together, these results are an example of maternal experience-induced plasticity in the ACtx PV population that is dysregulated in PVMHETs.

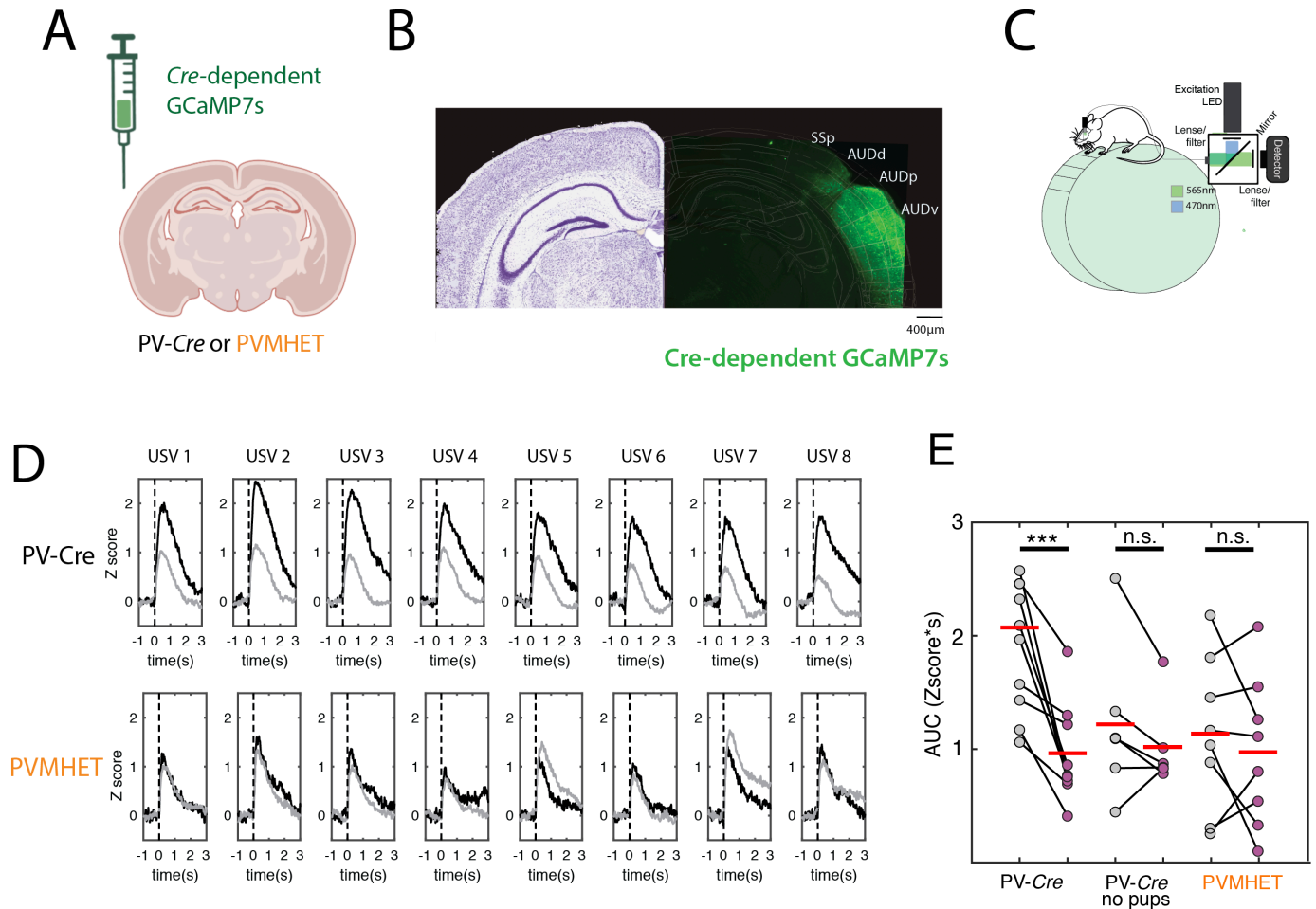


Figure 2.2: Changes in ACtx PV responses to USVs depend upon maternal experience and functional MeCP2. **A)** Viral strategy for fiber photometry to monitor the ACtx PV population. **B)** Representative example of histological confirmation of GCaMP7s expression in ACtx with the Allen Brain Atlas for reference. **C)** Headfixed fiber photometry set up for passive playback of auditory stimuli. **D)** Representative traces from a PV-Cre and PVMHET surrogate (top row and bottom row, respectively) showing responses to the 8 different pup USVs that comprised an auditory stimulus set played back to surrogates every day from a naive time point (prior to the onset of maternal experience) though P5. Each column is the average response to one of the USVs in the stimulus set (each USV was repeated in the set 20 times per session). The black traces indicate the average response taken on the naive timepoint. The grey traces indicate the average response taken at experienced timepoints (averaged P3-P5). **E)** Scatter plot of mean naive and experienced ACtx PV responses to all USVs for all mice in each condition. Grey dots indicate the average naive and purple dots indicate the average experienced values. Each dot-dot pair represents one animal. Responses were quantified as the AUC of the Z-scored fluorescence trace during the first 2 seconds after the USV stimulus onset. PV-Cre mice showed a consistent and significant decrease in response strength to USVs between naive and experienced timepoints (N=9; paired t-test, *** $p < 0.001$). No significant differences between the naive and experienced timepoints were found for PV-Cre animals that were not exposed to pups, but were imaged on the same schedule as surrogate littermates (N=5; paired t-test, $p = 0.14$), or for PVMHET surrogates (N=8; paired t-test, $p = 0.62$). Figure modified from Rupert, Pagliaro, et al., 2023.

2.3 Low Frequency ACtx PV Fluctuations are Absent in PVMHET Surrogates

We now turn to the first major objective of the current study – to uncover what the ACtx PV network is doing *during* maternal pup retrieval and how this may differ in PVMHETs that fail to learn the behavior. To address this question, we used the same surrogates that were used for the previous headfixed studies, and subjected them to a standard retrieval behavior assay every day from P0 – P5 immediately following the headfixed USV presentation sessions (Figure 2.3). In a cursory glance, we observed a stark difference between the ACtx PV activity of PVMHET surrogates and their wild type counterparts. In wild type surrogates, the ACtx PV activity was highly dynamic throughout the entire retrieval trial, with several clear peaks and troughs in the signal. In contrast, the ACtx PV activity of the PVMHET surrogates was noticeably stagnant and static, and did not exhibit the same dynamic quality as that of the wild type (Figure 2.3). In order to quantify this obvious qualitative discrepancy, we implemented a power spectral density analysis to compare low frequency signal content between genotypes. The observed fluctuations in the wild type ACtx PV signal were occurring on a timescale spanning multiple seconds; therefore, we computed the power below 0.5 Hz represented as a fraction of the total signal power (capped at 20 Hz). As expected, this value was significantly higher in wild type surrogates as compared to PVMHETs during the retrieval sessions (Figure 2.3). Importantly, we know that the overall lack of signal dynamism in the PVMHETs is not a reflection of poor signal in these animals – the use of the same surrogates for the headfixed experiments has allowed us to confirm both signal integrity and auditory responsivity in these animals (Figure 2.2). Taken together, these data demonstrate that ACtx PV activity is highly

dynamic during retrieval sessions in wild type surrogates, but ACtx PV activity in PVMHETs grossly lacks these low frequency fluctuations.

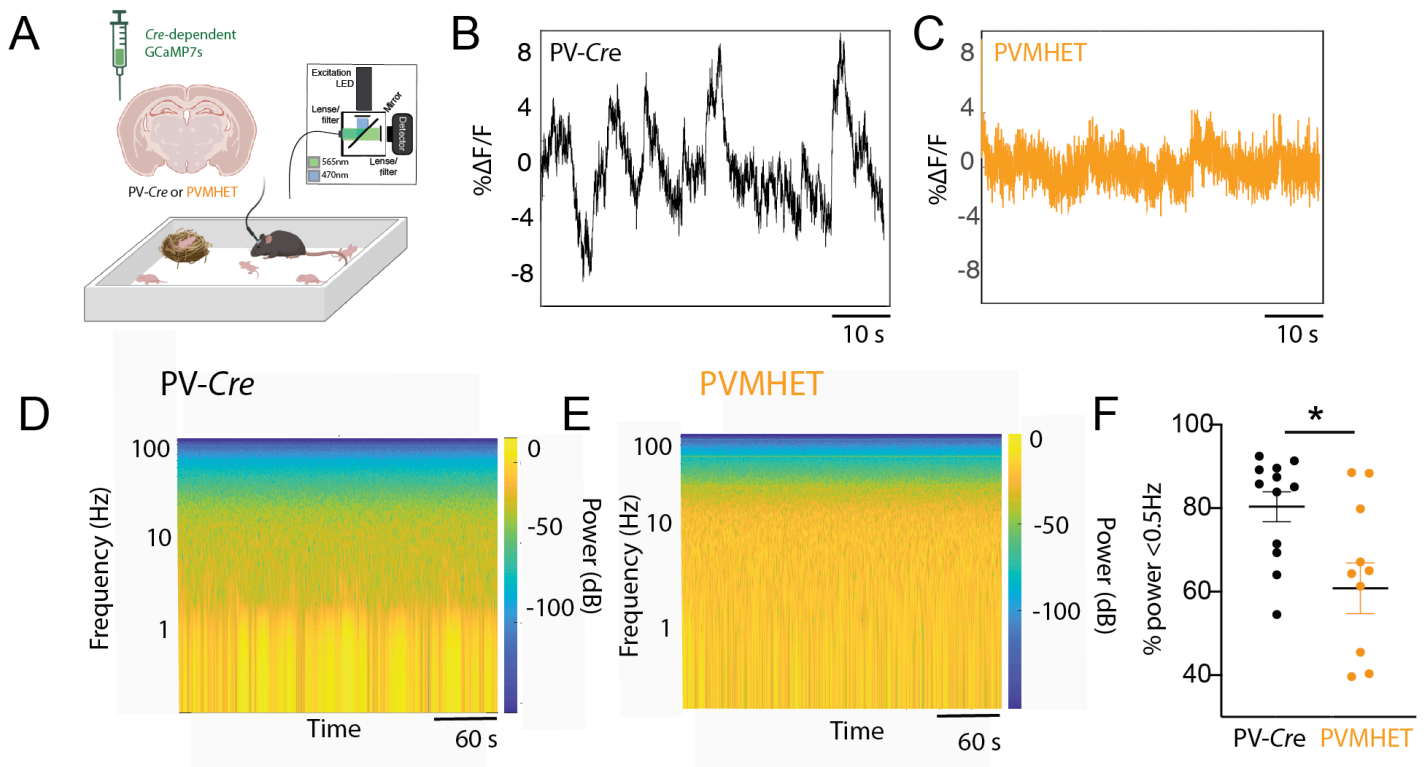


Figure 2.3: PVMHET surrogates lack low frequency ACTx PV fluctuations. **A)** Viral strategy and freely behaving fiber photometry set up for recording from the ACTx PV population in PV-Cre (WT) and PVMHET surrogates. **B)** Representative ACTx PV activity during a retrieval behavior assay in a PV-Cre surrogate. **C)** Representative ACTx PV activity during a retrieval behavior assay in a PVMHET surrogate. **D)** Representative power spectra of the ACTx PV fluorescence signal over the course of a retrieval session for a PV-Cre (**D**) and PVMHET (**E**) surrogate. Notice the much stronger contribution of lower frequency signal components in the PV-Cre power spectrum compared to the PVMHET power spectrum. **F)** Quantification of power spectral density analysis. We computed the ACTx PV signal power below 0.5Hz as a fraction of the total signal power (0-20Hz). This quantity was significantly higher in PV-Cre (black, N=12 mice) than in PVMHET (orange, N=10 mice) surrogates (Mann-Whitney U test, $p=0.0156$). Each dot represents the average value for an individual animal across all recording sessions.

At this time, it is critical to note that we have been slightly oversimplifying the complexity of PVMHET retrieval behavior for the sake of clarity. While, on average, PVMHET surrogates perform significantly worse than wild type littermates, there is a great deal of variability across animals when it comes to retrieval behavior performance. Namely, PVMHETs (and MeCP2^{hets} as similarly seen in Krishnan et al., 2016) exhibit a bimodal distribution of retrieval performance – some PVMHETs learn the behavior relatively well over postnatal days, while others consistently fail to retrieve pups (Figure 2.4) (Krishnan et al. 2017). Given this behavioral spread, we were interested to see if variability amongst low frequency ACtx PV fluctuation power in PVMHETs was related to retrieval success, hypothesizing that the PVMHETs that learned to successfully retrieve would exhibit more pronounced low frequency fluctuations. Looking across all experimental subjects from the freely behaving fiber photometry study, there is a correlative relationship between retrieval performance and low frequency signal power that approaches significance (Pearson's $R=0.4122$, $p=0.0507$; Figure 2.4).

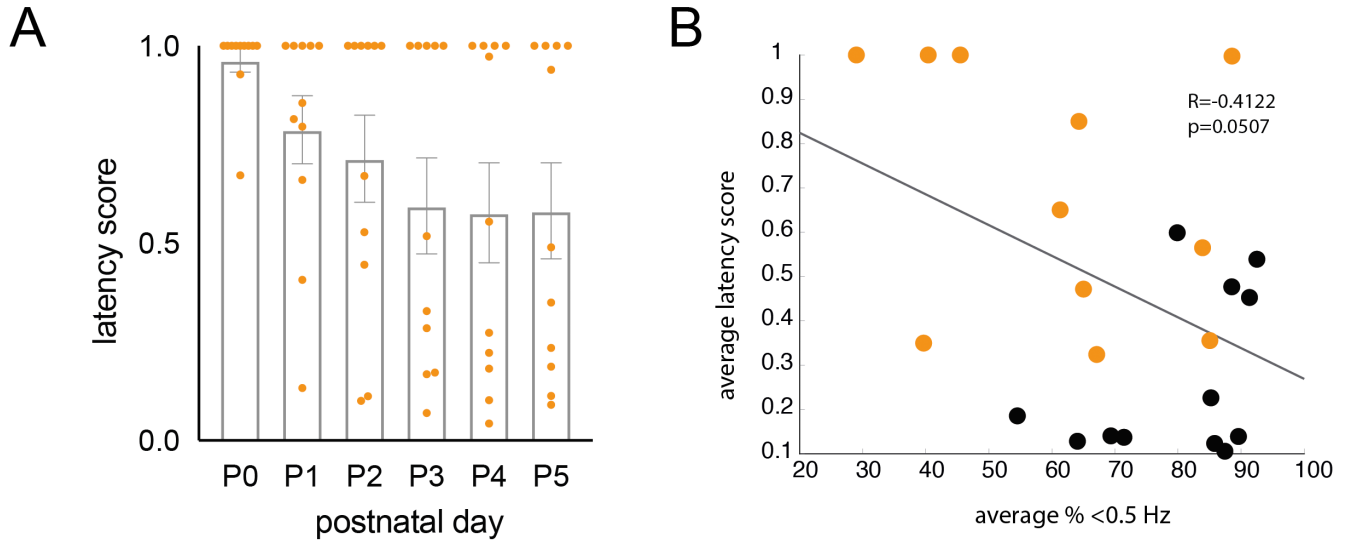


Figure 2.4: Pup retrieval performance correlation with ACtx PV low frequency fluctuations. **A)** Latency scores for individual PVMHET surrogates across days. Bars represent group mean +/- SEM, orange dots are values for individual animals. Note that there is a near bimodal distribution in performance – about half of the group fails to retrieve pups across postnatal days (latency score =1), and the other half performs the behavior with varying degrees of success. **B)** Correlation between the average latency score across postnatal days and the average percentage of ACtx PV signal power under 0.5Hz across all recording sessions. Each dot represents one animal. Black dots are PV-*Cre* surrogates, orange dots are PVMHET surrogates. Pearson’s correlation $R = 0.4122$, $p=0.0507$.

2.4 ACtx PV Activity Reflects Sensory and Behavioral Events in Wild Type, but not PVMHET, Surrogates

Given that PVMHET surrogates fail to retrieve pups, the low frequency ACtx PV fluctuations seen in wild type, but not PVMHET, surrogates may be meaningful and integral to the successful execution of the pup retrieval behavior. Therefore, the next logical question pertains to the functional role of these fluctuations. In order to gain insight into what these fluctuations may reflect, we began by aligning ACtx PV activity to different documented events that comprise the retrieval trial. Because we are looking at activity from ACtx, a sensory cortex, we first aligned the ACtx PV traces to pup USVs that were produced during the retrieval session. Perhaps unsurprisingly, there was a robust and reliable auditory stimulus-evoked response to these pup USVs in wild type surrogates (Figure 2.5). However, we noticed that pup USVs accounted for a very small proportion of the larger fluctuations that occurred throughout the entirety of the retrieval session. To better understand what may be driving the majority of the fluctuations, we constructed behavioral ethograms for each retrieval session, and aligned the ACtx PV activity to various behavioral events with significance to retrieval (see Table 5.2 for a complete list of scored behaviors). Notably, there was a robust response to pup contact – the moment that a surrogate lifts the pup off of the ground to retrieve it back to the nest (Figure 2.5), which occurred independently of overlap with pup USVs (Figure 2.6). Furthermore, large ACtx PV responses were also seen when a small door was removed to reveal a pup during ‘single pup retrieval’ trials (Figure 2.5). We conducted these ‘single pup retrieval’ trials immediately following the standard retrieval assay in order to investigate USV-evoked retrieval of individual pups – in the standard retrieval assay it is unclear which pups are producing USVs at a given moment and how that may influence the surrogate’s behavior.

In these ‘single pup retrieval’ trials, the lone pup is originally hidden behind a door that can be removed by the experimenter at any time after the start of the trial. The use of the door was originally included so as to prevent the surrogate from immediately rushing to retrieve the pup on later postnatal days when they became quite proficient in the behavior.

Unsurprisingly given the overall lack of fluctuations in PVMHET activity, there were no significant USV-evoked nor pup contact-evoked responses in PVMHET surrogates during the retrieval sessions (Figure 2.5). However, we confirmed that we are able to detect event evoked responses in PVMHETs in the freely moving condition – PVMHETs exhibited strong auditory responses to the USV stimulus set not only in a headfixed, but also in a freely moving context, and across a range of presentation volumes (Figure 2.7). Taken together, these results suggest that ACtx PV activity reflects not only sensory information, but also behavioral events in wild type surrogates.

2.5 ACtx PV Activity Does Not Regulate Retrieval on a Moment-to-Moment Basis

Because of the non-sensory associated peaks in the ACtx PV activity during retrieval sessions, we trained a linear encoding model to elucidate the unique sensory and behavioral contributions to the ACtx PV signal. In doing so, we tested the hypothesis that ACtx PV activity is dynamically regulating retrieval behavior on a moment-to-moment basis during a retrieval session, fulfilling a role far beyond basic sensory processing. Despite the inclusion of USV occurrences, various behavioral events (see Table 5.2 for complete list), and continuous variables such as the animal’s instantaneous velocity, the linear encoding model failed to

adequately explain the fluctuations in the ACtx PV signal (Figure 2.8). One explanation for the model's failure would be the exclusion of relevant covariates – a valid possibility given both the complexity of the behavior, and the existence of latent variables such as affect or internal state that we could not incorporate into the model as naive observers. An alternative possibility is that our hypothesis was incorrect and ACtx PV activity is not regulating retrieval behavior on a moment-to-moment basis.

In order to distinguish between these two possibilities, we needed to determine if ACtx PV activity is acutely necessary for retrieval behavior to be executed. If ACtx PV activity regulates retrieval performance on a moment-to-moment basis, then ACtx PV activity during retrieval would be required for its successful execution. To test this idea, we silenced ACtx PV activity in surrogates during daily pup retrieval assays. We took a chemogenetic approach, using a Pharmacologically Selective Actuator Module (PSAM)/Pharmacologically Selective Effector Molecule (PSEM) system to inactivate ACtx PV neurons during retrieval behavior upon PSEM delivery via IP injection. To our surprise, ACtx PV inactivation in wild type surrogates did not impair retrieval performance (Figure 2.9). We confirmed the efficacy of ACtx PV silencing in a separate cohort of animals that were expressing both the PSAM construct and GCaMP7s in the left ACtx PV population. We used fiber photometry to record spontaneous ACtx PV activity before and after an IP injection of the PSEM agonist, which showed a dramatic reduction in ACtx PV activity following the agonist administration (Figure 2.9). Taken together, these results suggest that acute ACtx PV activity does not regulate maternal retrieval behavior on a moment-to-moment basis.

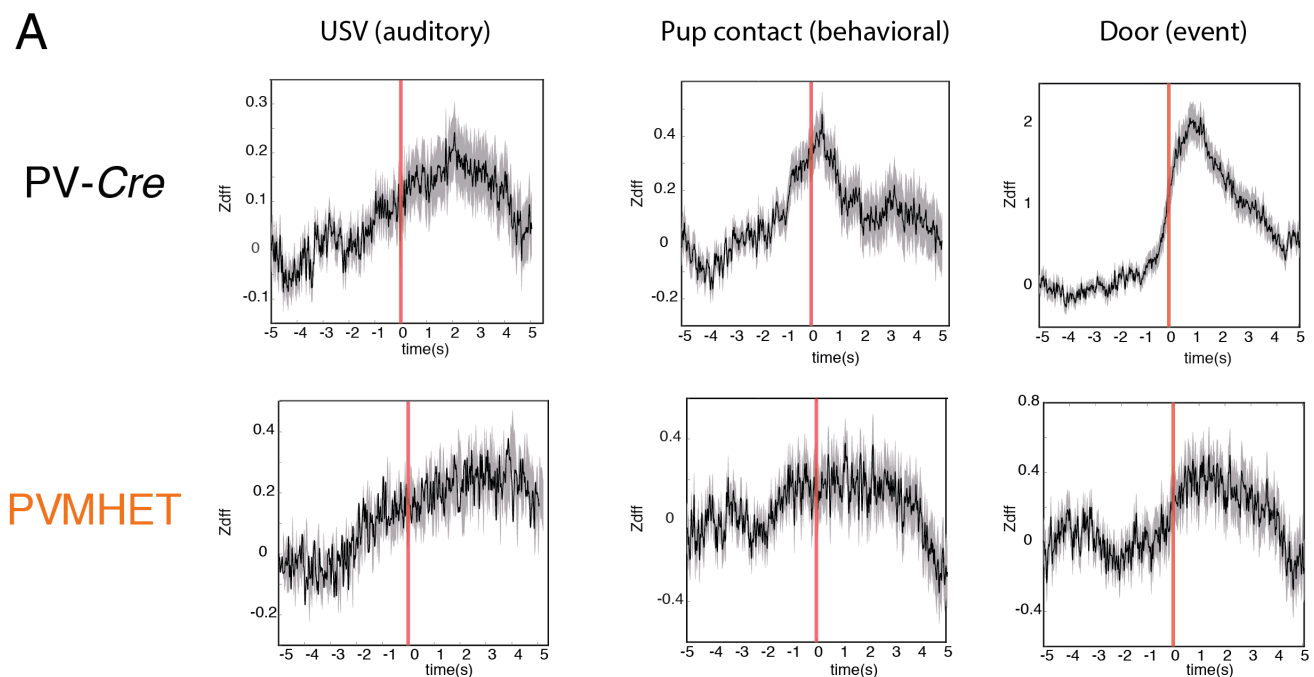


Figure 2.5: ACtx PV activity reflects sensory and behavioral events in *PV-Cre*, but not *PVMHET*, surrogates. A) Average baseline subtracted Z-scored deltaF/F (Zdff) ACtx PV activity aligned to various events occurring during retrieval sessions. Grey shading indicates SEM. Responses are averaged across all sessions from all *PV-Cre* (top row, N=12) and *PVMHET* (bottom row, N=10) surrogates. ACtx PV activity is aligned to USVs (left), the moment a surrogate contacts a pup to retrieve it back to the nest (center), and the moment a door is removed to reveal a single pup for retrieval during separate ‘single pup retrieval trials’ conducted after the standard retrieval assay. The event occurrence is denoted by the red vertical line at time 0.

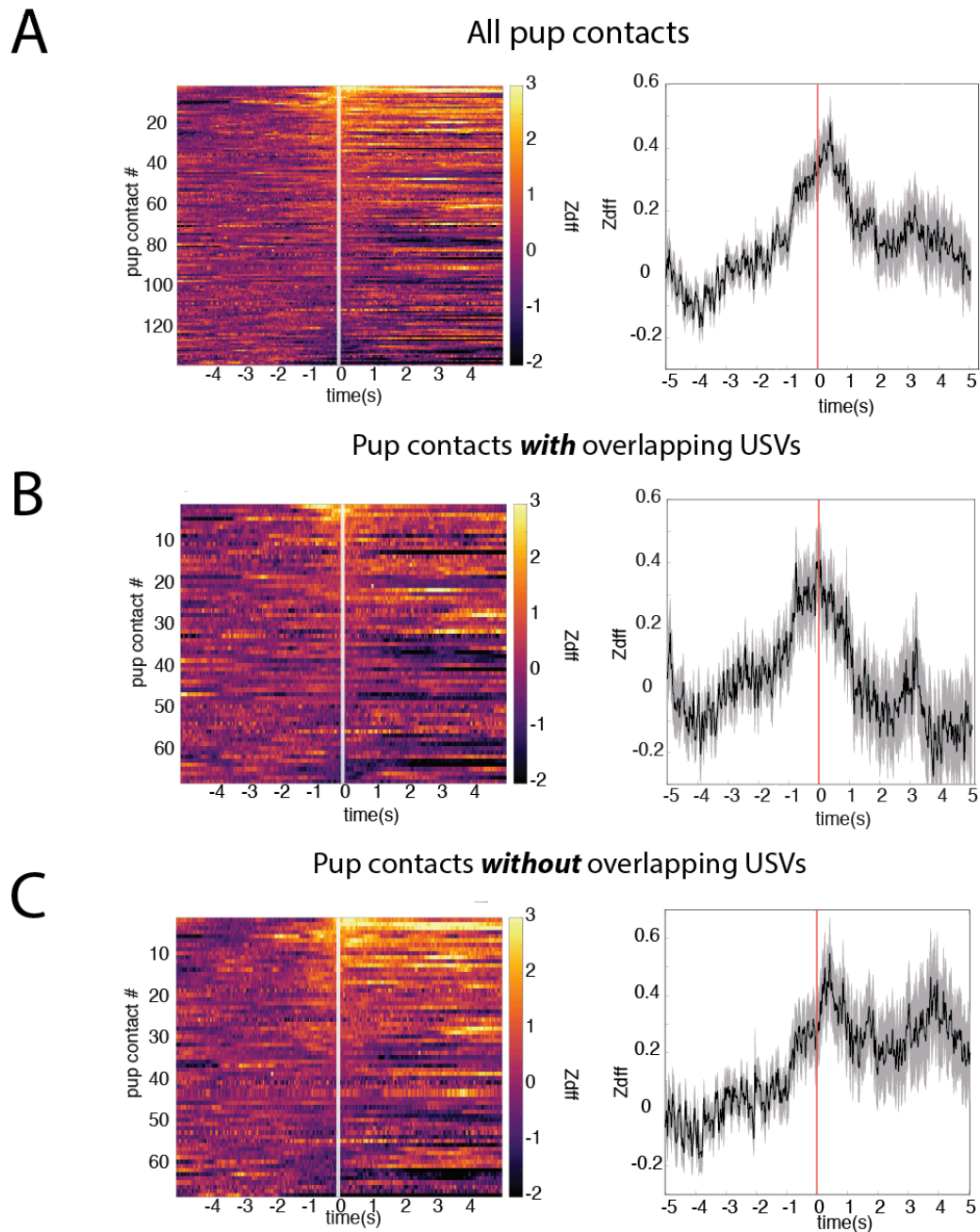
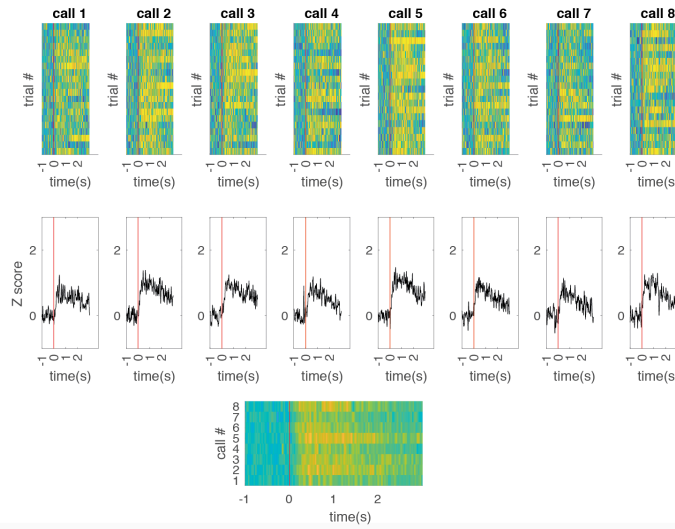

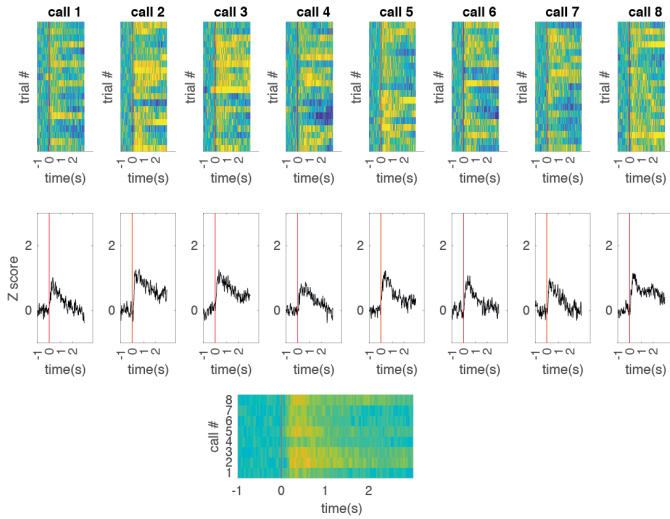


Figure 2.6: ACTx PV responses to behavioral events occur independently of auditory stimuli. **A)** (Left) Heatmap of baseline subtracted, Z-scored $\Delta F/F$ (Zdff) ACTx PV activity surrounding all pup contacts across PV-Cre surrogates. Each row in the heatmap is a unique pup contact event, aligned to the moment the pup is lifted off of the ground to be retrieved to the nest (time=0, white vertical line). Rows are sorted with the most excitatory event response at the top. (Right) Average (\pm SEM in grey) baseline subtracted ACTx PV activity aligned to pup contact (time=0, red vertical line). **B)** Same as in (A), but only for pup contacts that occurred at the same time as a pup USV during the retrieval session. **C)** Same as in (A), but only for pup contacts that occurred when there were no pup USVs being produced at the same time during the retrieval session. A pup contact was considered to overlap with a pup USV if a pup USV occurred within 2 seconds of the pup contact event.

A Headfixed USV playback



B Freely moving USV playback 



C Freely moving USV playback   

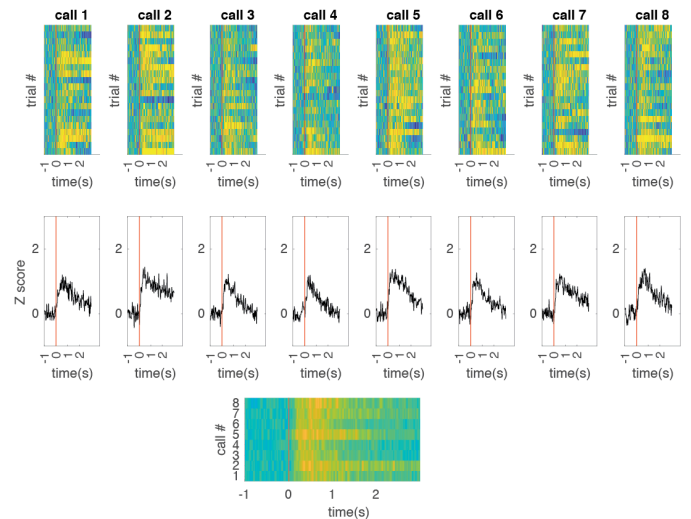


Figure 2.7: PVMHET surrogate responses to USV playback in a freely moving context. Comparison of a representative PVMHET surrogate’s ACtx PV responses to a USV stimulus set taken on the same day in headfixed (A) and freely moving (B) and (C) conditions. To determine whether playback volume had an effect on USV-evoked responses, the stimulus set was presented at either 45 dB (B) or 70 dB (C) in the freely moving condition. For reference, the headfixed playback occurred at 70 dB (A). The top row of heatmaps for each panel reflects the ACtx PV response to each of the 8 USV stimuli that comprise the stimulus set. Each USV was presented 20 times in a pseudorandom order, and each row of the heatmap reflects an individual presentation occurrence. The traces in each panel reflect the average USV-evoked response for each of the 8 USV stimuli that comprise the stimulus set. The bottom heatmap in each panel reflects the average response to each USV, where each row is a different USV in the stimulus set.

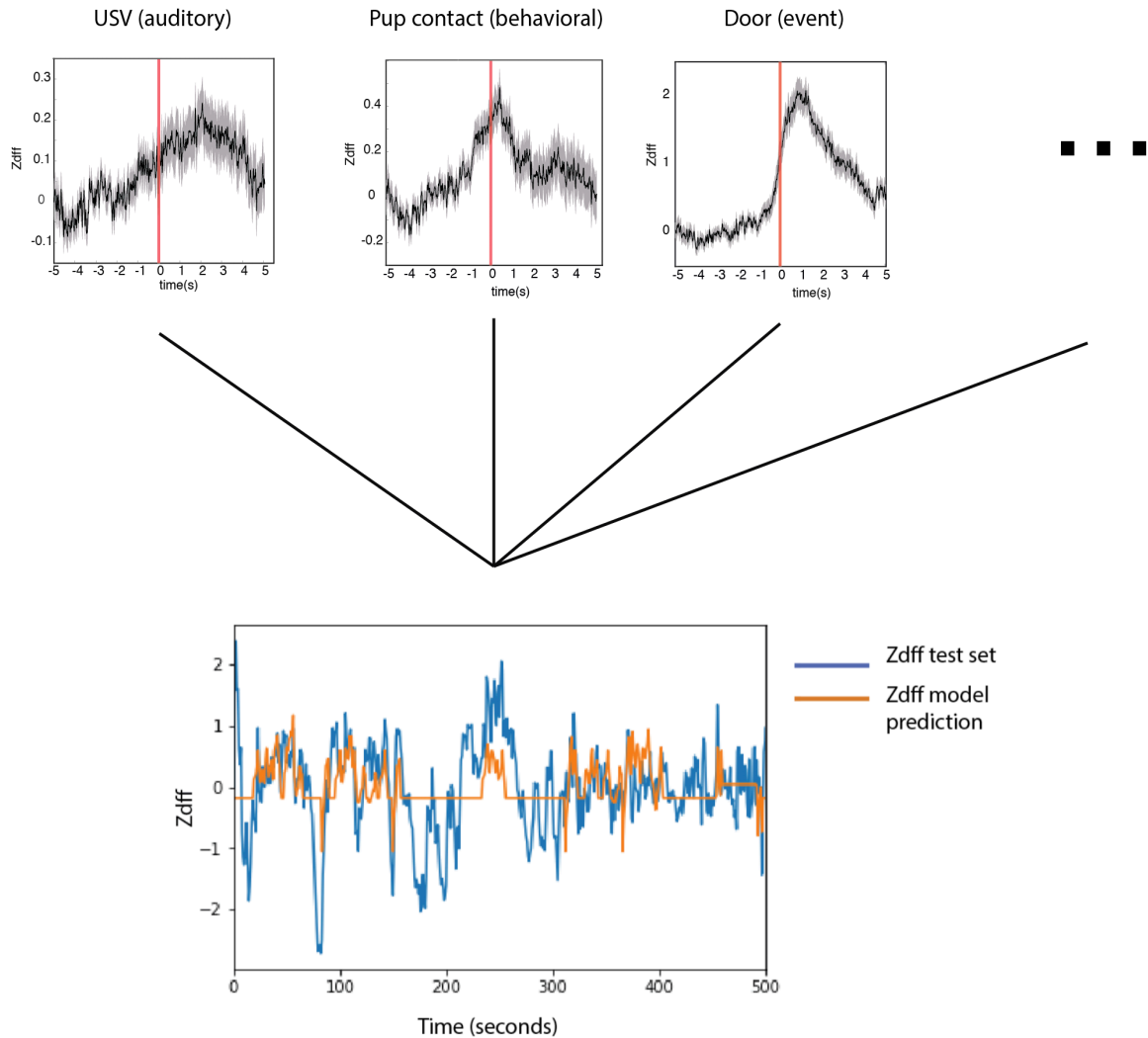


Figure 2.8: Sensory and behavioral events are insufficient covariates for a robust linear encoding model. Given the sensory and behavioral events reflected in wild type ACtx PV activity, we trained a linear encoding model in an attempt to elucidate the unique sensory and behavioral contributors to the overall signal. A complete list of covariates used to train the model is shown in Table 5.2. Separate models were trained for each mouse using all available sessions from that animal. The bottom graph illustrates the model results for one mouse. Time is not continuous, but rather reflects data concatenated from individual sessions. The blue trace is the ground truth ACtx PV activity recorded during freely behaving fiber photometry sessions, and the orange is the linear encoding model’s prediction of the ACtx PV activity.

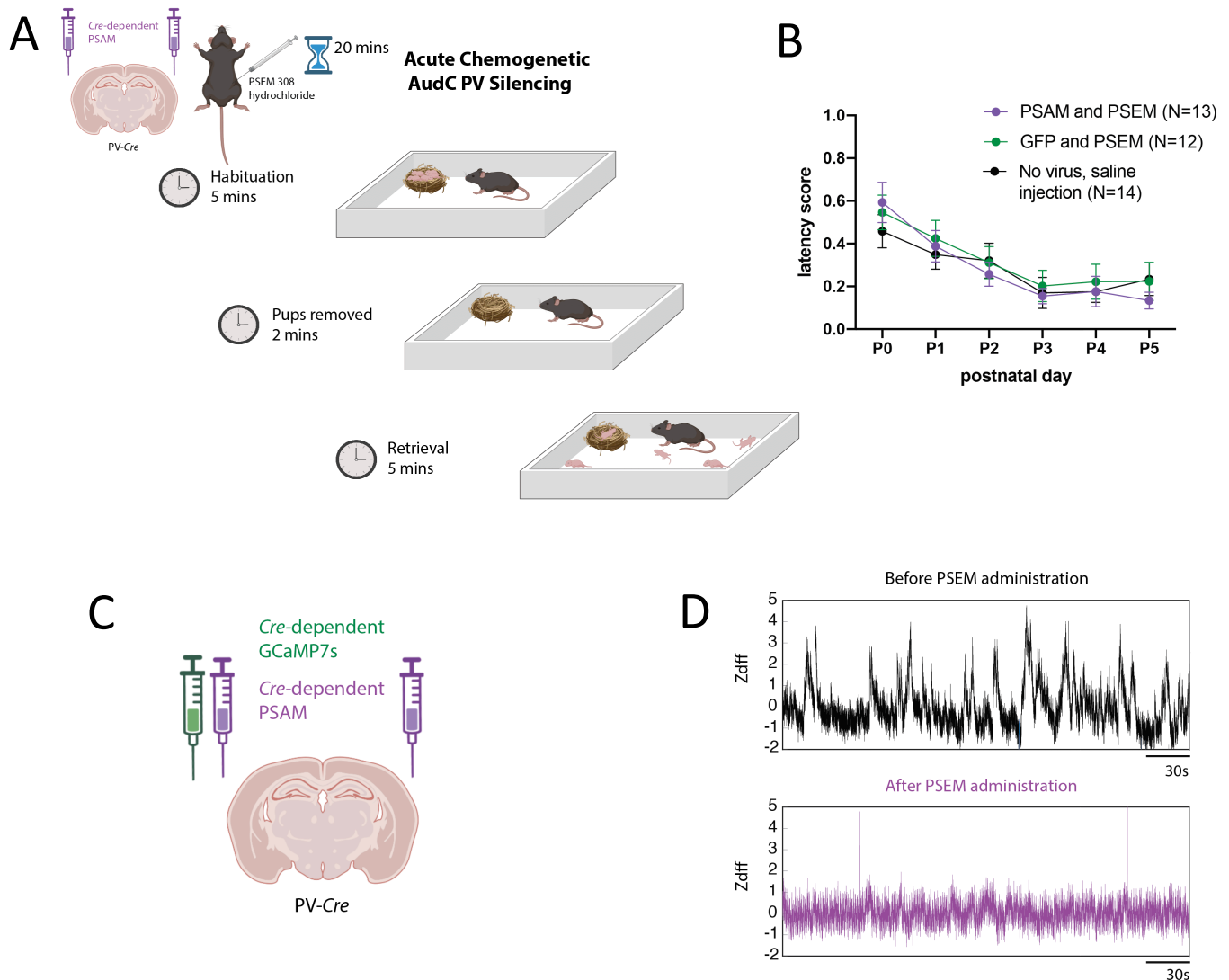


Figure 2.9: ACtx PV inhibition does not impair retrieval. **A)** Acute chemogenetic silencing paradigm. A Cre-dependent inhibitory PSAM receptor domain was delivered bilaterally to the ACtx of PV-Cre females via AAV. PV-Cre females were given maternal experience in the form of surrogacy. Every day from P0 – P5, PSEM 308 hydrochloride was delivered via IP injection 20 minutes prior to the start of a retrieval behavior assay. **B)** Average latency scores from retrieval behavior assays across postnatal days. N= 13 PSAM/PSEM injection surrogates (purple), N = 12 GFP/PSEM injection surrogates (green), N= 14 saline injected controls for comparison (black). There was no effect of ACtx PV inhibition on retrieval performance (Kruskal-Wallis test, $p=0.7761$). **C)** Viral strategy to confirm ACtx PV silencing via PSAM/PSEM mediated inhibition. GCaMP7s was also expressed in the left hemisphere ACtx PV population of surrogates expressing the PSAM receptor construct bilaterally in the ACtx PV population. **D)** ACtx PV activity before and after PSEM agonist administration to induce ACtx PV inhibition. ACtx PV activity was monitored with fiber photometry for 5 minutes as the animal moved freely about the cage (black trace, top). PSEM (3mg/kg) was then administered via IP injection. 20 minutes later, ACtx PV activity was monitored with fiber photometry for 5 minutes as the animal moved freely about the cage (purple trace, bottom).

2.6 Discussion

2.6.1 Technical Considerations for Fiber Photometry Studies

The primary goal of this chapter was to monitor ACtx PV activity during retrieval behavior, and compare activity patterns between wild type and PVMHET surrogates. In doing so, we uncovered a stark difference between the ACtx PV activity of wild types and their PVMHET counterparts. In wild type surrogates, the ACtx PV activity was highly dynamic throughout the entire retrieval trial, with several clear peaks and troughs in the signal. In stark contrast, the ACtx PV activity of the PVMHET surrogates was noticeably stagnant and static. We were initially concerned that the lack of fluctuations indicated poor signal quality disproportionately affecting the PVMHET group of surrogates. However, not only were we able to histologically confirm GCaMP7s expression in these animals (Figure 2.2), but we were also able to cross validate signal integrity from the headfixed experiments conducted in the same mice. Indeed, every postnatal day immediately prior to freely behaving retrieval sessions, the same surrogates were subject to headfixed USV playback experiments and displayed robust USV-evoked responses (Figure 2.2). This experimental design afforded a powerful cross-context comparison, and gave us confidence in the biological significance of the stagnant ACtx PV activity when PVMHET surrogates were placed in a freely moving environment. In addition, we confirmed that the implementation of a movement correction algorithm for freely moving recording sessions (that was not necessary for the headfixed experiments) was not eliminating stimulus evoked responses by broadcasting the same headfixed USV stimulus set to PVMHETs freely behaving in the home cage. Furthermore, we presented this stimulus set over a range of volumes to ensure that pup USVs occurring during retrieval were not eliciting

a response because they were too quiet (Figure 2.7). However, given their primary role as distress cries to attract caregiving attention from afar, it is highly unlikely that such vocalizations would be sufficiently quiet for this to be a major concern.

As with all methods, fiber photometry is not without its limitations. While our headfixed USV-evoked response results follow the same trends as previously reported single cell electrophysiological data, our selection of fiber photometry methodology restricts our interpretation to the level of population activity (Lau et al. 2020). However, given their sparse distribution and strong reciprocal connectivity, there is no strong evidence pointing towards significant heterogeneity amongst ACtx PV interneurons (Galarreta and Hestrin 1999; Rudy et al. 2011; Tamamaki et al. 2003; DeFelipe 1993). Because of this, we determined that fiber photometry and a population-level view of PV activity were sufficient for our purposes. Nevertheless, future studies may wish to employ miniaturized endoscopy-based strategies for a calcium-imaging technique capable of single cell resolution. Indeed, this would be particularly interesting to directly assess ACtx PV synchrony, and network activity and connectivity changes associated with learning across the postnatal period. Recent advances in dual color miniaturized endoscopy imaging could also provide insight into ACtx PV neurons interactions with other neuronal subpopulations that comprise the ACtx microcircuit.

2.6.2 Auditory Cortex as a Higher-Order Processing Area

Given that the ACtx PV activity reflected both sensory and behavioral events, we hypothesized that this network may be dynamically regulating and guiding the retrieval behavior on a moment-to-moment basis. This was an ambitious hypothesis for several reasons. First, maternal behavior is an ethologically critical behavior, and its successful performance is

necessary for offspring survival. From an evolutionary perspective, it would be logical for there to be some degree of system redundancy distributed across the brain to safeguard its performance, so that its successful execution would not be driven by a single regional subpopulation. Indeed, we found that transient ACtx PV inactivation during retrieval did not impact wild type surrogate performance (Figure 2.9). Furthermore, pup retrieval is an incredibly complex, multisensory behavior with many diverse regions and signaling pathways implicated in its execution – the MPOA, LC, ACC, amygdala, and VTA to name a few (Fang et al. 2018; Dvorkin and Shea 2022; Corona et al. 2022; Nowlan et al. 2022; Xie et al. 2023). Therefore, it is unlikely that such a small inhibitory interneuron population would be a significant inter-regional regulator. It is more likely that the ACtx is a key node in a multifaceted network with critical projections to interconnected downstream areas. This may also explain why inter-animal variation in low frequency ACtx fluctuations is not an exceptionally strong predictor of individual retrieval performance – dysregulation in other cortical and subcortical regions implicated in retrieval behavior and their relative *MeCP2* mutational burdens likely also contribute to retrieval performance. Nevertheless, our initial hypothesis of ACtx PV-based regulation of behavior was motivated by the documented necessity of the ACtx for successful retrieval performance, the non-sensory evoked responses seen in the ACtx during retrieval, and the fact that, despite its designation as a primary sensory area, the ACtx has a history of serving as a higher-order processing area.

Given the widespread encoding capabilities of the ACtx, we have also considered the possibility that the low frequency ACtx PV fluctuations may reflect physiological processes – namely the animal’s locomotion and/or breathing. This stems from several studies showing that movement modulates ACtx activity – for instance, running has been shown to increase

spontaneous, but decrease evoked firing rates in this area (Yavorska and Wehr 2021; Schneider and Mooney 2018). However, when monitoring the instantaneous velocity of surrogates using DeepLabCut markerless position tracking, we found no significant correlation between locomotion and ACtx PV activity (Mathis et al. 2018) (Figure 2.10). We did not monitor breathing in the current experiments, but future studies may seek to explore a relationship between the low frequency ACtx PV fluctuations and inhalation patterns. Breathing is a critical input source for multisensory integration that could potentially occur in the ACtx, providing the network with information regarding pup odors. Indeed, pup odors alone can modulate ACtx neural responses to both pure tones and USV stimuli (Cohen et al. 2011).

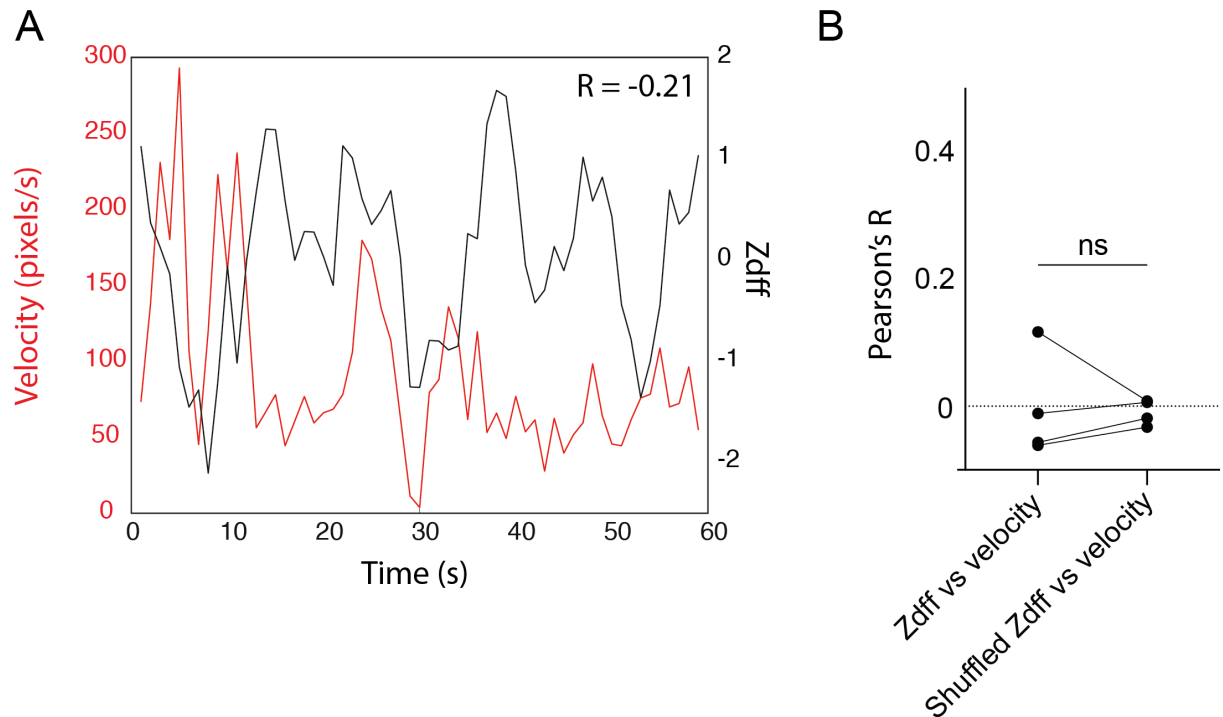


Figure 2.10: Surrogates' instantaneous velocity is not correlated with ACtx PV fluctuations. **A)** Plot of a representative *PV-Cre* surrogate's instantaneous velocity (red) and simultaneously recorded ACtx PV activity (black). Both velocity and Zdff have been down sampled into 1 second bins. Pearson's R value for the correlation between the two signals is shown in the upper right (Pearson's $R = -0.21$). **B)** Average Pearson's R value per animal for the subset of all surrogates that underwent this analysis ($N = 4$). Each dot-dot pair represents one mouse, comparing the actual Pearson's R between the signals (Zdff vs velocity), with a correlation computed with a randomized time lag in the ACtx PV signal (Shuffled Zdff vs velocity). The values for each mouse are the average values taken from all retrieval sessions. A paired t-test revealed no significant difference between the actual and shuffled correlations ($p=0.8731$).

2.6.3 Circuit Interactions for Retrieval Behavior – Within and Beyond Auditory Cortex

As previously mentioned, the ACtx does not function in isolation, but is a key node in the larger circuit-level orchestration of the complex retrieval behavior. That being said, it is unclear how generalizable our findings may be across cortical regions implicated in the behavior. We have chosen to focus on the ACtx not only because of its necessity for successful retrieval, but also because of the role for USVs in guiding the behavior, and the well documented plasticity in this region that is induced by the onset of maternal experience (Marlin et al. 2015; Krishnan et al. 2017; Ehret 2005; Sewell 1970; Liu and Schreiner 2007; Galindo-Leon et al. 2009; Lin et al. 2013; Cohen and Mizrahi 2015; Marlin et al. 2015; Lau et al. 2020; Tasaka et al. 2018; Liu et al. 2006). This has provided us with a detailed look at the PV interneuron network of the ACtx and its dysregulation in PVMHETs, but provides no insight into how PV interneuron networks in other sensory cortices may be affected by *MeCP2* mutations. Namely, the lack of low frequency fluctuations seen in PVMHETs may span cortical regions nonspecifically, or the low frequency fluctuations (and lack thereof in PVMHETs) may be a signature specific to the ACtx PV network.

Nevertheless, the lack of low frequency ACtx PV fluctuations in PVMHETs highlights an aberrant population-level activity pattern that would presumably impact both the ACtx microcircuit, and ACtx projections to downstream targets. At the microcircuit level, future studies may wish to monitor either gross excitatory network activity in the ACtx using fiber photometry in both wild type and *MeCP2*^{het} backgrounds, or other ACtx inhibitory interneuron populations. Notably, selective *MeCP2* deletion in PV cells is sufficient to disrupt retrieval behavior, but *MeCP2* deletion restricted to either vasoactive intestinal polypeptide (VIP) or

somatostatin (SST) inhibitory neurons is not (Rupert et al. 2023). This is somewhat unsurprising given the role of PV interneurons in regulating critical periods for plasticity, but also suggests that perhaps the significant dysregulation seen in the PVMHET ACtx PV population would not extend to other inhibitory subpopulations. Future studies may also seek to understand the downstream effects of impaired ACtx computations in PVMHETs by monitoring select ACtx projection outputs. One particularly interesting group may be auditory corticostriatal projection neurons given that they have previously been shown to carry auditory information to the striatum to drive an auditory frequency discrimination task (Znamenskiy and Zador 2013). Even in a headfixed context, it would be interesting to see if this projection population responds to pup USVs, if that response changes with maternal experience, and how those responses may vary in MeCP2^{hets}. Finally, future work may seek to monitor ACtx inputs as a way to gauge at what level of processing aberrations emerge in MeCP2^{hets}. Given the ubiquitous expression of MeCP2 throughout both the brain and body, it is likely that basic sensory processing in areas such as the inferior colliculus may also be impacted, which will in turn dictate what is transmitted to the ACtx, and how the ACtx goes about internal computations with that input. Furthermore, as discussed in Chapter 3, aberrations in certain neuromodulatory systems (particularly the cholinergic) may influence aberrant ACtx PV activity and may merit future study. In sum, the ACtx PV abnormalities seen in PVMHETs most likely reflect a more global dysregulation of interconnected circuitry manifesting in deficits not limited to pup retrieval. Nevertheless, this does not undermine the value of studying the ACtx PV population specifically for our investigation into basic plasticity mechanisms underlying learning, especially given the well documented role of PV interneurons in regulating critical periods.

Chapter 3: ACtx PV Fluctuations May Reflect a PV Network Configuration that Favors Plasticity

The results presented in Chapter 2, namely that acute silencing of ACtx PV activity during pup retrieval in wild type surrogates has no effect on retrieval performance, refute our initial hypothesis that ACtx PV activity dynamically regulates retrieval behavior on a moment-to-moment basis. However, the direct consequences of the lack of low frequency ACtx PV fluctuations in PVMHETs remain to be discovered. To further probe the significance of these fluctuations, we hypothesized that they were the signature of a constitutive network state in a favorable configuration to facilitate plasticity and learning. To support this hypothesis, we looked across behavioral contexts to show that the presence of such fluctuations was not restricted to pup retrieval settings. We next hypothesized that such a PV network state may reflect attention and arousal, which would favor learning. In support of this hypothesis, we showed that ACtx PV activity is closely coupled to pupil diameter – an established proxy for attention and arousal. Based on the results presented in this chapter, we propose that the low frequency ACtx PV fluctuations reflect a constitutive state of the PV network, and that this state may reflect a PV network configuration that is ready to meet heightened plasticity demands when needed.

3.1 Wild Type ACtx PV Fluctuations Occur Independently of Context

Given that acute ACtx PV fluctuations during retrieval are not necessary for the successful performance of the behavior, we hypothesized that the low frequency fluctuations seen in wild type surrogates are a signature of a PV network state. We reasoned that such a

state reflects a network configuration equipped to meet plasticity demands as they arise, thereby facilitating the successful learning of the retrieval behavior. By extension, the lack of such fluctuations in the PVMHET surrogates may reflect a PV network incapable of meeting the plasticity demands necessary for successfully learning the behavior.

A first indication that the ACtx PV fluctuations may be capturing a network state stems from the fact that they are not exclusively present during retrieval sessions. Indeed, large low frequency fluctuations are also present in different behavioral contexts – namely we recorded ACtx PV activity when the surrogate was alone in the cage or with the pups safe in the nest (Figure 3.1). Perhaps most dramatically, naive virgin females that are yet to have experience with pups also exhibit marked low frequency ACtx PV fluctuations when they are alone in a cage (Figure 3.1). These results suggest that the ACtx PV fluctuations do not reflect a retrieval specific context per se, but may be indicative of an ACtx PV network state ready to accommodate experience-dependent plasticity demands such as those induced by parturition.

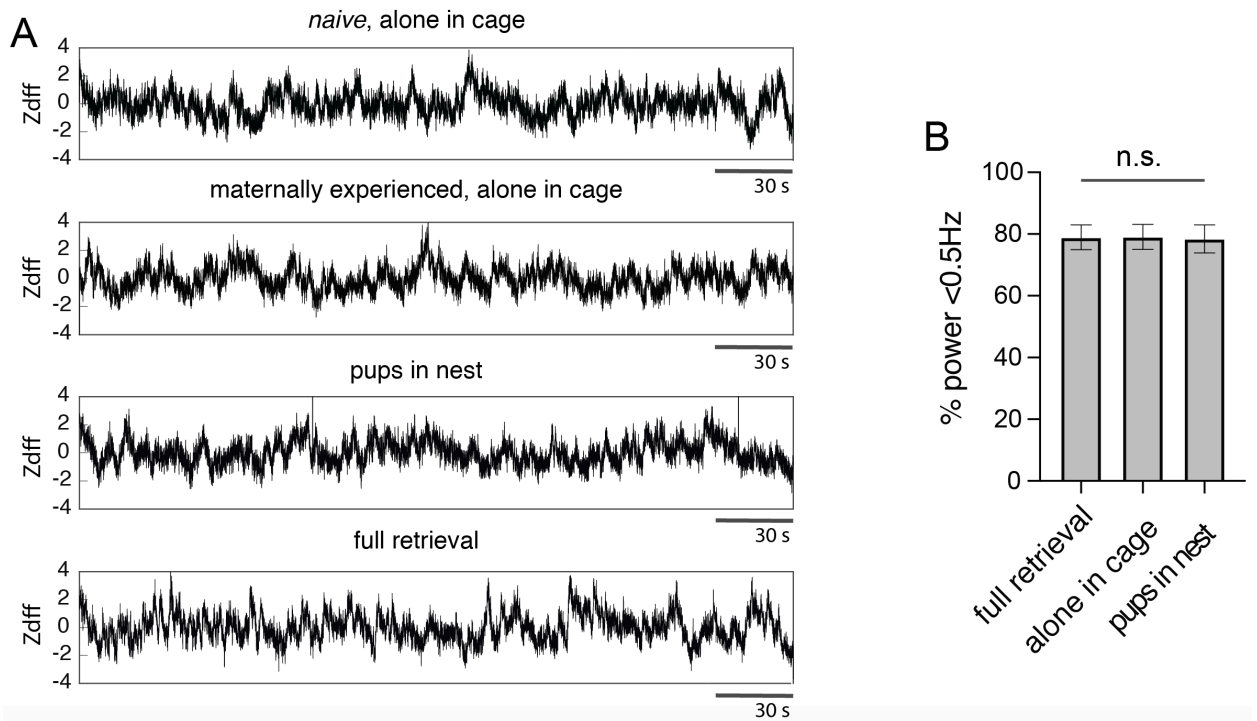


Figure 3.1: ACtx PV fluctuations occur independently of context. **A)** Representative ACtx PV traces from a PV-Cre female across various conditions. **B)** Quantification of the percentage of ACtx PV signal power below 0.5 Hz from recording sessions in various conditions. Full retrieval, 78.99 +/- 3.989%; alone in cage, 79.10 +/- 4.042%; pups in nest, 78.44 +/- 4.529% (mean +/- SEM). A One-Way ANOVA revealed no significant difference in low frequency content across the conditions ($p=0.9937$). N = 11 animals.

3.2 ACtx PV Activity and ACtx Acetylcholine Release are Highly Correlated with Pupil Diameter

There are a variety of factors that may characterize a network state that facilitates experience-dependent learning. One such factor may be the ability to support an adequate attentional capacity, which would require an appropriate level of behavioral arousal. As such, the ACtx PV fluctuations in wild type mice may reflect an attentional state, or even be actively facilitating attentional state transitions. To test the hypothesis that ACtx PV activity reflects attention and arousal, we recorded the ACtx PV population while simultaneously monitoring pupil diameter in a head fixed setting (pupil diameter is an established proxy for attention and arousal) (Bradley et al. 2008; Reimer et al. 2016, 2014; McGinley et al. 2015; Steinhauer et al. 2004; Tursky et al. 1969; Zekveld et al. 2018; Privitera et al. 2010; Lisi et al. 2015; Zhao et al. 2019; Zekveld et al. 2010; Winn et al. 2015; Poulet 2014; Vinck et al. 2015; Bala and Takahashi 2000). In doing so, we found a very tight coupling between pupil diameter and ACtx PV activity (Figure 3.2). This correlation appeared to be independent of the animal's movement – ACtx PV activity tracked with pupil size regardless of whether the mouse was actively running on the wheel or not (Figure 3.3). We next reasoned that this relationship may break down in PVMHETs, which might partially explain their inability to retrieve pups – an insufficient ability to attend to relevant stimuli (namely pup USVs) that prompt the behavior. However, to our surprise, ACtx PV activity was also correlated with pupil diameter in PVMHETs (Figure 3.2).

To further explore the possibility that an insufficient attentional capacity may contribute to the retrieval deficits seen in *MeCP2^{hets}*, we repeated the pupillometry experiments, only this time simultaneously monitoring pupil diameter while using fiber

photometry to record acetylcholine (ACh) release in the ACtx with a GRAB ACh sensor (Jing et al. 2020). We chose to monitor ACh activity given that this neuromodulator is heavily implicated in arousal, sensory processing, and cognition, and that cholinergic dysfunction has been linked to numerous neuronal degenerative diseases (Guillem et al. 2011; Goard and Dan 2009; Everitt and Robbins 1997; Schliebs and Arendt 2011). Similar to our findings with ACtx PV activity, ACh release was highly correlated with pupil diameter in wild type mice (Figure 3.4). Because cortical interneurons are a major target of basal forebrain-derived nicotinic signaling, we reasoned that altered cholinergic input onto ACtx PV neurons in MeCP2^{hets} may reflect a source of dysregulation upstream of the ACtx PV network itself that possibly contributes to the lack of low frequency ACtx PV fluctuations seen in MeCP2^{hets} (Alitto and Dan 2012; Bloem et al. 2014; Arroyo et al. 2012; Demars and Morishita 2014). However, similar to the ACtx PV fluctuations themselves, we also found that ACh release in the ACtx was significantly correlated with pupil diameter in MeCP2^{hets} (Figure 3.4). Taken together, these results suggest that the pronounced low frequency fluctuations in wild type surrogates may reflect a PV network state that is also closely tuned to behavioral arousal and attention.

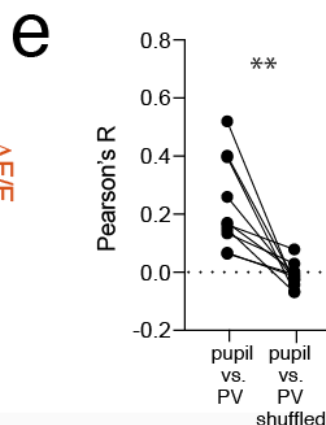
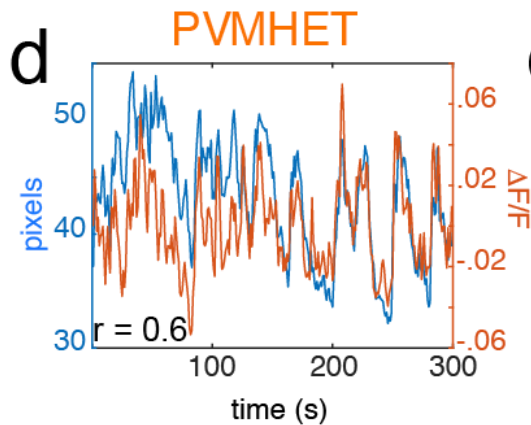
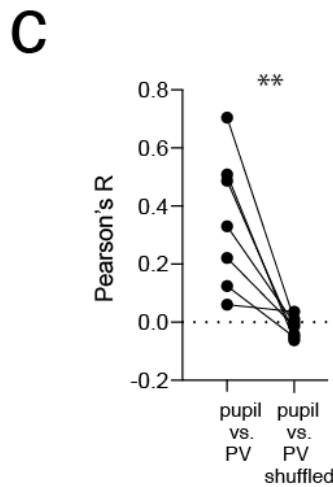
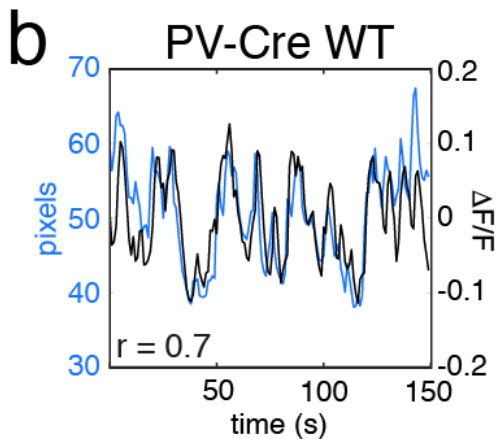
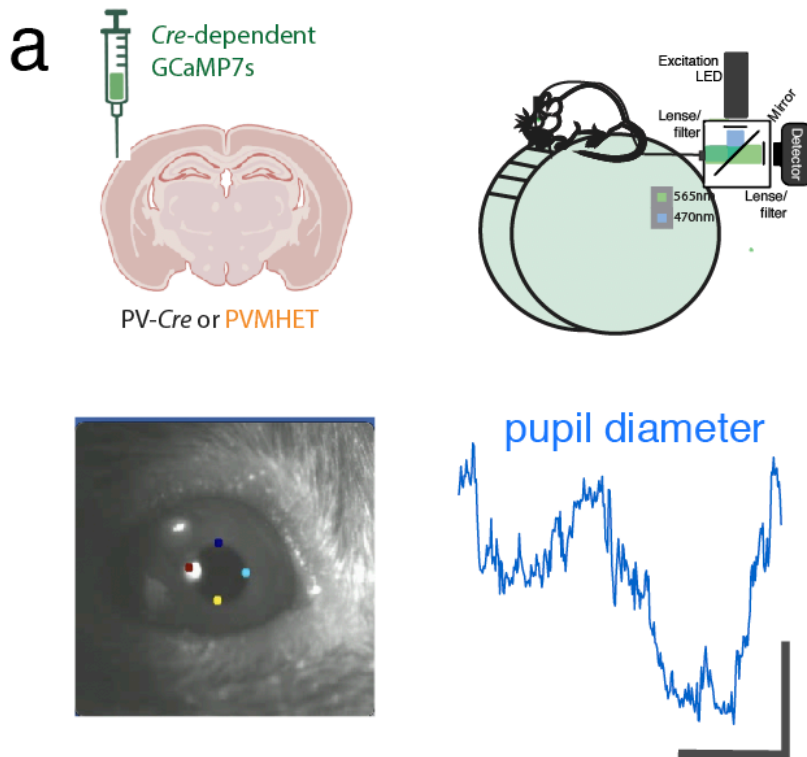


Figure 3.2: ACtx PV activity is correlated with pupil size.

A) Experimental details of simultaneous ACtx PV fiber photometry and pupillometry. Pupil size was determined using DeepLabCut machine learning software. Colored markers denote anatomical landmarks used to compute pupil diameter, fluctuations in which are shown from an example trace on the bottom right (scale bar = 20s, 10 pixels). **B)** Representative trace from simultaneous fiber photometry (black) and pupillometry (blue) recordings in a PV-Cre mouse. The R value for a Pearson correlation between the two signals is shown in the lower left. **C)** Quantification of the ACtx PV/pupil correlation in PV-Cre mice. Correlations between PV activity and pupil diameter were significantly higher than a correlation computed with a randomized time lag in the ACtx PV signal. Each pair of points is an individual animal representing the mean correlation across all recordings collected from that animal (N=7 mice, paired t-test, **p=0.0069). **D)** and **E)** show the same as **B)** and **C)**, but for PVMHET mice (N=7 mice, paired t-test, **p=0.0019).

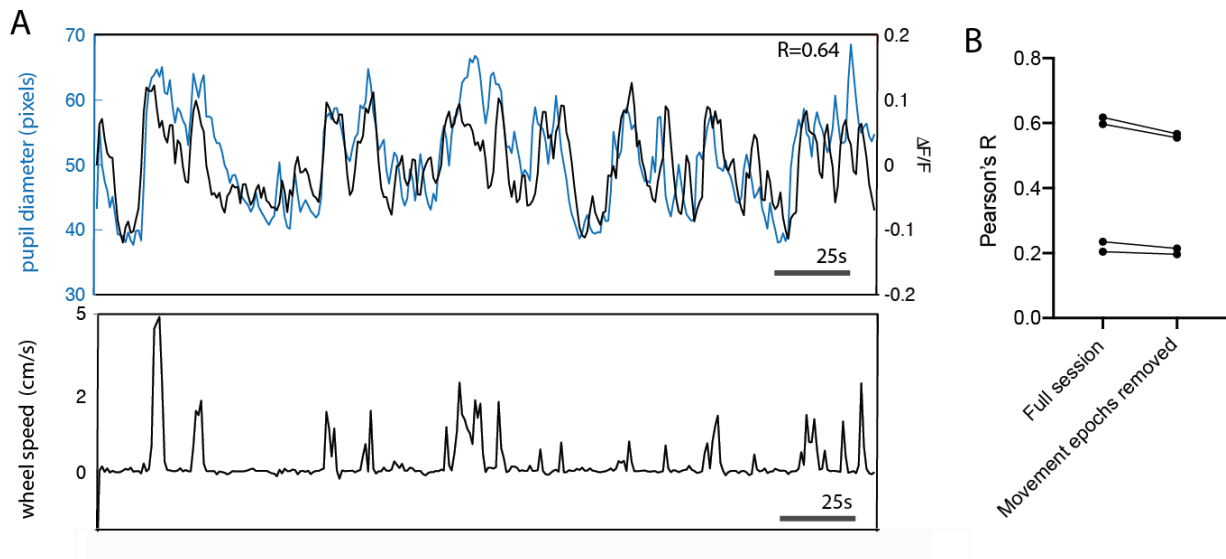


Figure 3.3: ACTx PV correlation with pupil is independent of locomotion. A) (Top) Representative trace comparing pupil diameter and ACTx PV activity. Pearson's R value for the correlation is shown in the top right corner. **(Bottom)** Simultaneously acquired wheel speed that was monitored during the same pupillometry/fiber photometry recording session as shown on top. **B)** Quantification of session correlations with and without epochs of movement removed, as determined by instantaneous wheel speed. Each dot-dot pair reflects the average Pearson's R value across all sessions for an individual animal. We performed this analysis on a subset (N=4) of all experimental animals, intentionally balancing the group with 2 individuals that had overall higher average correlation values, and 2 that had overall lower correlation values. A paired t-test revealed no significant difference between the actual and shuffled correlations (full session: mean = 0.4135, SEM = 0.1122; movement epochs removed: mean = 0.3831, SEM = 0.1028; paired t-test $p=0.0525$).

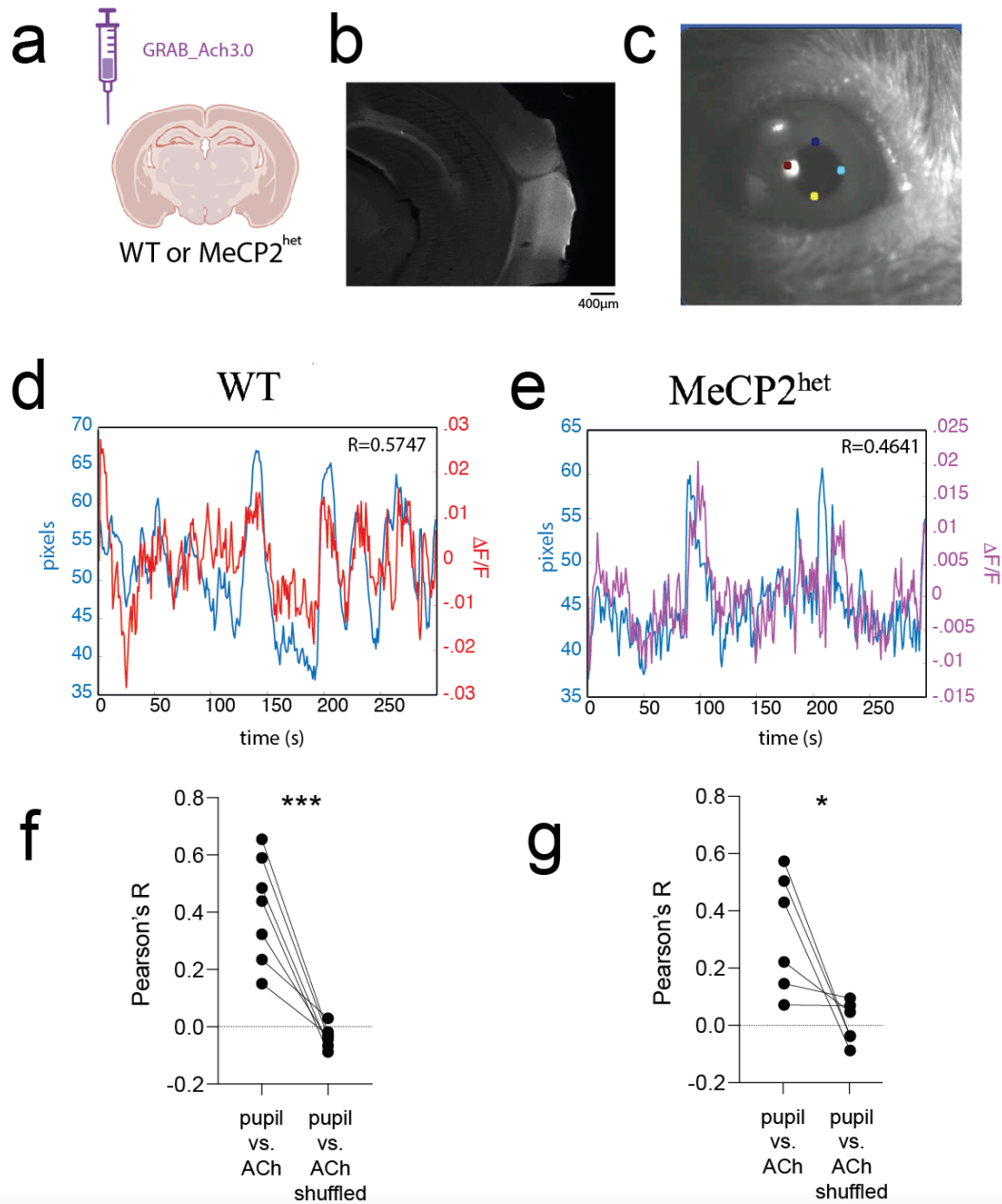


Figure 3.4: ACTx ACh release is correlated with pupil size. **A)** The GRAB_ACh3.0 sensor was delivered to the left ACTx to monitor ACh release with fiber photometry in WT (BL6) or MeCP2^{het} females. **B)** Histological confirmation of GRAB_ACh3.0 expression in left ACTx. **C)** Pupil size was determined using DeepLabCut machine learning software. Colored markers denote anatomical landmarks used to compute pupil diameter. **D)** Representative trace from simultaneous ACh (red) and pupillometry (blue) recordings in a WT mouse. The R value for a Pearson correlation between the two signals is shown in the upper right. **E)** Same as **D)**, but for a MeCP2^{het} mouse (ACh signal is purple). **F)** Quantification of the ACTx ACh/pupil correlation in WT mice. Correlations between ACh release and pupil diameter were significantly higher than correlations computed with a randomized time lag in the ACTx ACh signal. Each pair of points is an individual animal representing the mean correlation across all recordings collected from that animal (N=7 mice, paired t-test, ***p=0.0010). **G)** same as **F)** but for MeCP2^{het} mice (N=6 mice, paired t- test, *p=0.0352).

3.3 Discussion

3.3.1 What do we Mean by a PV Network State?

Here we show that the signature low frequency ACtx PV fluctuations present in wild type surrogates during retrieval sessions are *not* context dependent – similar fluctuations are evident in non-retrieval settings, and they are present prior to the onset of maternal experience. This raises the possibility that these fluctuations reflect a constitutive state of the PV network, and we propose that this state may reflect a PV network configuration that is ready to meet heightened plasticity demands when needed.

This proposition requires a definition – what do we mean by a PV network state? We are not the first to hypothesize the existence of such a state; indeed, both ‘low’ and ‘high’ PV network configurations have been described in the hippocampus. In the hippocampus, these PV network designations are tied to learning and memory, and the PV network state reconfigures from a low-PV activity to a high-PV activity state upon learning completion (Donato et al. 2013). This shift following learning is consistent with our conceptual framework – we propose that PVMHETs have a premature ‘high-PV state’ that impairs learning and is characterized by elevated ACtx PV activity at the onset of maternal experience.

Given that PV activity positively regulates PNN formation, another characteristic of our proposed ‘PV network state’ includes a PV activity-dependent PNN presence (Härtig et al. 1992; Pizzorusso et al. 2002; Dityatev et al. 2007; Reimers et al. 2007; Favuzzi et al. 2017; Devienne et al. 2021). Consistent with a ‘high PV network configuration’, elevated PV activity in PVMHETs is evident in both the sustained high ACtx PV response strength to USVs in our headfixed studies, and the corresponding increased PNN density seen in the ACtx following

parturition (Krishnan et al. 2017). However, the relationship between PNNs and low frequency ACtx PV fluctuations remains unclear. Interestingly, PNNs have been shown to lock PV neurons into patterns of high firing activity, potentially serving as additional calcium buffers in the extracellular matrix (Härtig et al. 1999; Brückner et al. 1993; Wingert and Sorg 2021). It is possible that such high firing patterns are not conducive to widespread, coordinated population activity that would present as the signature slow fluctuations in the wild type fiber photometry traces. Furthermore, the stagnant ACtx PV traces in PVMHETs could reflect an activity ‘ceiling effect’ where uncoordinated baseline population activity is so high that there is a limited range for large fluctuations to be detected. Future studies may employ electrophysiological techniques such as Neuropixels probes to gain more insight into these possibilities, as fiber photometry methods are not appropriate for this level of analysis.

While we will expand on this and other facets of our proposed PV network state in Chapter 6, we essentially suggest that a ‘plasticity favorable PV network configuration’ is marked by low ACtx PV activity, limited PNN presence, and signature low frequency ACtx PV fluctuations. A ‘high PV network state’ would therefore be characterized by elevated ACtx PV activity, heightened PNN presence, and the notable absence of low frequency ACtx fluctuations.

3.3.2 A Possible Relationship Between ACtx PV Activity and Attention

While there are a range of processes that a plasticity-favorable network state might support, one may be the facilitation of an adequate attentional capacity, which would require an appropriate level of behavioral arousal. Indeed, adequate attention is critical for successful learning, and may also improve stimulus detection of crucial pup USVs during retrieval

epochs. Furthermore, the large ACtx PV response to the door opening to reveal a pup during single pup retrieval trials may reflect a certain level of attentional engagement at the start of the trial. In support of an attentional component to the plasticity-favorable ACtx PV network state, we observed a tight coupling of both ACtx PV activity and ACh release in the ACtx with pupil diameter. While we have not established a direct relationship between ACtx PV activity and cholinergic modulation in the current experiments, it is noteworthy that both of these measures are coupled to pupil diameter (an established proxy for attention and arousal). This is particularly interesting given that ACh is heavily implicated in arousal, sensory processing, and cognition, and that cholinergic dysfunction has been linked to numerous neuronal degenerative diseases - most notably Alzheimer's Disease (Guillem et al. 2011; Goard and Dan 2009; Everitt and Robbins 1997; Schliebs and Arendt 2011). Future work may seek to more directly probe the relationship between ACh release and ACtx PV activity, and any differences in this relationship in MeCP2^{hets}. Given that cortical interneurons are a major target of basal forebrain-derived nicotinic signaling, altered cholinergic input onto ACtx PV neurons in MeCP2^{hets} may indeed reflect a source of dysregulation upstream of the ACtx PV network itself (Alitto and Dan 2012; Bloem et al. 2014; Arroyo et al. 2012; Demars and Morishita 2014). Therefore, future studies may investigate ACh receptor distribution and sensitivity on ACtx PV neurons and any differences in MeCP2^{hets}, or directly monitor basal forebrain projection neuron activity onto ACtx PV cells.

It is worth noting that we attempted to monitor ACtx ACh release during retrieval sessions using fiber photometry in a similar configuration to our freely moving fiber photometry experiments recording the ACtx PV population. However, the signal strength of the ACh GRAB sensor was very weak compared to the strong signals we have seen with

GCaMP7s. While this was not an issue in our pupillometry experiments where the animal was headfixed (thereby eliminating movement artifacts), the true ACh signal became drowned out following the application of our motion correction algorithm in the freely moving paradigm and we deemed the results uninterpretable.

3.3.3 A Correlation that Persists in PVMHETs...

We hypothesized that the correlative relationship between ACtx PV activity and pupil diameter in wild type mice would break down in PVMHETs, potentially pointing towards attentional deficits that may impair pup retrieval learning. To our surprise, we found that this relationship was actually maintained in the PVMHETs, for both ACtx PV activity and ACtx ACh release. However, with regards to the ACtx PV activity, it is critical to note that the spread of $\Delta F/F$ values in PVMHET traces was typically smaller than that of wild types, consistent with the ‘stunted and stagnant’ characterization of their qualitative appearance (compare the right Y axes in Figure 3.2). Therefore, a correlational relationship between ACtx PV activity and pupil diameter could be and was indeed maintained in the PVMHETs, as a correlation would not be affected by a diminished range of possible values in that group of traces. In essence, this result, although surprising, does not undermine the significance of the wild type finding in which the ACtx PV network is coupled to pupil diameter and affiliated with attention.

It goes without saying that the pupillometry experiments are limited in the sense that a head-fixed set up is a very contrived and artificial context. Although we presented the mice with different sensory stimuli while they were headfixed on the wheel, this experience in no way recapitulates the complexities of freely moving behavior, and the multisensory

environment created in the pup retrieval assay. Therefore, an alternative and purely speculative interpretation of the persistent correlation between ACtx PV activity and pupil diameter in the PVMHETs is that the overall lack of robust fluctuations in the PVMHET traces creates a tenuous relationship between ACtx PV activity and pupil diameter. Therefore, it is possible that this coupling could break down once the mouse is put into a more complex environment such as that surrounding retrieval where attentional demands are greater. In order to test this hypothesis, pupil diameter must be monitored in freely behaving mice which, although technically viable, is beyond the scope of the current study (Sattler and Wehr 2021).

Chapter 4: Manipulation of the ACtx PV Network to Rescue Retrieval Performance in PVMHETs

The results presented in Chapters 2 and 3 suggest that the low frequency ACtx PV fluctuations seen in wild type, but not PVMHET, surrogates reflect a constitutive state of the PV network, and that this state may reflect a PV network configuration that is ready to meet heightened plasticity demands when needed. Given the lack of low frequency ACtx PV fluctuations seen in PVMHETs, the primary aim of this chapter is to reconfigure the ACtx PV network of PVMHETs into a more plasticity-favorable state. In doing so, we aim to not only induce the emergence of low frequency ACtx PV fluctuations, but also rescue performance of the retrieval behavior. To achieve this goal, we inhibited the ACtx PV population and found that chronic, but not acute, ACtx PV suppression ameliorated the retrieval deficits seen in PVMHETs. Furthermore, this behavioral rescue was accompanied by a removal of PNNs in the ACtx, and a modest emergence of low frequency activity in the ACtx PV signal.

4.1 Chronic, but not Acute, ACtx PV Inhibition Improves Retrieval Behavior in PVMHETs

Our accumulating evidence suggests that the ACtx PV fluctuations present in wild type surrogates are not regulating retrieval behavior on a moment-to-moment basis, but rather reflect a PV network state that supports plasticity and facilitates learning. The question now becomes – can we induce this PV network state in the PVMHETs to rescue their retrieval behavior? Given that PVMHETs exhibit markers of a hyperactive and hypermature ACtx PV network, we hypothesized that inhibiting ACtx PV neurons would rescue retrieval behavior in PVMHET surrogates (Krishnan et al. 2017; Lau et al. 2020; Cisneros-Franco and de Villers-

Sidani 2019; Donato et al. 2013; Rowlands et al. 2018). To test this hypothesis, we inhibited ACtx PV neurons during retrieval sessions every day from P0 – P5. We initially used optogenetic methods to achieve temporally precise ACtx PV inhibition during retrieval (Figure 4.1). However, we noticed that the PVMHET surrogates in both our optogenetic and GFP control groups were retrieving pups with greater levels of success than a typical group of PVMHET surrogates. At the same time, we were experiencing higher than average mortality rates during surgical procedures – mice with the *MeCP2*^{het} background are particularly sensitive to anesthesia, but significantly more animals did not survive this surgery compared to other, shorter procedures (those performed for fiber photometry experiments, for example). Given the bimodal distribution of PVMHET surrogate behavior (Figure 2.4), we reasoned that the particularly long surgery required for this experiment (bilateral multi-site injections and bilateral optic fiber implants) was inadvertently selecting for more robust PVMHETs that carried a lower *MeCP2* mutational burden, were less affected by the anesthesia, and would naturally comprise the subgroup of PVMHETs that performed the retrieval with some success. Because of this, we pivoted technical strategies to employ chemogenetic inhibition which required a much shorter surgery. We used a PSAM receptor/PSEM agonist system to bilaterally inhibit the ACtx PV population during daily pup retrieval assays by administering PSEM via IP injection 20 minutes prior to the start of the retrieval session. This acute inhibition during retrieval assays (one IP injection each day from P0-P5, 6 injections total) was insufficient to improve retrieval performance (Figure 4.3).

While ACtx inhibition during retrieval did not affect retrieval performance, it is possible that such limited inhibition (restricted to daily retrieval assays) was insufficient to adequately reorganize the ACtx PV network into a more favorable configuration for plasticity.

Therefore, we sought to increase the extent of the ACtx PV inhibition achieved in the PVMHET surrogates. In lieu of increasing the number of IP injections each surrogate received (which would introduce additional confounds such as handling and injection stress), we chronically inhibited the ACtx PV network by dissolving clozapine-N-oxide (CNO, the ligand for an inhibitory DREADD (Designer Receptors Exclusively Activated by Designer Drugs)) in the surrogate's drinking water for the entirety of the perinatal period (approximately P-1 through P5). Unlike the acute ACtx PV inhibition, this chronic manipulation significantly improved retrieval performance in PVMHET surrogates (Figure 4.4).

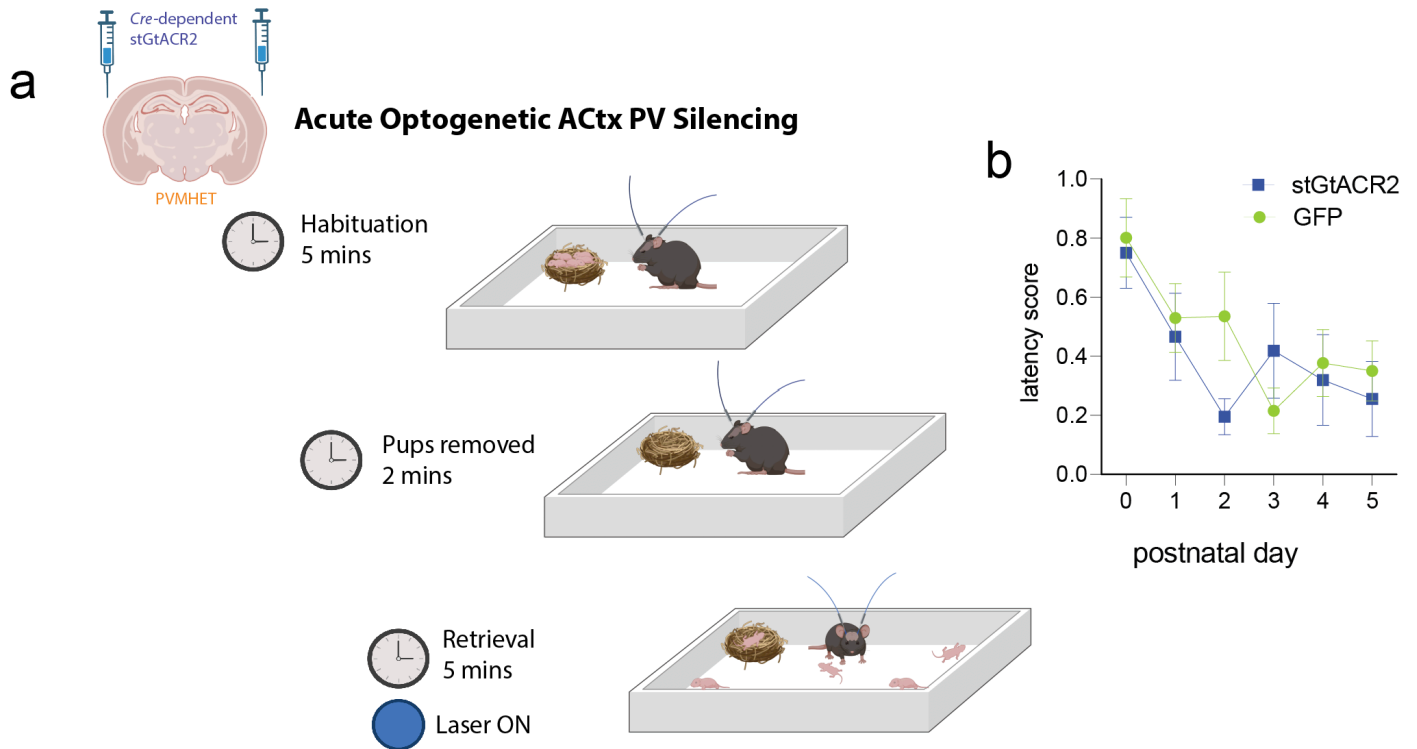


Figure 4.1: Acute optogenetic ACtx PV silencing in PVMHETs does not rescue retrieval performance. **A)** Acute optogenetic silencing paradigm. A *Cre*-dependent inhibitory stGtACR2 construct was delivered bilaterally to the ACtx of PVMHET females via AAV. PVMHET females were then given maternal experience in the form of surrogacy. Every day from P0 – P5, constant blue light (10mW at fiber tip) was delivered during the retrieval behavior assay, only during the 5 minute retrieval epoch. **B)** Average latency scores from retrieval behavior assays. N=7 stGtACR2 PVMHET surrogates (blue), N=6 GFP PVMHET surrogates (green). A Two-Way ANOVA revealed a main effect for postnatal day ($p=0.0015$), but not for treatment condition ($p=0.5889$). There was no significant interaction between postnatal day and treatment condition ($p=0.2423$).

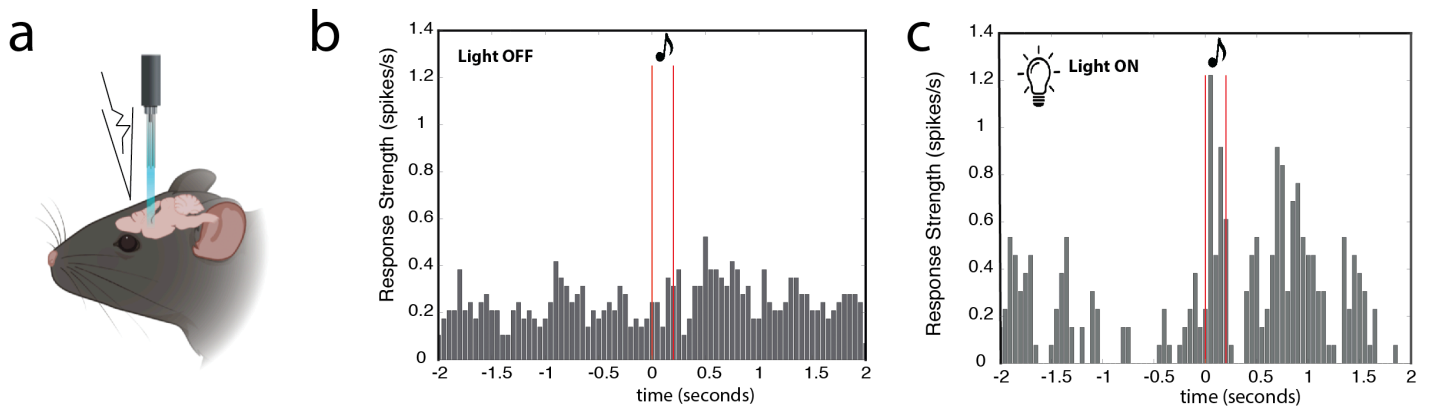


Figure 4.2: Optogenetic construct validation. **A)** To validate the efficacy of the stGtACR2 construct, we conducted *in vivo* single cell loose-patch electrophysiological recordings from the ACtx of PV-*Cre* females expressing the *Cre*-dependent stGtACR2 construct in PV neurons. We recorded from single ACtx units during playback of a set of recorded pup USVs (to promote ACtx activity). Each single unit was recorded as we presented the stimulus set to the animal twice – once through with no blue light present, once through with blue light shining directly at the cortical surface for the duration of the stimulus set (approximately 12 minutes, a timescale similar to that of the 5 minute length of a retrieval assay). **(B)** and **(C)** represent the average response to all stimuli for when blue light was either off or on, respectively. We expected that silencing ACtx PV neurons (an inhibitory population) would cause overall cortical disinhibition. Indeed, putative pyramidal neurons such as the one shown here (identified by spike waveform) exhibited a disinhibited response to the USV stimulus set when presented with the light on.

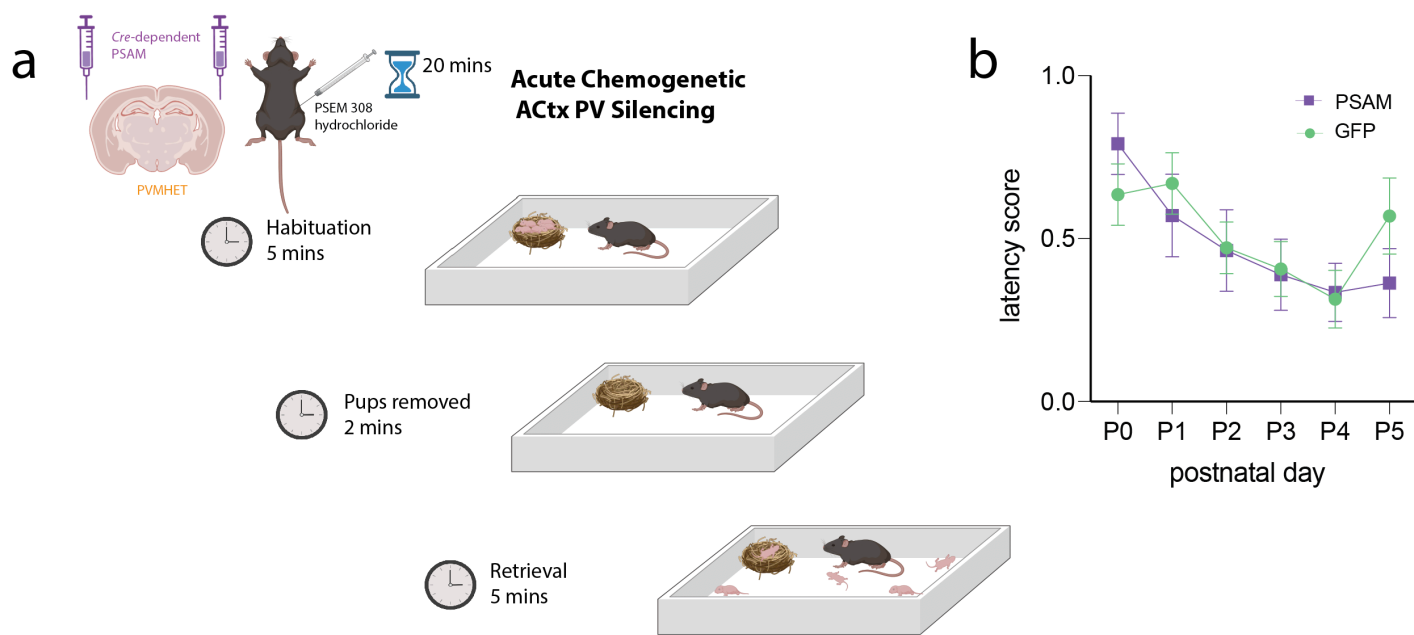


Figure 4.3: Acute chemogenetic ACTx PV silencing in PVMHETs does not rescue retrieval performance. **A)** Acute chemogenetic silencing paradigm. A *Cre*-dependent inhibitory PSAM receptor domain was delivered bilaterally to the ACTx of PVMHET females via AAV. PVMHET females were then given maternal experience in the form of surrogacy. Every day from P0 – P5, PSEM 308 hydrochloride was delivered via IP injection 20 minutes prior to the start of a retrieval behavior assay. **B)** Average latency scores from retrieval behavior assays across postnatal days. N = 10 PSAM/PSEM injection PVMHET surrogates (purple), N = 10 GFP/PSEM injection PVMHET surrogates (green). A Two-Way ANOVA revealed a main effect for postnatal day ($p=0.0002$), but not for treatment condition ($p=0.8706$). There was no significant interaction between postnatal day and treatment condition ($p=0.3100$).

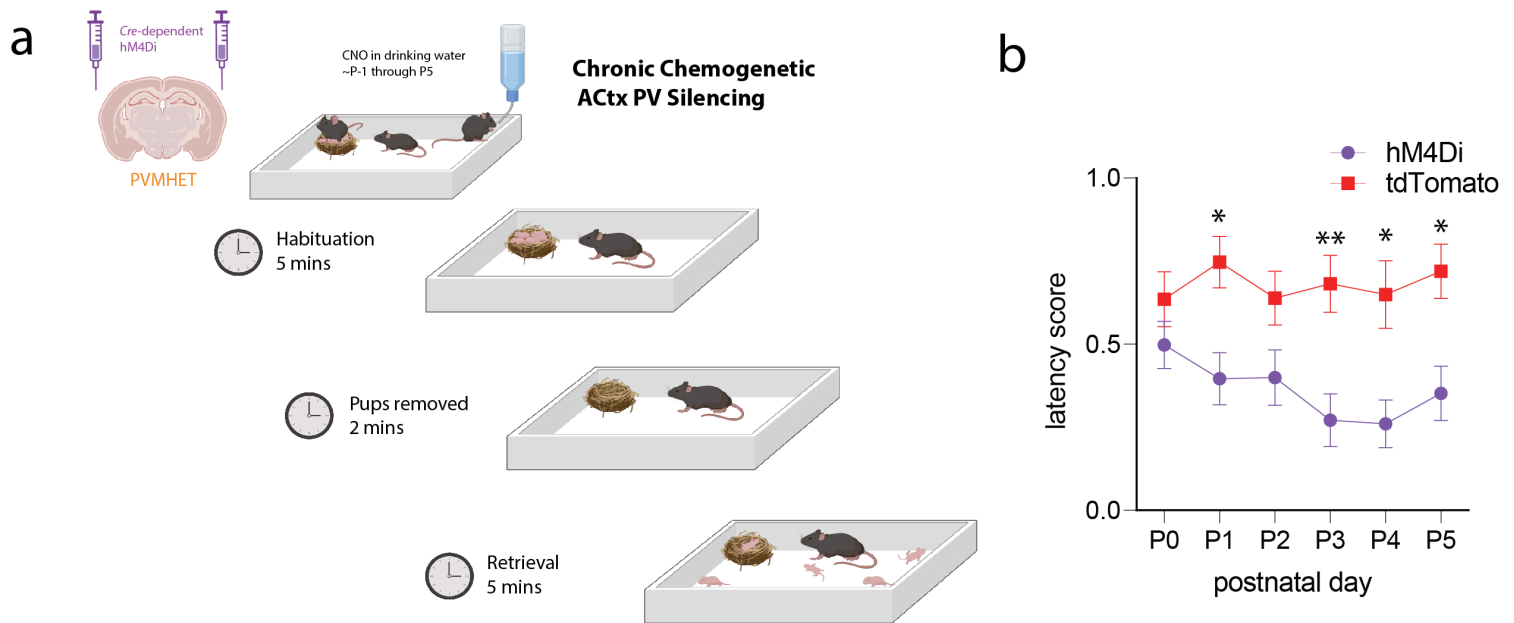


Figure 4.4: Chronic ACtx PV silencing in PVMHETs rescues retrieval performance. **A)** Chronic ACtx PV silencing paradigm. A *Cre*-dependent inhibitory hM4Di construct was delivered bilaterally to the ACtx of PVMHET females via AAV. PVMHET females were then given maternal experience in the form of surrogacy. From just before pup birth (beginning approximately P-1) through P5, CNO (the hM4Di ligand) was dissolved into the drinking water of the home cage to achieve chronic inhibition throughout the course of the experiment. Each day P0-P5, surrogates underwent a standard pup retrieval assay. **B)** hM4Di-injected surrogates (purple; N=19) outperformed tdTomato-injected controls (red, N=16) on the retrieval behavior. A Two-Way ANOVA revealed a significant main effect for treatment condition (hM4Di vs tdTomato, $p=0.0018$), but no main effect for postnatal day ($p=0.1833$). There was no significant interaction between treatment condition and postnatal day ($p=0.0851$). Post hoc Sidak's test revealed significant differences between the hM4Di and tdTomato surrogates on four postnatal days (P0, $p=0.7655$; P1, $p=0.0188$; P2, $p=0.2572$; P3, $p=0.0080$; P4, $p=0.0250$; P5, $p=0.0194$; * $p<0.05$, ** $p<0.01$).

4.2 Chronic ACtx PV Inhibition in PVMHETs Disassembles PNNs

Since chronic ACtx PV inhibition was able to rescue retrieval performance in PVMHETs, we wondered how this treatment affected established plasticity markers such as PNNs. Given PNN's canonical role as molecular 'brakes' on plasticity, and the elevated PNN presence typically seen in PVMHETs surrounding parturition, we hypothesized that the improvement in retrieval behavior from chronic ACtx PV inhibition was accompanied by a decrease in ACtx PNNs. To test this hypothesis, we compared PNN immunolabeling from ACtx sections taken from surrogates either expressing the inhibitory DREADD (hM4Di) or tdTomato in ACtx PV neurons. Importantly, all surrogates had chronic access to CNO, the hM4Di ligand, in the home cage drinking water for the duration of the experiment.

Consistent with the improvement in behavior, we found that chronic ACtx PV inhibition led to the disassembly of PNNs surrounding ACtx PV neurons (Figure 4.5). Interestingly, this PNN dissolution was more pronounced on transduced ACtx PV cells that were expressing the inhibitory hM4Di than on their untransduced neighbors within individual hM4Di-injected surrogates, suggesting a cell autonomous regulation of PNN assembly based on the activity of individual neurons (Figure 4.5). Indeed, we found this intra-subject measure to be more informative and compelling than a comparison of gross PNN densities between the hM4Di and tdTomato groups, especially given the qualitative nuances of PNN assemblies and the subjective measures such as thresholding invoked in their quantification. Taken together, these results demonstrate that chronic, but not acute, ACtx PV inhibition rescues retrieval behavior in PVMHETs, and the resulting ACtx PV network assumes a more plasticity-favorable configuration featuring PNN disassembly.

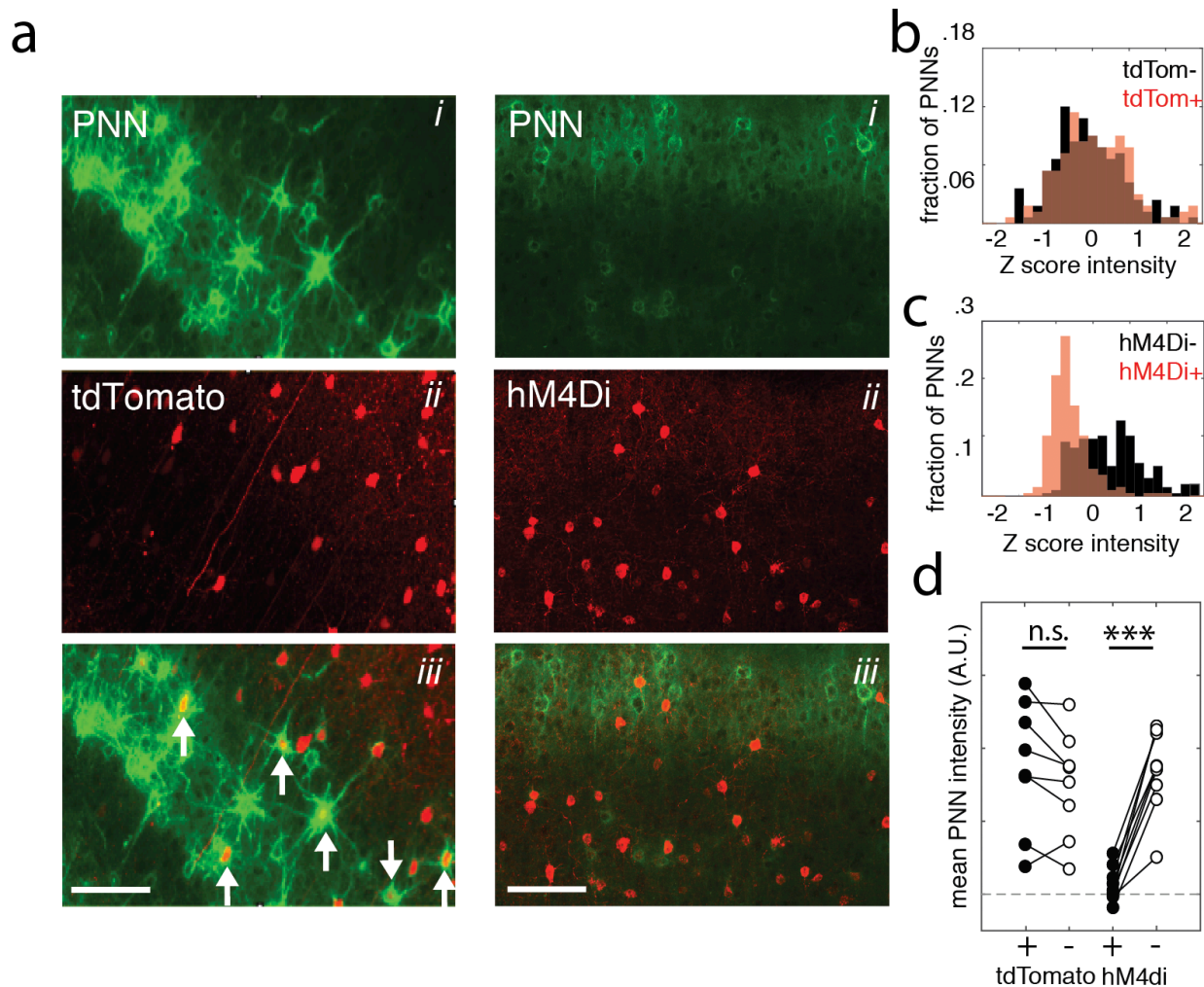


Figure 4.5: Chronic ACtx PV inhibition in PVMHETs leads to disassembly of PNNs. **A)** Representative photomicrographs taken of the ACtx of a *Cre*-dependent tdTomato-injected (left column) and *Cre*-dependent hM4Di-injected (right column) PVMHET surrogate. Surrogates were delivered CNO via drinking water for the duration of the experiment (approx. P-1 through P5) to achieve chronic inhibition of the ACtx PV population. Sections are stained for PNNs (*i*, green), and either tdTomato or the mCherry tag on the hM4Di construct (*ii*, red). The composite image is shown in (*iii*) with white arrows indicating cells engulfed by PNNs. **B)** Histogram comparing the intensity of PNNs engulfing neurons with and without expression of tdTomato. **C)** Histogram comparing the intensity of PNNs engulfing neurons with and without expression of hM4Di. **D)** Comparison of mean PNN intensity for virally transduced vs non-transduced neurons. Each dot-dot pair represents one animal. hM4di-transduced cells had less developed PNNs surrounding them compared to their non-transduced neighbors (paired t-test, *** $p < 0.001$).

4.3 Chronic ACtx PV Inhibition Increases Low Frequency Fluctuations in PVMHETs

At this point, we have shown that chronic ACtx PV inhibition ameliorated the retrieval deficits in PVMHETs, and disassembled PNNs surrounding ACtx PV neurons. We hypothesized that these changes were also accompanied by the appearance of the signature low frequency PV fluctuations that were previously only seen in wild type surrogates that successfully performed the retrieval behavior (see Chapter 2). To test this hypothesis, we expressed both the inhibitory hM4Di construct and GCaMP7s in the ACtx PV population of PVMHET surrogates. These surrogates underwent the same chronic ACtx PV inhibition paradigm as previously described, with CNO dissolved in the drinking water of the home cage. We used fiber photometry to record from the ACtx PV population in these surrogates every day from P0 – P5. Consistent with a gradual transition from a high to low PV network state as hM4Di-mediated ACtx PV inhibition accrued over time, we saw that the power of low frequency fluctuations (<0.5 Hz) in the ACtx PV signal modestly increased over the course of postnatal days (Figure 4.6).

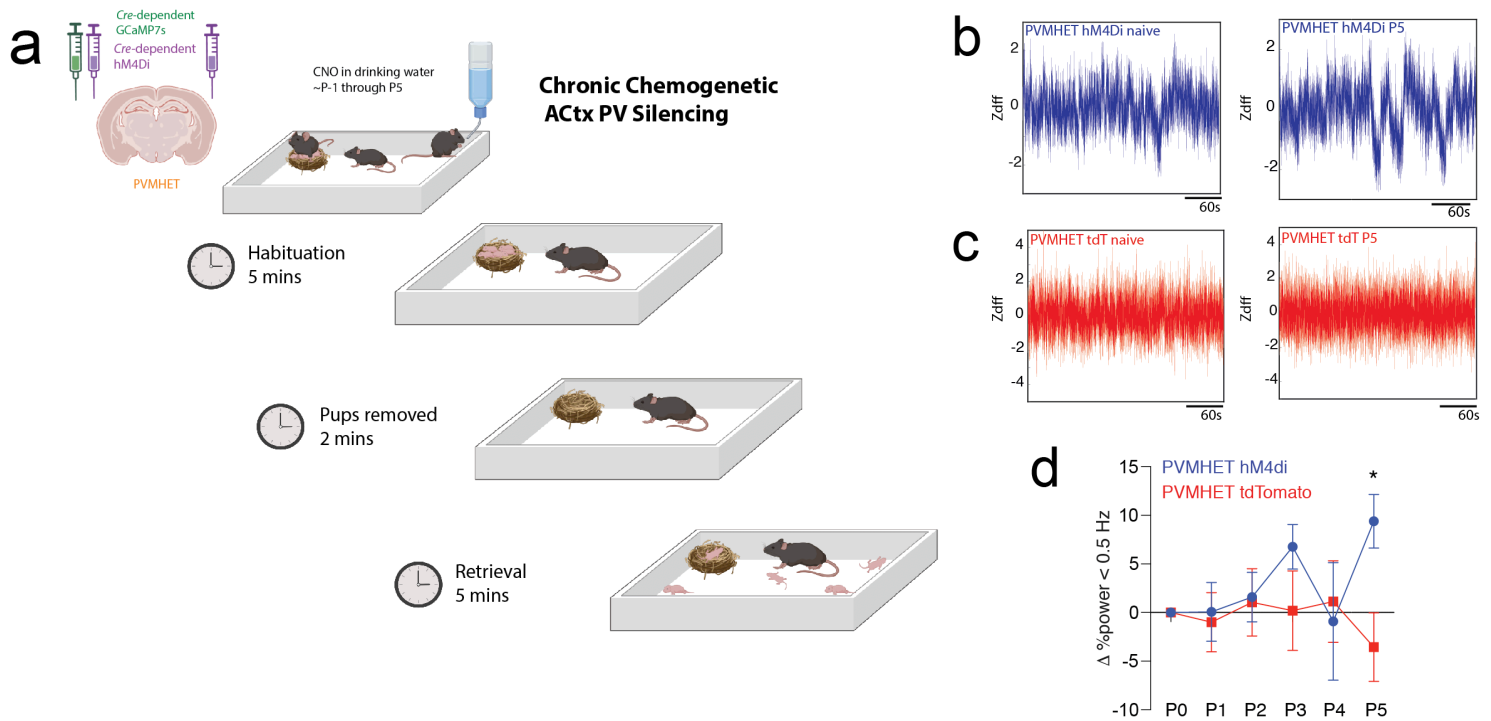


Figure 4.6: Chronic ACtx PV inhibition in PVMHETs modestly restores low frequency fluctuations. **A)** Experimental schematic of chronic ACtx PV inhibition achieved by dissolving CNO in the home cage drinking water. **B)** Representative ACtx PV fiber photometry traces recorded from a PVMHET surrogate under the chronic inhibition paradigm at a naive timepoint (left) and on P5 (right) **C)** Same as in **(B)**, but for a representative control PVMHET surrogate that received a tdTomato injection in lieu of the inhibitory hM4di construct. **D)** Mean net change in ACtx PV low frequency power for all recorded sessions across postnatal days for mice either expressing the inhibitory hM4di construct (blue, N=8) or tdTomato (red, N=7) with CNO dissolved in their drinking water. ACtx recordings from each animal included the 5 minute habituation period, the 5 minute retrieval period, and an additional 5 minutes where the surrogate was alone in the cage. A Two-Way ANOVA revealed no significant interaction between treatment condition and time with $p=0.0555$. A post hoc Sidak test revealed a significant difference between the hM4di and tdTomato groups on P5 ($p=0.0388$).

4.4 Discussion

4.4.1 A Time Course for PV Network Reconfiguration

Here we show that chronic, but not acute, ACtx PV network inhibition ameliorates retrieval deficits seen in PVMHET surrogates. This raises the interesting possibility that prolonged PV inhibition (and the resulting cortical disinhibition) is necessary for sufficient network remodeling to accommodate increased plasticity demands. However, the molecular and cellular underpinnings of such a reconfiguration, and the time course of its effects remain to be elucidated. That being said, the cell-autonomous dissolution of PNNs surrounding hM4Di-transduced cells (but not their uninfected neighbors) may provide some early insight. Devienne and colleagues took a similar experimental approach and also reported a cell autonomous dissolution of PNNs based on whether a given PV neuron was transfected with an inhibitory DREADD (Devienne et al. 2021). However, in that study, CNO was administered via 4 IP injections spaced 12 hours apart. This raises a critical question – what is the minimal amount of PV inhibition needed to achieve such a network reconfiguration? The answer to this question would also be intertwined with one regarding the dynamics of PNN assembly – how quickly are PNNs able to assemble and disassemble in the context of experience-dependent learning? Aberrantly heightened levels of PNNs in the ACtx of surrogates with an MeCP2 KO restricted to PV neurons have been reported as early as P1, despite their presence being indistinguishable from wild type at a naive timepoint (Rupert et al. 2023). This would suggest that PNN reconfiguration is largely flexible and expedient (on the order of minimal days if not quicker), which would be desirable for a network responsible for learning and solidifying new information. The fact that the once daily IP injections in the current study (acute inhibition)

were insufficient to incite such a reconfiguration may also point to the system's resistance to transient activity fluctuations that may reflect noise in the network. Therefore, future studies may seek to identify the threshold for PV suppression that is required to alter the network configuration and begin PNN disassembly in PVMHETs. Such a study coupled with transcriptomic analyses of PV neurons may also identify key changes in gene expression underlying this switch, the mechanisms by which PV neurons regulate their PNN assemblies, and elucidate a more mechanistic understanding of how this network reconfiguration is accomplished.

4.4.2 Technical Limitations

A significant technical limitation of the current study is that we were unable to quantify the exact dosage of CNO received by each surrogate throughout the chronic ACtx PV inhibition experiment. This was unavoidable given the nature of our experimental design in which surrogates forgo physical pregnancy to mitigate confounds introduced by maternal hormonal fluctuations. In this paradigm, surrogates must be co-housed with a dam and drink from the same available water source (in which the CNO was dissolved). Because of this, more traditional measures of DREADD efficacy and inter-subject variability are less informative. For example, assessing the DREADD injection spread for insight into behavioral performance would be relatively meaningless given that we do not know how much ligand was introduced to the system and at what time intervals (water was available *ad libitum*). Nevertheless, given the cell-autonomous disassembly of PNNs surrounding hMD4i+ neurons, we are fairly confident that a sufficient level of chronic ACtx PV inhibition was achieved. In support of this assertion, the same PV cell autonomous PNN disassembly resulting from DREADD-mediated

PV inhibition has been previously described by Devienne and colleagues (Devienne et al. 2021). Furthermore, dissolving CNO in the animal's drinking water served two purposes (Zhan et al. 2019). First, it eliminated additional handling and injection stress for the animals that would be introduced from multiple IP injections per day over the course of the multi-day experiment. Second, it administered CNO at much lower levels than direct IP injections, which mitigates the risk for some of the adverse effects seen following administration of high doses of CNO (MacLaren et al. 2016).

4.4.3 Enzymatic Dissolution of PNNs in PVMHETs

While it was encouraging that chronic ACtx PV inhibition appeared to tackle both behavior and PNN architecture in PVMHET surrogates, its ability to induce the characteristic low frequency fluctuations of wild types was modest. This could be for a number of reasons. Primarily, we sought to monitor the activity of the very ACtx PV population that we were constitutively inhibiting. Indeed, it is unlikely that such pronounced activity as that seen in wild type surrogates would materialize under these conditions. In an attempt to circumvent this issue, in a separate cohort of animals we enzymatically dissolved ACtx PNNs immediately prior to maternal experience. This treatment has previously been shown to rescue retrieval behavior in MeCP2^{het} surrogates, but no neural activity of any kind was monitored (Krishnan et al. 2017).

To incorporate this additional layer of experimental complexity, surrogates underwent two surgical procedures. The first involved the injection of *Cre*-dependent GCaMP7s into the left ACtx delivered via AAV. 3 weeks later in a second surgical procedure, the enzyme Chondroitinase ABC was bilaterally injected into the ACtx, and an optical fiber implant was

inserted into the left ACtx (Figure 4.7). The different timescales on which the AAV and enzymatic processes occur necessitated this two-tiered process – the AAV required sufficient time to express before imaging, but the Chondroitinase ABC enzyme needed to be introduced as close to maternal experience as possible so PNNs would be dissolved during the perinatal period. Therefore, surrogates were paired with dams that were about to give birth immediately following their second surgery, and pups were born anywhere from 1-3 days later. However, we ran into numerous challenges attempting to perform fiber photometry in animals with such recent surgical history. Namely, mice typically exhibited very little measurable ACtx PV activity. Interestingly, in the few animals that did display adequate signal, the strength of the signal would increase over the course of postnatal days. Animals with barely any USV-evoked headfixed responses on the first few days post-surgery would exhibit measurable USV-evoked responses by P5 (Figure 4.7). Encouragingly, in this small subset of surrogates that exhibited auditory-evoked responses, we found low frequency ACtx PV fluctuations similar to those seen in wild types (Figure 4.7). However, because of the emerging nature of the signal, we were hesitant to attribute the presence of any low frequency fluctuations specifically to PNN degradation - it was impossible to disentangle the source of their onset from simply the overall improvement in signal quality as time went on.

We believe that the reason for the lack of signal, or emerging signal, in this group of animals stems from a combination of inflammation following surgery, and the Chondroitinase ABC itself which introduced a significant volume of fluid into the ACtx around the onset of imaging epochs. Because of these factors, we determined that the signal integrity from these experimental animals was not sufficiently reliable to draw any meaningful conclusions. That being said, slice electrophysiology may be the most technically feasible strategy to assess the

direct effect of PNN degradation on ACtx PV activity in PVMHETs. Indeed, a protocol written by Tewari and Sontheimer outlines optimal experimental parameters for monitoring Chondroitinase ABC – induced PNN degradation in real time using this approach (Tewari and Sontheimer 2019). While this technique would not be able to ascertain information concerning population level dynamics and overall ACtx PV fluctuations, single unit changes in neural activity patterns following PNN disassembly in PVMHETs would offer valuable insight into how interneurons comprising this subpopulation would differentially behave in the presence and absence of PNNs.

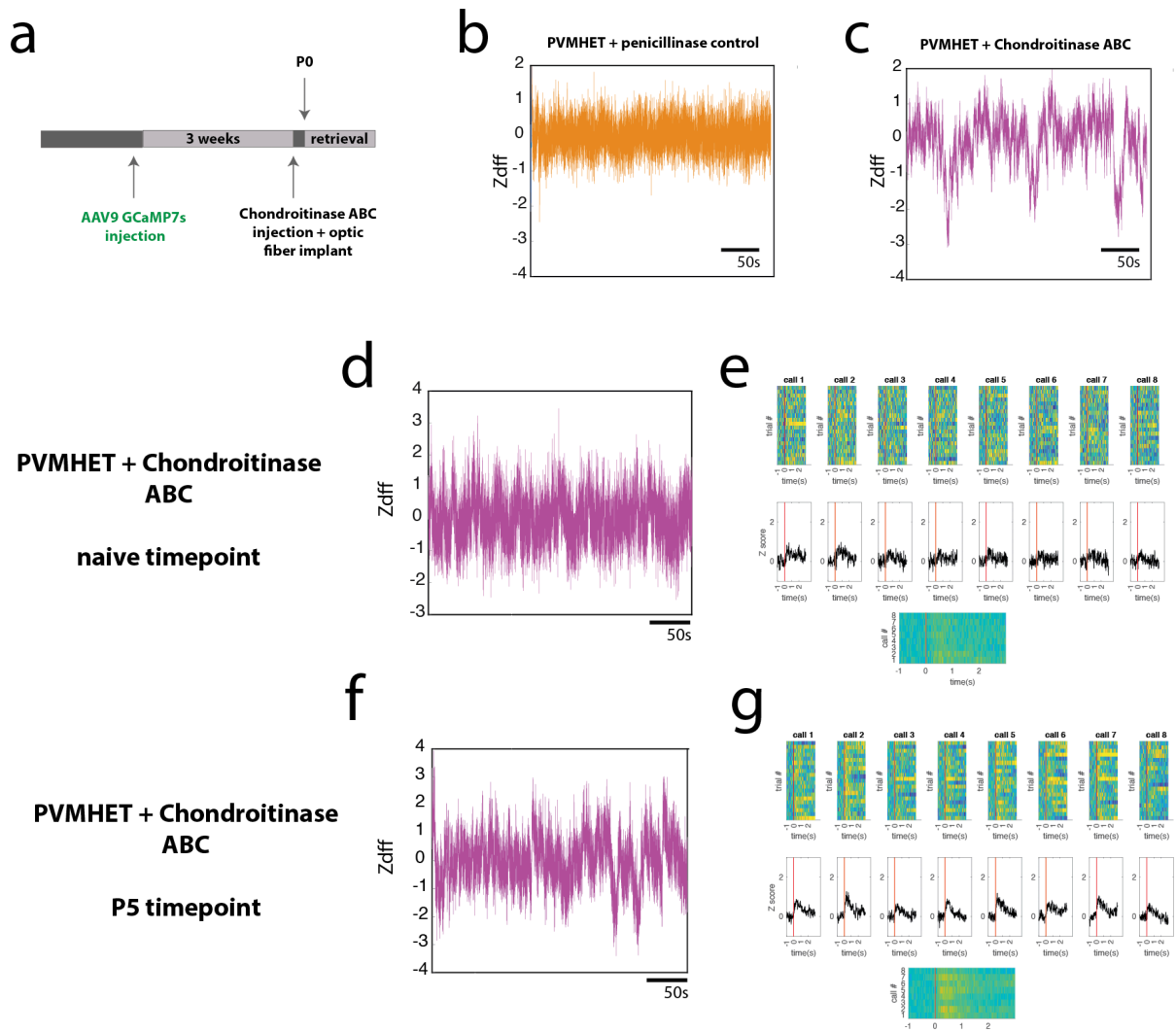


Figure 4.7: Enzymatic dissolution of PNNs is not conducive to stable recordings. **A)** Experimental timeline. The different timescales on which AAV and enzymatic processes occur necessitated two surgical procedures. The first surgery injected *Cre*-dependent GCaMP7s via AAV into the ACTx of PVMHETs. After 3 weeks (to allow sufficient time for GCaMP7s expression), a second surgery injected the enzyme Chondroitinase ABC (or penicillinase for controls) bilaterally into the ACTx. For our purposes, we wanted PNNs to be dissolved around the time of pup birth when retrieval behavior was being learned and assayed. Given that enzymatic processes occur on the order of days, surrogates had to be paired with expectant dams that were about to drop around the time of the surrogate's second surgery. This typically resulted in surrogates beginning retrieval assays anywhere from 1 day to 3 days after surgery. **B)** ACTx PV activity recorded with fiber photometry during a retrieval session in a control surrogate, and a **C)** Chondroitinase ABC-injected surrogate. **D)** ACTx PV activity from a surrogate alone in the home cage and **E)** in response to a pup USV stimulus set comprised of 20 repetitions of 8 recorded pup USVs, prior to maternal experience. **F)** and **G)** show the same recording conditions from the same animal, this time recorded on P5. It is critical to note that both auditory responses and low frequency fluctuations appear to emerge over time (in the small portion of animals that would eventually develop signal following the second surgical procedure).

Chapter 5: Materials and Methods

5.1 Experimental Subjects

All animal procedures and experiments were conducted under the National Institutes of Health's Guide for the Care and Use of Laboratory Animals and approved by the Cold Spring Harbor Laboratory Animal Care and Use Committee. All experiments were performed in adult female mice (7-12 weeks of age) that were maintained on a 12h-12h light-dark cycle and received food and water *ad libitum*. CBA/CaJ females were used as dams for all studies - pregnant CBA/CaJ females were transferred to a cage with surrogates (experimental subjects) approximately one week before expected pup drop. Additional mouse lines used were PV-*ires-Cre* (B6;129P2-Pvalbtm1(cre)Arbr/J; referred to as "PV-*Cre*" throughout), and *Mecp2*^{het} (C57BL/6 background; B6.129P2(C)-*Mecp2*tm1.1Bird/J; referred to as "*Mecp2*^{het}" throughout, in which exons 3 and 4 of the *MeCP2* gene are deleted (Guy et al. 2001). For studies in which PV interneuron activity was monitored or manipulated in the *Mecp2*^{het} background, "PVMHET" females were used as experimental subjects. PVMHET females were generated by crossing homozygous PV-*Cre* males and *Mecp2*^{het} females (heterozygous for the *MeCP2* loss of function allele). Mendelian genetics dictate all offspring to be PV-*Cre* heterozygous, and 50% of offspring to have the desired *Mecp2*^{het} genotype. PCR based genotyping was performed on all offspring to select females that both express *Cre* in PV cells and are heterozygous for the loss of function *MeCP2* allele that defines the Rett Syndrome mouse model. For brevity, females that meet these criteria are referred to as PVMHET females. The offspring without the desired *Mecp2*^{het} genotype (*Mecp2*^{wt}) resulting from this cross were used as wild type littermate controls.

5.1.1 Genotyping Procedures

All animals were genotyped via ear punch at the time of weaning (approximately 3-4 weeks old). Genotyping was carried out both in house, and occasionally, by an external genotyping service (TransnetYX). Table 5.1 lists the primers, recommended by Jackson Laboratories, that were utilized for genotyping purposes.

Table 5.1: Primer sequences used for genotyping mouse lines

Genetic Mouse Line	Allele Type	Forward Primer Sequence	Reverse Primer Sequence
<i>PV-Cre</i>	Wild type	GCAGAATTCTCCACTCTGGTG	GACTGAGATGGGGCGTTG
<i>PV-Cre</i>	Mutant	TCTAATTCCATCAGAAGCTGGT	GACTGAGATGGGGCGTTG
MeCP2-het	Wild type	AAATTGGGTTACACCGCTGA	CTGTATCCTTGGGTCAAGCTG
MeCP2-het	Mutant	AAATTGGGTTACACCGCTGA	CCACCTAGCCTGCCTGTACT

5.2 Maternal Pup Retrieval Behavior

In order to eliminate potential confounds introduced by hormonal fluctuations in mothers, experimental subjects were given maternal experience via co-habitation with a pregnant dam and her pups. A female with this maternal experience is referred to as a “surrogate” throughout. Beginning approximately one week prior to pup drop, two surrogates were co-housed with a pregnant dam. Every day from postnatal day 0 (P0) through P5, surrogates underwent a pup retrieval assay. First, the surrogate is habituated in the home cage, inside of a soundproof box, for 5 minutes. Subsequently, pups were placed in the nest with the surrogate in the cage for 5 minutes. Finally, the pups were removed from the cage for 2 minutes, and then scattered around the 4 corners of the cage. The surrogate had a maximum of 5 minutes to gather the pups to the nest. After the standard retrieval assay, 4 ‘single pup trials’ were performed, where only 1 pup was placed in the cage at a time and the surrogate was given 1 minute to retrieve. We incorporated these trials in an effort to disambiguate the source of individual pup USVs, and observe how surrogates interacted with the specific pup that was vocalizing. In some instances, wild type surrogates became so proficient at retrieval, that they would retrieve the single pup within the first few seconds of the assay. To combat this, we constructed a small cardboard ‘door’ attached to a pulley system that would conceal the pup, and allow the experimenter to reveal the pup without opening the door to the behavior box after the session had begun. All behavior assays were performed in the dark, during the dark cycle, and in the subject’s home cage. Videos were recorded in the dark under infrared light using a Logitech webcam (c920) with the infrared filter removed.

5.2.1 Ultrasound Recording during Pup Retrieval Behavior

During pup retrieval assays, ultrasonic vocalizations were recorded using a polarized condenser ultrasound microphone (CM16/CMPA Avisoft Bioacoustics) that was positioned 12 inches directly above the center of the cage. The microphone digitally sampled at 200kHz via a National Instruments DAQ (NI-USB 6211) using custom MATLAB software. Onsets and offsets of pup ultrasonic vocalizations were confirmed manually using custom MATLAB software.

5.2.2 Analysis of Maternal Pup Retrieval Behavior

Each maternal pup retrieval behavior assay was assessed using a latency retrieval score. The normalized latency of each mouse to gather the scattered pups was calculated using the following formula, where n = # of pups outside the nest, t_0 = start of trial, t_n = time of n^{th} pup gathered, L = trial length.

$$\text{latency index} = [(t_1 - t_0) + (t_2 - t_0) + \dots + (t_n - t_0)] / (n \times L)$$

The resulting latency index score is a number from 0 to 1 where a smaller number indicates a more expedient, efficient retrieval.

To assess event evoked responses during retrieval behavior in fiber photometry experiments, behavioral ethograms were created using BORIS (Behavior Observation Research Interactive Software) (Friard and Gamba 2016). A trained experimenter manually annotated retrieval assay videos for the onset and offset of behaviorally relevant events. The

behavioral ethograms generated in BORIS were subsequently exported to MATLAB for further analysis. A complete list of the annotated behavioral events is found in Table 5.2.

5.3 Linear Encoding Model

To assess the unique sensory and behavioral contributions to the overall PV interneuron activity, we trained a linear encoding model similar to that employed by Musall et al. (Musall et al. 2019). Behavioral epochs were deemed as point (single time bin) or state (spanning multiple time bins) events, and manually annotated using BORIS software (Friard and Gamba 2016). Each time bin was 1 second. A complete list of the input variables to the model are found in Table 5.2. Instantaneous velocity was calculated using positional markers labeled with DeepLabCut (Mathis et al. 2018). Briefly, the center of the mouse's head was tracked for the duration of each video, and its positional changes through the session were used to calculate the mouse's instantaneous velocity (per second resolution) using custom MATLAB software. A separate model was trained for each animal using all freely moving data collected from that mouse across postnatal days.

Table 5.2: Linear Encoding Model Covariates

Covariate name	Description	Event Type
Initial pup contact	The first frame that the surrogate contacts the pup to be returned to the nest	Point event
Pup contact	The first frame when the pup is lifted off of the ground to be returned to the nest	Point event
Pup investigation	The surrogate sniffs/licks the pup, but does not return the pup to the nest	State event
Pup drop	The pup is retrieved and dropped down in the nest	Point event
Enter nest	The surrogate crosses into the nest with a pup (counted as the first frame there is overlap with any part of the surrogate's body and the nest)	Point event
Leave nest	The surrogate leaves the nest to retrieve a pup (counted as the first frame to lack overlap with any part of the surrogate's body and the nest)	Point event
Door	For single pup trials, when the door was lifted to reveal a pup	Point event
Nesting	The surrogate engages in nesting behavior (either collecting material to build the nest or rearranging material in the existing nest)	State event
Grooming	The surrogate grooms herself	State event
Rearing	The surrogate rears onto her hind legs	State event
Ultrasonic vocalization	Ultrasonic vocalization train occurs	State event
Instantaneous velocity	Surrogate's instantaneous velocity binned per second	Continuous event

5.4 Surgical Procedures

Prior to all surgical procedures, mice were initially anesthetized with an intraperitoneal injection (1.25ml/kg) of an 80:20 mixture of ketamine (100mg/ml) and xylazine (20mg/ml) prior to being stabilized in a stereotaxic frame (KOPF). Anesthesia was subsequently maintained throughout by vaporized isoflurane (1-2% as needed), and the depth of the anesthesia was assessed by both monitoring the animal's respiration and by performing periodic toe pinches. Preoperative analgesia was given in the form of a subcutaneous meloxicam injection (2mg/ml). An ophthalmic lubricant was applied to the eyes and maintained throughout the duration of the surgical procedures. An incision was made to expose the bregma and lambda sutures of the skull, and the brain was levelled in the stereotax such that the sagittal suture was centered, and lambda was +0.15mm – 0.30mm dorsal/ventral relative to bregma.

5.4.1 Viral Injections

After the brain was levelled in the stereotax, a craniotomy was drilled over the ACtx, and the dura mater was removed. Depending on the specific experiment, one or more adeno-associated viruses were injected into the ACtx craniotomy. Injection coordinates for the ACtx were informed by the Allen Brain Atlas: Anterior/Posterior -2.3mm, 2.6mm, and -2.9mm from bregma, Medial/Lateral 4.0mm and 4.5mm from bregma for 6 unique injection sites.

Table 5.3: Viral Constructs for Injection

Construct	Purchasing Information
AAV9-syn-FLEX-jGCaMP7s-WPRE	Addgene Plasmid #104491
AAV9-syn-FLEX-PSAM4-GlyR-IRES-EGFP	Addgene Plasmid #119741
AAV9-hSyn-DIO-hM4D(Gi)-mCherry	Addgene Plasmid #44362
GFP; AAV9-synP-DIO-EGFP-WPRE-hGH	Addgene Plasmid #100043
AAV9-FLEX-tdTomato	Addgene Plasmid #28306
AAV9_hSyn1-SIO-stGtACR2-FusionRed	Addgene Plasmid #105677
AAV9-hSyn-DIO-GRAB_Ach3.0	WZ Biosciences

5.4.1.1 Procedures for Fiber Photometry Experiments

For fiber photometry experiments, *Cre*-dependent GCaMP7s (AAV9-syn-FLEX-jGCaMP7s-WPRE; Addgene Plasmid #104491) was injected into the left ACtx of either PV-*Cre* or PVMHET females at the injection site coordinates listed above in 5.4.1 *Viral Injections*. At each injection site, 90nL of virus was expelled at a depth of -0.830mm from the cortical surface. A 200 μ m optical fiber (0.39NA, ThorLabs) was implanted in the center of the injection site craniotomy at a depth of -0.780mm from the cortical surface. The optical fiber and a titanium head fixation bar were secured to the skull using Metabond dental cement, and the scalp was sutured shut. Micropipettes for viral injections were prepared using a P-97 horizontal micropipette puller, and tips were manually clipped at a width of 20-30 microns (Sutter Instruments).

5.4.1.2 Procedures for Chemogenetic Experiments

Chemogenetic experiments required bilateral injections of adeno-associated viruses into the ACtx. Therefore, craniotomies were opened over both the left and the right hemisphere ACtx. Injection sites were similarly determined as in the fiber photometry experiments described above, with the exception that virus was expelled at 3 distinct depths within each injection site so as to more comprehensively cover the dorsal/ventral span of the ACtx. Here, 45nl of virus was expelled at dorsal/ventral coordinates of -1.00mm, -0.550mm, and -0.350mm from the cortical surface. For acute chemogenetic manipulation of PV interneurons, an inhibitory *Cre*-dependent PSAM receptor AAV was bilaterally injected (AAV9-syn-FLEX-PSAM4-GlyR-IRES-EGFP; Addgene Plasmid #119741) into the ACtx of either PV-*Cre* or

PVMHET females. For chronic chemogenetic manipulation of PV interneurons, an inhibitory DREADD (Designer Receptors Exclusively Activated by Designed Drugs) was bilaterally injected (AAV9-hSyn-DIO-hM4D(Gi)-mCherry; Addgene Plasmid #44362) into the ACtx of PVMHET females. Depending on the experiment, control animals for chemogenetic studies were injected with either *Cre*-dependent green fluorescent protein (GFP; AAV9-synP-DIO-EGFP-WPRE-hGH, Addgene Plasmid #100043), or *Cre*-dependent tdTomato (AAV9-FLEX-tdTomato, Addgene Plasmid #28306).

5.5 Chemogenetic Manipulation of PV Interneurons

5.5.1 Acute Chemogenetic Manipulation of PV Interneurons

Acute chemogenetic manipulation of PV interneurons was achieved using an inhibitory PSAM/PSEM system (AAV-syn-FLEX-PSAM4-GlyR-IRES-EGFP, Addgene Plasmid #119741; PSEM 308 hydrochloride, Tocris Bioscience). 20 minutes prior to a daily pup retrieval assay, surrogates received an intraperitoneal injection of PSEM (3mg/kg dissolved in sterile saline). Control animals received the same PSEM injection prior to each retrieval assay, but expressed GFP in PV interneurons as opposed to PSAM. To validate the efficacy of the PSAM/PSEM system, PV-*Cre* females received a dual injection of both *Cre*-dependent GCaMP7s and *Cre*-dependent PSAM into the left ACtx, along with a 200 μ m optical fiber to allow for fiber photometry experiments. PV activity was monitored using fiber photometry before and 20 minutes after an intraperitoneal PSEM injection.

5.5.2 Chronic Chemogenetic Manipulation of PV Interneurons

A DREADD system was implemented for chronic chemogenetic inhibition of PV interneurons (AAV9-hSyn-DIO-hM4D(Gi)-mCherry, Addgene Plasmid #44362) (Sternson and Roth 2014; Krashes et al. 2011; Roth 2016). To chronically suppress PV activity, CNO (the DREADD receptor agonist) was dissolved in the subject's drinking water beginning at approximately P -1 and continuing through P5 at a desired dose of 1mg/kg as described by Zhan et al. (Zhan et al. 2019). A fresh solution was made daily, and bottles were wrapped in aluminum foil to shield it from the light. This delivery strategy was particularly advantageous as it omitted the need for continual intraperitoneal injections (eliminating additional stress and handling confounds), and allowed for a low enough effective dose to mitigate adverse behavioral effects from the CNO, given that CNO is not entirely pharmacologically inert (Zhan et al. 2019; MacLaren et al. 2016). The exact effective dose could not be determined for each subject because water was shared amongst all mice in a cage (two surrogates and the dam). Note that a subset of the surrogates shown in Figure 4.4b were also used for the experiment described in Figure 4.6 (8/19 hM4Di and 7/16 tdTomato injected surrogates were also injected with GGaMP7s to monitor the emergence of low frequency ACtx PV fluctuations resulting from chronic ACtx PV inhibition). Since both groups received the same chronic ACtx PV inhibition and were not significantly different from each other, we combined them for the analysis of the behavioral effect of prolonged ACtx PV inhibition on retrieval performance.

5.6 Optogenetic Manipulation of PV neurons

A *Cre*-dependent, blue light sensitive, soma-targeted anion-conducting channelrhodopsin (stGtACR2; AAV9_hSyn1-SIO-stGtACR2-FusionRed; Addgene Plasmid #105677) was employed to inhibit PV cells in the ACtx (Mahn et al. 2018). Bilateral injections were made in the ACtx as described above for chemogenetic manipulation of ACtx PV neurons (See 5.4.1.2 *Procedures for Chemogenetic Experiments*). In addition to the bilateral viral injections, 200 μ m tapered optical fibers were implanted in each hemisphere at a depth of -1.10mm from the cortical surface (Optogenix), and cemented in place with Metabond. Unlike blunt optical fibers that emit light only from the fiber tip, tapered fibers emit light down the length of the implant, effectively increasing the illuminated cortical area (ideal to maximize light delivery to large cortical regions such as the ACtx).

5.6.1 Optogenetic Stimulation Paradigm

The output power of a 473nm laser (MBL III, 100mW) was measured immediately prior to all experimental sessions using a compact power and energy meter console (Thorlabs, PM100D), and refined until 10mW was emitted at the tip of each optical fiber. Dual fiber optic patch cords for bilateral stimulation (NA=0.22) and rotary joints were obtained from Doric lenses. Using a ceramic mating sleeve, surrogates were attached to the dual fiber optic patch cord and, following the protocol for maternal pup retrieval assays described above, allowed to habituate to the home cage alone for 5 minutes before pups were removed for 2 minutes. Then, the 473nm laser was turned on, and pups were scattered around the nest for the 5 minute retrieval session. The 473nm light was delivered constantly during the 5 minute retrieval. The stGtACR2 construct was specifically chosen for these experiments due to the construct's favorability for temporally extended manipulations (those on the order of minutes to hours).

Indeed, favorable stoichiometry allows for a more light sensitive, efficient silencing that reduces the risk of heat-induced tissue damage from prolonged laser exposure (Mahn et al. 2018).

5.7 Electrophysiological Validation of Optogenetic Silencing

5.7.1 Single Cell Loose-Patch Electrophysiology

The electrophysiology recording rig is equipped with a sound-attenuation chamber and installed air table, digital oscilloscope (Tektronix), audio monitor (Grass), 1401 power board I/O (CED), BA-03x intracellular amplifier and pressure injector (NPI), Master 8 multichannel pulse stimulator (AMPI), Microelectrode AC amplifier – extracellular (AM Systems), piezoelectric micromanipulator (Sutter Instrument SOLO/E-116), and Spike 2 software (version 7; Cambridge Electronic Design) for playback of auditory stimuli.

Before recording sessions, mice were anesthetized with an 80:20 mixture (1.25ml/kg) of ketamine (100mg/ml) and xylazine (20mg/ml), and a small craniotomy was opened above the left ACtx. Micropipettes were pulled from borosilicate glass filaments (BF150-86-10, Sutter Instruments) using a horizontal micropipette puller (P-97, Sutter Instruments). Micropipettes were back-filled with intracellular solution comprised of 125mM potassium gluconate, 10mM potassium chloride, 2mM magnesium chloride, and 10mM HEPES (pH 7.2) for a final resistance of 10-30 M Ω . Isolated single unit activity was recorded with a BA-03X bridge amplifier (npi), low-pass filtered at 3kHz, digitized at 10kHz, and acquired using Spike2 software. Recording depth was determined with a piezoelectric micromanipulator (Sutter

Instrument SOLO/E-116), and all recorded neurons were located between 300 μ m and 1200 μ m from the cortical surface (encapsulating layers II-VI of ACtx).

5.7.2 Presentation of Auditory Stimuli

Individual unit responses to a series of pup ultrasonic vocalizations and pure tones were compared in the presence and absence of optogenetic PV inhibition. Auditory stimuli were presented using one of the output channels on a Power1401 ADC/DAC board (Cambridge Electronic Design), low-pass filtered at 100kHz, and amplified using a custom filter and preamp (Kiwa Electronics). Output was sent through an electrostatic speaker driver powering an electrostatic speaker (ED1/ESI, Tucker-Davis Technologies) positioned 4 inches in front of the mouse's head. All auditory stimuli were calibrated to RMS of 65dB SPL at the mouse's head using a sound level-meter (Ex-Tech, model 407736). Stimuli consisted of 7 log-spaced pure tones from 4-32 kHz in frequency, and 8 pup ultrasonic vocalizations recorded from CBA/CaJ mouse pups in-house on either postnatal day 2 (calls 1-4) or postnatal day 4 (calls 5-8). Auditory stimuli were presented for 100ms with an inter-stimulus interval of 4 seconds, with each unique stimulus occurring 10 times in a session in a pseudorandomized order. All electrophysiology data was subsequently manually spike sorted into single unit spike trains with Spike2 (CED).

5.7.3 Optogenetic Inactivation During Electrophysiological Recordings

In vivo single cell loose-patch electrophysiology was performed in the left ACtx of PV-*Cre* females expressing the *Cre*-dependent inhibitory optogenetic construct used for optogenetic silencing of PV neurons during retrieval behavior (stGtaCR2; AAV9_hSyn1-SIO-

stGtACR2-FusionRed; Addgene Plasmid #105677). To optogenetically silence PV neurons during electrophysiology recording sessions, the tip of a 400 μ m optical fiber (NA 0.39, ThorLabs) was positioned directly over the surface of the craniotomy and held in place by a micromanipulator such that light shone directly on the cortical surface. Laser (473nm, MBL III 100mW) power was 30mW measured at the tip of the optic fiber. Based on this configuration, the light intensity would have an estimated power of 2-10mW/mm² at a depth of 300-100 μ m from the cortical surface, where electrophysiological recordings were made (Yizhar et al. 2011). Recordings for each single neuron (a session of 10 stimulus repetitions) were collected twice – once with the laser off and once with the laser on with continuous light.

5.8 Fiber Photometry

5.8.1 Fiber Photometry Acquisition system

Experiments were performed using a custom-built two-color fiber photometry system. The output from two LEDs (470nm and 565nm, Thorlabs M470F3 and M565F3) was focused into a fiber launch holding a 200 μ m optical fiber (0.37 NA, Doric) which was coupled to the implanted optical fiber via a lightweight, flexible cable and ceramic mating sleeve (Thorlabs). The two LEDs were sinusoidally modulated 180 degrees out of phase at 211 Hz by LED drivers (Thorlabs, LEDD1B), and the emitted green and red light was collected from the optical fiber. The two color channels were separated, bandpass filtered, and detected by distinct photoreceivers (#2151, Newport Corporation). The signal from each photoreceiver was digitized at a sampling rate of 6100 Hz and acquired via a National Instruments DAQ device (NI-USBB6211). Mice attached to the patch cord for imaging were afforded free movement

within the cage via connection with an optical swivel (Doric). Light delivered to the brain was measured at $\sim 30\text{mW}$ at the fiber tip before each imaging session using a digital handheld optical power and energy meter console (Thorlabs, PM100D).

5.8.2 Fiber Photometry Data Analysis

$\Delta F/F$ (change in fluorescence over fluorescence) signals from the output of the fiber photometry acquisition system were calculated with custom written MATLAB software. The value at each peak in the sinusoidal signal for both color channels was detected, resulting in an effective sampling rate of 211 Hz. Each signal was low-pass filtered with a Butterworth filter at 15Hz and fit to a double exponential decay function, which was subtracted to correct for photobleaching that may have occurred over the course of the recording session. The red channel was used to correct for any movement artifact in the signal during freely moving recording sessions. To achieve this, a robust regression was used to compute a linear function for predicting the activity-independent component of the green signal based on the red. This prediction was then subtracted from the actual green channel signal. Finally, the result was mean subtracted and divided by the mean to calculate $\Delta F/F$. $\Delta F/F$ signals from each mouse were Z-scored across all recording sessions from that mouse to compare activity across postnatal days (denoted as Z_{dff} for “Z-scored $\Delta F/F$ ”). For freely behaving event associated responses (Figure 2.5, Figure 2.6), Z_{dff} responses were background subtracted (background taken was the period 10 seconds before event onset to 5 seconds before event onset). This range for background subtraction was chosen so as to not interfere with any pre-event activity (we had noticed that responses to pup contact in particular would tend to ramp up before the actual event). Headfixed responses to pup USV presentation were used to confirm signal in

experimental subjects. Paired t tests of the average Zdff ACtx PV activity 2 seconds before and 2 seconds after each stimulus onset were used to determine if subjects demonstrated sufficient signal to be included in further analysis.

5.9 Low Frequency Fluctuations in Fiber Photometry Signal

The percentage of power in the 0 to 0.5Hz frequency band of the fiber photometry Zdff signal for each recording was used to quantify the presence and absence of fluctuations in fiber photometry traces of PV-*Cre* and PVMHET surrogates, respectively. The 0 to 0.5Hz frequency range was chosen to incorporate the distinctive, low frequency fluctuations in the PV-*Cre* surrogate's traces, as an initial manual inspection of the traces determined that these fluctuations had durations on the order of 2-3 seconds. Total power in the signal was capped at 20Hz for computations of the percentage of total power, given anything above this frequency exceeds the imaging limitations set by the use of *Cre*-dependent GCaMP7s. The built-in MATLAB function "bandpower" was fed the Zdff traces of individual sessions as input, and calculated the average power within the specified frequency band. A single value was reported for each animal, and was comprised of the average value for all recorded trials across all postnatal days for that mouse (trials included "alone in cage", "pups in nest habituation", and "full retrieval").

5.10 Presentation of Ultrasonic Vocalizations

During headfixed fiber photometry sessions, two auditory stimulus sets were presented to experimental subjects. The first was a set of tones, consisting of 7 log spaced pure tones

from 4-32 kHz in frequency, and the second consisted of 8 pup ultrasonic vocalizations recorded from CBA/CaJ mouse pups in-house on either postnatal day 2 (calls 1-4) or postnatal day 4 (calls 5-8). Auditory stimuli were presented in a pseudo-random order over 20 trials with a 10 second inter-stimulus interval. A National Instruments DAQ (NI-USB 6211) was used to trigger auditory stimuli during simultaneous acquisition of fiber photometry data using custom written MATLAB software. Stimuli were triggered through an electrostatic speaker driver to an electrostatic speaker (ED1/ES1, Tucker-Davis Technologies) positioned 4 inches behind the animal's head. Stimuli were low-pass filtered and amplified at 100kHz using a custom filter and preamp (Kiwa Electronics). A sound level meter (Extech Model 407736) was used to calibrate the RMS for all stimuli to 70 dB at the position of the animal's head. The head fixed data shown in Figure 2.2E was taken from Rupert et al., 2023 and includes results from 9 PV-*Cre* and 8 PVMHET surrogates (Rupert et al. 2023). Since the publication of that pre-print, additional animals have been used for freely-moving behavior studies (PV-*Cre*, N=12 total (3 additional); PVMHET, N=10 total (2 additional)). These animals were also subject to the headfixed USV playback paradigm to ensure sufficient fiber photometry signal, but are not included in Figure 2.2E.

5.11 Fiber Photometry and Chondroitinase ABC Removal of PNNs

In order to determine if directly disassembling PNNs would result in low frequency ACTx PV fluctuations in PVMHETs, we used the enzyme Chondroitinase ABC to dissolve PNNs while monitoring ACTx PV activity using fiber photometry. The differing timescales for enzymatic and viral processes necessitated a two-tiered surgical approach – experimental mice underwent 2 procedures that occurred 3 weeks apart. First, PVMHET females were injected in

the left ACtx with *Cre*-dependent GCaMP7s as previously described in section 5.4.1.1 (*Procedures for Fiber Photometry Experiments*). 3 weeks later in a second surgical procedure, the enzyme Chondroitinase ABC (0.3 μ l of 50 U ml⁻¹ per site, 6 sites per hemisphere, in 0.1% BSA/0.9% NaCl solution; Sigma Aldrich) was bilaterally injected into the ACtx, and an optical fiber implant was inserted into the left ACtx. Control animals were subject to the same procedures, but instead were injected with the control enzyme penicillinase (0.3 μ l of 50 U ml⁻¹ per site, 6 sites per hemisphere, in 0.1% BSA/0.9% NaCl solution; Sigma Aldrich). The different timescales on which the AAV and enzymatic processes occur necessitated the separate surgical procedures– the AAV required sufficient time to express before imaging, but the Chondroitinase ABC enzyme needed to be introduced as close to maternal experience as possible so PNNs would be dissolved during the perinatal period. Therefore, surrogates were paired with dams that were about to give birth immediately following their second surgery, and pups were born anywhere from 1-3 days later. Following pup birth, surrogates were subject to the same freely moving and headfixed fiber photometry experiments as described in Figures 2.2 and 2.3.

5.12 Pupillometry Setup

Pupil activity was monitored during headfixed fiber photometry sessions to assess the relationship between ACtx PV interneuron activity and pupil diameter (an established proxy for arousal and attention) (Bradley et al. 2008; Reimer et al. 2016, 2014; McGinley et al. 2015; Steinhauer et al. 2004; Tursky et al. 1969; Zekveld et al. 2018; Privitera et al. 2010; Lisi et al. 2015; Zhao et al. 2019; Zekveld et al. 2010; Winn et al. 2015; Poulet 2014; Vinck et al. 2015; Bala and Takahashi 2000). The pupil was captured using a DCC1545M High-Resolution

CMOS camera with 10Hz resolution (ThorLabs), and the pupillometry video was synced to the simultaneously acquired fiber photometry data using a time-locked infrared light flash visible in the pupillometry video that was automatically triggered at the onset of the fiber photometry data acquisition. Each pupillometry session consisted of a series of trials in the following sequence: no stimulus (5 minutes), pure tones playback (12 minutes), pup ultrasonic vocalizations playback (12 minutes), tactile stimulus (5 minutes, experimenter would touch the mouse on the back with a cotton swab at approximately 30 second intervals), no stimulus (30 minutes), no stimulus (5 minutes). The Pearson's R value for each mouse was the average of the Pearson's R value of all trials for that subject. Pupillometry experiments were conducted while either monitoring PV interneuron activity in the ACtx (AAV9-syn-FLEX-jGCaMP7s-WPRE; Addgene Plasmid #104491), or ACh detection in the ACtx (AAV9-hSyn-DIO-GRAB_Ach3.0, WZ Biosciences).

In addition to monitoring the pupil and acquiring fiber photometry data, the mouse's locomotion was also tracked based on wheel movement. To assess whether pupil diameter was only correlated with ACtx PV activity while the subject was running, the time vector of the experiment was binned into seconds, and wheel movement was binarized into movement or no movement bins. The correlation between the two signals was computed and compared between the entire duration of the session, and the session with the movement epochs removed.

5.13 Pupil tracking with DeepLabCut

The machine learning software package, DeepLabCut was implemented to track pupil diameter in the acquired pupillometry videos (Mathis et al. 2018). 4 markers were used to train the model – the top edge of the pupil, the right edge of the pupil, the bottom edge of the pupil,

and the left edge of the pupil. 15 frames from each video were used to train the model to ensure a robust and diverse training set. The labeled data, where the 4 edges of the pupil are represented as coordinates in each frame of every video, was exported to MATLAB for further analysis. Pupil diameter was calculated in units of pixels, based on the linear distance between the top and bottom edge of the pupil in each frame. In rare cases where one or both of these markers was obscured throughout the video recording (ex. under the eyelid), the linear distance between the left and right edges of the pupil was used to calculate the pupil diameter.

5.13.1 Correlation of Pupillometry and PV Interneuron (or Acetylcholine) Activity

Given the sampling rate of 211Hz for fiber photometry data acquisition, and the 10Hz sampling rate for the acquired pupillometry video, both signals were down sampled to a common denominator of seconds. At this resolution, the relationship between Zdff and pupil diameter were compared, and a Pearson's correlation coefficient between the two was computed for each trial. The Pearson's correlation coefficient for all trials from a mouse were averaged to yield a single value per mouse.

5.14 Histology

Immediately following the maternal pup retrieval assay on P5, mice received a lethal dose of pentobarbital (Euthasol), and were transcardially perfused with PBS followed by 4% paraformaldehyde. Following the perfusion, the brain was immediately extracted and post-fixed overnight at 4°C. Brains were then transferred to a solution of 30% sucrose in PBS and stored at -4°C. Brains were sectioned in the sagittal plane on a freezing microtome (Leica) at

a thickness of 50 μ m and stored in cryoprotectant (a combination of sucrose (.3g/ml), polyvinylpyrrolidone (.01g/ml), and ethylene glycol (.5ml/ml) in .1 M in PB) at -20°C. For visualization of GCaMP7s expression from fiber photometry animals, brain sections were first incubated with a primary antibody raised against GFP in chicken diluted 1:1000 in PDT (0.5% normal donkey serum, 0.1% Triton X-100 in PBS) at 4 degrees overnight, and then stained with a secondary anti-chicken Alexa 488 fluorophore raised in goat and diluted 1:500 in PDT for 2 hours at room temperature.

For immunolabeling of perineuronal nets and the quantification of DREADD spread for the chronic inhibition of PV interneurons experiment, brains were cut in half down the midline at the time of sectioning and separated into the left and right hemispheres before acquiring sagittal sections. Right hemisphere sections were stained for perineuronal nets and the mCherry tag on the DREADD construct. Left hemisphere sections were stained for GFP (to visualize GCaMP7s expression), and the mCherry tag on the DREADD construct. For right hemisphere sections, brain sections were first incubated with primary antibodies raised against Lectin in *Wisteria floribunda* with biotin conjugate (WFA) diluted 1:500, and against mCherry in rabbit diluted 1:1000 in PDT (0.5% normal donkey serum, 0.1% Triton X-100 in PBS) at 4 degrees overnight. The next day they were stained with a secondary Alexa 488 conjugate fluorophore and a secondary anti-rabbit Alexa 594 fluorophore raised in goat, both diluted 1:500 in PDT for 2 hours at room temperature. Left hemisphere sections were stained for GFP (to visualize GCaMP7s expression), and the mCherry tag on the DREADD construct. Left hemisphere brain sections were first incubated with primary antibodies raised against GFP in chicken diluted 1:1000, and against mCherry in rabbit diluted 1:1000 in PDT (0.5% normal donkey serum, 0.1% Triton X-100 in PBS) at 4 degrees overnight. The next day they were

stained with a secondary anti-chicken Alexa 488 fluorophore raised in goat and a secondary anti-rabbit Alexa 594 fluorophore raised in goat, both diluted 1:500 in PDT for 2 hours at room temperature. All antibodies are from Thermo Fisher Scientific, except for the primary antibody against lectin which is from Sigma-Aldrich. Sections were mounted onto slides using Fluoromount (SouthernBioTech), coverslipped, and stored at -4°C.

5.15 Fluorescence Microscopy

For all imaging excluding that involving PNN analysis, slides were imaged under an epifluorescence microscope (Olympus BX43) at either 4x or 10x magnification. For images used to analyze PNNs, 20x magnification Z-stack images were taken on a 710 confocal microscope (Zeiss) in line scan mode. The spectra for each channel were adjusted to optimize the signal to noise ratio from representative sections. Settings included: bit depth = 12 bit; laser power = 1%; gain = 700 for green channel, 750 for red channel; pin hole size = 1 airy unit; full dynamic range 1024x1024 smoothness; averaging = 4; image tiling set to a 2x3 configuration for acquisition. Tiled images were stitched together using ZEN software (2012 SP5) before being exported to FIJI for further analysis.

5.16 Quantification of Perineuronal Nets

Confocal images from the right hemisphere ACtx of animals from the chronic PV inhibition experiments were acquired as described above. Images were subsequently exported to FIJI for PNN quantification (Schindelin et al. 2012). 4 sagittal images were taken from similar anterior/posterior planes of section from each mouse, guided by the Allen Brain Atlas

(Lein et al., 2007). Z stacks were collapsed to generate a maximum projection image for each color channel. 10 PNNs were randomly selected from the same dorsal/ventral location within ACtx, and were categorized as either surrounding hM4Di/tdTomato-positive cells or not surrounding hM4Di/tdTomato-positive cells. The intensity of each PNN was determined by manually outlining the structure and applying the area integrated density function in FIJI. Background fluorescence intensity for each section was subtracted from each PNN intensity value.

5.17 Statistical Analysis and Figure Generation

GraphPad Prism was used for all statistical analysis. Throughout the thesis, the following notation style is used: $p < 0.05$ (*), $p < 0.01$ (**), $p < 0.001$ (***). Figures were generated either in MATLAB or Python, and experimental schematics were created using BioRender and Adobe Illustrator.

Chapter 6: Conclusions and Perspectives

Through this work, we endeavored to reveal the real-time contributions of the ACtx PV network to maternal pup retrieval behavior, and any aberrations that may underlie retrieval deficits in a mouse model of Rett Syndrome (RTT). Previous studies implicating the ACtx PV network as a key site of dysregulation during the perinatal period were limited in their ability to address this question – either revealing ACtx PV abnormalities in postmortem histology, or monitoring single unit activity in a headfixed experimental set up (Krishnan et al. 2017; Lau et al. 2020; Rupert et al. 2023). These restrictions have so far impeded our understanding of the real-time ACtx PV network contributions to retrieval, and the direct behavioral consequences of its dysregulation in the RTT model. Here, for the first time, we have monitored ACtx PV activity *during* retrieval behavior over the course of the postnatal period. Our results provide hitherto unequaled insight into ACtx PV dynamics in freely behaving animals, and a cell-type specific network underlying adult experience-dependent plasticity. Our findings have contributed several key results towards our understanding of this complex, learned behavior and the network-level processes that facilitate it:

- Using fiber photometry to monitor the ACtx PV population in both wild type and RTT model surrogates, we discovered a lack of low frequency ACtx PV fluctuations in RTT model surrogates that were a characteristic signature of wild type ACtx PV activity (Chapter 2).
- For a primary sensory cortex, ACtx PV activity in wild type surrogates reflected far more than merely sensory information (Chapter 2).

- Low frequency ACtx PV fluctuations were tightly coupled with pupil size, a proxy for arousal and attention. This observation gave rise to the possibility that the ACtx PV fluctuations are reflective of a network state that facilitates adult experience-dependent plasticity and learning (Chapter 3).
- Chronic, but not acute, ACtx PV inhibition in the RTT model rescued pup retrieval performance, disassembled PNNs in a PV cell autonomous fashion, and induced the emergence of modest low frequency ACtx PV fluctuations (Chapter 4).

6.1 Where Does the ACtx PV Network Fit into the Overall Execution of Maternal Pup Retrieval Behavior?

For the first time, we directly monitored ACtx PV activity in freely moving animals as they engaged in maternal pup retrieval behavior. In doing so, we were able to elaborate on the role of the ACtx PV network for learning during a naturally occurring period of adult experience-dependent plasticity. However, our focus on this limited inhibitory subpopulation is merely one piece of an elaborate puzzle that supports the complex social behavior that is pup retrieval.

As key integrators and orchestrators of neural activity, the ACtx PV population exerts considerable influence on local microcircuit dynamics. Indeed, restricting MeCP2 knockout to distinct subpopulations (namely PV, VIP, SST, or EMX neurons) has revealed that only MeCP2 knockout in PV or EMX-positive neurons is sufficient to disrupt retrieval behavior (Rupert et al. 2023). When considering the relative proportion of neurons that each of these populations represent (PV comprising ~20% of all cortical neurons, EMX the ~80% of cortical excitatory neurons), it is impressive that such a small population of inhibitory interneurons is capable of achieving the same overall effect on behavior as the manipulation of 80% of the neocortex

(Markram et al. 2004; Petilla Interneuron Nomenclature Group et al. 2008; Tremblay et al. 2016; DeFelipe et al. 2013). However, the cell-type specific effects of *MeCP2* mutation and how the resulting aberrations to activity patterns of individual subpopulations may feed into each other and alter dynamics within the ACtx microcircuit remain unclear. Indeed, it is particularly difficult to disentangle and pinpoint wholly disparate sources of dysregulation within such an interconnected circuit.

Zooming out from the ACtx microcircuit, a larger question remains as to exactly how the ACtx may be supporting the retrieval behavior, and how ACtx PV activity may influence ACtx output that is utilized by downstream targets for additional computations. Through the current work, we have contributed to the ever-growing body of evidence that the ACtx is capable of much more sophisticated computations apart from mere sensory processing. Indeed, we have shown that ACtx PV activity not only reflects non-auditory events (Chapter 2), but also may be more intimately linked to the animal's overall state of arousal which may aid in pup retrieval (Chapter 3). One of the early indications that the ACtx was not exclusively reflecting auditory information came in the 1950s when Hubel and colleagues discovered what they coined "attention units" in the cat ACtx. These single units would only be responsive if a cat was "paying attention" to the sound source (Hubel et al. 1959). Indeed, the idea that there could be some neural representation of attention in the ACtx is a particularly attractive idea for the interpretation of our findings from Chapter 3 in which we propose the ACtx PV network fluctuations may in some way reflect attention given their close coupling to pupil diameter. In further support of this idea, we propose that the exceptionally strong response that we see in the ACtx PV population to the door opening during single pup retrieval trials may also reflect an event that engages the animal's attention as it signals the start of a retrieval trial. Apart from attention, the events, processes, and states that ACtx

activity appears to encode has only grown over time— many far removed from pure sensory processing. Several studies have now demonstrated that the ACtx plays a role in perceptual decision-making, performs multisensory integration, and reflects locomotion (Tsunada et al. 2016; Francis et al. 2018; Niwa et al. 2012; Znamenskiy and Zador 2013; Hackett and Schroeder 2009; Werner-Reiss et al. 2003; Ghazanfar and Schroeder 2006; Lakatos et al. 2007; Zatorre et al. 2007; Yavorska and Wehr 2021; Kuchibhotla and Bathellier 2018; Schneider and Mooney 2018). Thus, ACtx may serve as a critical circuit node linking sensory representations with behavioral variables. This status lends credence to our initial hypothesis proposing its role in the regulation of the sensory-driven behavior that is pup retrieval.

With regards to the retrieval deficits we report in the PVMHET surrogates, it is difficult to pinpoint the local ACtx PV network as the definitive site for behaviorally disruptive dysregulation. Indeed, pup retrieval is an incredibly complex, multisensory behavior with many brain regions implicated in its successful execution – the MPOA, LC, ACC, amygdala, and VTA to name a few (Fang et al. 2018; Dvorkin and Shea 2022; Xie et al. 2023; Corona et al. 2022; Nowlan et al. 2022). How aberrant ACtx PV network activity in the PVMHETs impacts overall ACtx output and projections to other key regions implicated in the behavior is unknown. The global penetrance of the *MeCP2* mutation and its mosaic expression pattern resulting from random X chromosome inactivation in these surrogates further exacerbates this issue, as dysregulation in other regions and their relative *MeCP2* mutational burdens is likely also reflected in retrieval performance. However, prior work by Rupert et al. have restricted the *MeCP2* knockout specifically to ACtx PV neurons in adulthood with a temporally and spatially restrictive viral strategy, and show that this manipulation delays the acquisition of pup retrieval (Rupert et al. 2023). Taken together, these results support the claim for the ACtx PV population as a critical node in the overall network

contributing to the learning and execution of pup retrieval, but we are currently unable to disentangle the unique contribution of ACtx PV network activity from that of downstream targets when it comes to their ultimate influence on behavior.

6.2 How We Think About PV Neurons in Plasticity Periods

Much of the discourse regarding the role for PV neurons in regulating critical periods for plasticity surrounds their maturity and concomitant engulfment by PNNs. Indeed, PV activity positively regulates PNN formation, and PNNs have been shown to lock encapsulated PV neurons into high firing rate activity patterns (Brückner et al. 1993; Härtig et al. 1999; Wingert and Sorg 2021; Reimers et al. 2007; Favuzzi et al. 2017). Therefore, we propose that chronically elevated ACtx PV activity is a plasticity deterrent, and reflective of a network state that is not conducive to learning. We are not the first to hypothesize the existence of such a state; indeed, both ‘low’ and ‘high’ PV network configurations have been described in the hippocampus based on PV activity levels. These PV network designations in the hippocampus are tied to learning and memory, and the PV network state reconfigures from a low-PV activity to a high-PV activity state upon learning completion (Donato et al. 2013). This shift following learning is consistent with our conceptual framework – we propose that PVMHETs have a premature ‘high-PV state’ at the onset of maternal experience that impairs learning. Interestingly, pharmacological hippocampal PV inhibition to induce the ‘low-PV-network configuration’ enhances memory consolidation and retrieval, similar to how chronic ACtx PV inhibition rescued PVMHET retrieval behavior in the current study (Chapter 4). Importantly, the pharmacological inhibition paradigm in both cases was designed so as to not capture the acute effects of agonist administration and PV network silencing during learning and memory tasks, but to reconfigure the PV network prior to testing (Donato et al. 2013).

Taken together, our proposed model for a PV network state shares many similarities with that described in the hippocampus by Donato and colleagues, and essentially suggests that elevated PV network activity is not conducive to learning (Donato et al. 2013).

While we and others have shown that PV activity cell-autonomously regulates PNN assembly, the population level consequences of widespread PNN assemblies on PV network activity are much less understood (Devienne et al. 2021; Härtig et al. 1992; Pizzorusso et al. 2002; Dityatev et al. 2007; Reimers et al. 2007; Favuzzi et al. 2017). The modest emergence of low frequency fluctuations in the ACtx PV activity following chronic PV inhibition (and the resulting degradation of PNNs) in PVMHETs suggests that PNNs do alter population-level PV activity dynamics. However, whether the emergence of these fluctuations is due to changes in synaptic connectivity following PNN disassembly, or coincident changes in the activity patterns of large groups of individual PV neurons remains unclear. The heightened PNN presence in PVMHETs may also affect PV-orchestrated gamma oscillations (cortical rhythms that typically emerge during periods of heightened arousal or attention). Indeed, both enzymatic degradation of PNNs by Chondroitinase ABC and PNN destabilization in mice deficient in a key extracellular matrix component critical for PNN formation have been shown to increase gamma power (Lensjø et al. 2017; Gurevicius et al. 2004; Wingert and Sorg 2021). Disrupted gamma oscillations in PVMHETs may also negatively impact retrieval behavior by limiting surrogates' attentional capacities.

While, to our knowledge, we are the first to report these low frequency fluctuations (and the lack thereof in MeCP2^{hets}), we are currently only able to speculate as to their functional significance and the underlying network computations that they reflect. We propose that, like the distribution of PNNs, this characteristic activity pattern represents a signature of a 'PV network state' that is equipped to meet plasticity demands as they arise. Indeed, these fluctuations are

consistently seen in freely behaving mice, are context-independent, and even precede the onset of maternal experience (Chapter 3). Clearly, these fluctuations are not required for the acute performance of pup retrieval, as pharmacological ACtx PV inhibition did not impair retrieval performance in wild type surrogates (Chapter 2). It may be that the bulk of the learning necessary to execute the behavior occurred during natural interactions with pups when the ACtx PV network was online (outside of the 15 minute retrieval assay). In this time, a more efficient motor program may have been consolidated and stored outside of the ACtx that allowed the surrogate to successfully execute the behavior during retrieval assays when the ACtx PV population was pharmacologically inhibited. Taken together, it appears that low frequency ACtx PV fluctuations are critical for successful learning to occur (although not necessarily needed during the performance of the behavior itself), and that their presence may reflect a network state prepared to meet plasticity demands in adulthood.

Given the tight coupling between pupil size (an established proxy for attention and arousal) and ACtx PV activity, we propose that the presence of low frequency fluctuations in the ACtx PV activity may either reflect or influence phenomena like cortical state transitions. Indeed, heightened attentive states may facilitate successful retrieval by allowing surrogates to more readily attend to pups in need. More specifically, an elevated attentional capacity may allow for more reliable detection of pup USV distress cries and increase the likelihood of retrieval. Given the strong thalamic and neuromodulatory (specifically cholinergic) inputs onto ACtx PV neurons, future work may look to understand their interaction and coordination with respect to cortical state transitions. Inhibitory interneurons often show both context and state-dependent activity modulation, although it is unclear whether this is a driving factor in state transitions, or a byproduct of such a cortical state change (Pakan et al. 2016; Petersen and Crochet 2013; Vinck et al. 2015).

However, the large magnitude of the low frequency fluctuations seen in ACtx PV activity with fiber photometry would suggest that there is strong reciprocal connectivity and synchronous activity within the PV network. Such a connectivity pattern is critical for the generation of cortical gamma rhythms which appear during times of heightened attention (Galarreta and Hestrin 1999; Sohal et al. 2009; Cardin et al. 2009; Bartos et al. 2007; Börgers et al. 2008; Bosman et al. 2012; Kim et al. 2016, 2015). Therefore, the low frequency fluctuation signature may also reflect a PV network state capable of strong gamma rhythm generation to facilitate attention and successful learning.

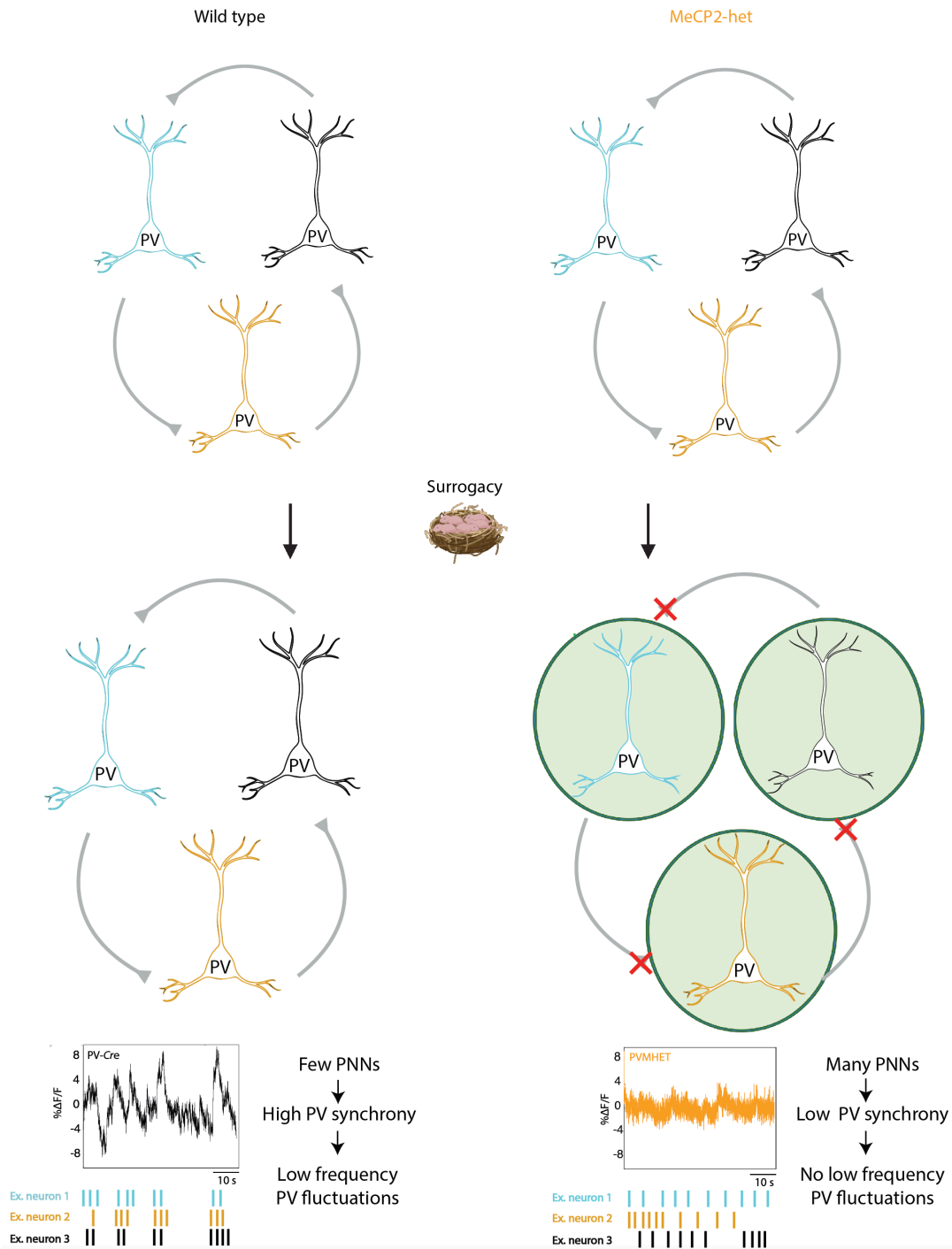


Figure 6.1: Proposed model for lack of ACTx PV low frequency fluctuations in MeCP2^{het} mice. We propose that the well-documented strong PV-PV connectivity in wild type mice results in highly synchronous ACTx PV neural activity. Such synchronous population activity is reflected in the pronounced peaks of the wild type fiber photometry signal. In contrast, we propose that the overexpression of PNNs in MeCP2^{het} surrogates impairs PV-PV connectivity. This weakened PV-PV connectivity results in less synchronous PV population activity, which is reflected in the lack of ACTx PV low frequency fluctuations.

6.3 Future directions

The results reported in this thesis shed significant light onto the role of the ACtx PV network in facilitating periods of adult experience-dependent plasticity, and the consequences of this network's dysregulation. Furthermore, our findings have bolstered the case for PV network-targeted therapeutic interventions for neurodevelopmental disorders such as RTT that are characterized by neural plasticity aberrations. Specifically, our results suggest that the timing of such interventions is critical, and would be optimal during periods of heightened plasticity demands. However, by no means do our findings leave us with a complete picture of how the ACtx PV network regulates critical periods for plasticity. While we have proposed various additional experiments to complement our current results throughout this thesis, here we will outline several broad directions for future study to address some of the outstanding ambiguities:

- How does aberrant ACtx PV activity affect other neuronal subpopulations within the ACtx microcircuit, and ACtx projections to downstream targets?
- How generalizable are the low frequency ACtx PV fluctuations? Are they specific to the ACtx, or are they seen in other cortical regions?
- How is PV-mediated inhibition modulated by behavioral states such as attention, arousal, or emotional salience, and how might the PV population may play a role in these state transitions?
- What are the cell-autonomous molecular events that relate PV activity and PNN assembly, and what role may MeCP2 play in this molecular cascade?

Taken together, investigations into these questions and more will help to refine our understanding of the ACtx PV network's role in facilitating adult experience-dependent plasticity, and the network and behavioral-level consequences of its dysregulation in the disease context.

Fin

Bibliography

- Alitto HJ, Dan Y. 2012. Cell-type-specific modulation of neocortical activity by basal forebrain input. *Front Syst Neurosci* **6**: 79.
- Alsina-Llanes M, De Brun V, Olazábal DE. 2015. Development and expression of maternal behavior in naïve female C57BL/6 mice. *Dev Psychobiol* **57**: 189–200.
- Amir RE, Van den Veyver IB, Wan M, Tran CQ, Francke U, Zoghbi HY. 1999. Rett syndrome is caused by mutations in X-linked MECP2, encoding methyl-CpG-binding protein 2. *Nat Genet* **23**: 185–188.
- Archer H, Evans J, Leonard H, Colvin L, Ravine D, Christodoulou J, Williamson S, Charman T, Bailey MES, Sampson J, et al. 2007. Correlation between clinical severity in patients with Rett syndrome with a p.R168X or p.T158M MECP2 mutation, and the direction and degree of skewing of X-chromosome inactivation. *J Med Genet* **44**: 148–152.
- Arroyo S, Bennett C, Aziz D, Brown SP, Hestrin S. 2012. Prolonged disynaptic inhibition in the cortex mediated by slow, non- $\alpha 7$ nicotinic excitation of a specific subset of cortical interneurons. *J Neurosci* **32**: 3859–3864.
- Baj G, Patrizio A, Montalbano A, Sciancalepore M, Tongiorgi E. 2014. Developmental and maintenance defects in Rett syndrome neurons identified by a new mouse staging system in vitro. *Front Cell Neurosci* **8**: 18.
- Bala AD, Takahashi TT. 2000. Pupillary dilation response as an indicator of auditory discrimination in the barn owl. *J Comp Physiol A* **186**: 425–434.
- Barnes SJ, Finnerty GT. 2010. Sensory experience and cortical rewiring. *The Neuroscientist* **16**: 186–198.
- Bartholome O, de la Brassinne Bonardeaux O, Neirinckx V, Rogister B. 2020. A Composite Sketch of Fast-Spiking Parvalbumin-Positive Neurons. *Cereb Cortex Commun* **1**: tga026.
- Bartos M, Vida I, Jonas P. 2007. Synaptic mechanisms of synchronized gamma oscillations in inhibitory interneuron networks. *Nat Rev Neurosci* **8**: 45–56.
- Bienvenu T, Carrié A, de Roux N, Vinet MC, Jonveaux P, Couvert P, Villard L, Arzimanoglou A, Beldjord C, Fontes M, et al. 2000. MECP2 mutations account for most cases of typical forms of Rett syndrome. *Hum Mol Genet* **9**: 1377–1384.
- Bloem B, Poorthuis RB, Mansvelder HD. 2014. Cholinergic modulation of the medial prefrontal cortex: the role of nicotinic receptors in attention and regulation of neuronal activity. *Front Neural Circuits* **8**: 17.

- Börgers C, Epstein S, Kopell NJ. 2008. Gamma oscillations mediate stimulus competition and attentional selection in a cortical network model. *Proceedings of the National Academy of Sciences* **105**: 18023–18028.
- Bosman CA, Schoffelen J-M, Brunet N, Oostenveld R, Bastos AM, Womelsdorf T, Rubehn B, Stieglitz T, De Weerd P, Fries P. 2012. Attentional stimulus selection through selective synchronization between monkey visual areas. *Neuron* **75**: 875–888.
- Boyes J, Bird A. 1991. DNA methylation inhibits transcription indirectly via a methyl-CpG binding protein. *Cell* **64**: 1123–1134.
- Bradley MM, Miccoli L, Escrig MA, Lang PJ. 2008. The pupil as a measure of emotional arousal and autonomic activation. *Psychophysiology* **45**: 602–607.
- Braunschweig D, Simcox T, Samaco RC, LaSalle JM. 2004. X-Chromosome inactivation ratios affect wild-type MeCP2 expression within mosaic Rett syndrome and *Mecp2*^{-/+} mouse brain. *Hum Mol Genet* **13**: 1275–1286.
- Brückner G, Brauer K, Härtig W, Wolff JR, Rickmann MJ, Derouiche A, Delpesch B, Girard N, Oertel WH, Reichenbach A. 1993. Perineuronal nets provide a polyanionic, glia-associated form of microenvironment around certain neurons in many parts of the rat brain. *Glia* **8**: 183–200.
- Busque L, Mio R, Mattioli J, Brais E, Blais N, Lalonde Y, Maragh M, Gilliland DG. 1996. Nonrandom X-Inactivation Patterns in Normal Females: Lyonization Ratios Vary With Age. *Blood* **88**: 59–65.
- Callaway EM. 2004. Feedforward, feedback and inhibitory connections in primate visual cortex. *Neural Netw* **17**: 625–632.
- Carcea I, Caraballo NL, Marlin BJ, Ooyama R, Riceberg JS, Mendoza Navarro JM, Opendak M, Diaz VE, Schuster L, Alvarado Torres MI, et al. 2021. Oxytocin neurons enable social transmission of maternal behaviour. *Nature* **596**: 553–557.
- Cardin JA, Carlén M, Meletis K, Knoblich U, Zhang F, Deisseroth K, Tsai L-H, Moore CI. 2009. Driving fast-spiking cells induces gamma rhythm and controls sensory responses. *Nature* **459**: 663–667.
- Carulli D, Pizzorusso T, Kwok JCF, Putignano E, Poli A, Forostyak S, Andrews MR, Deepa SS, Glant TT, Fawcett JW. 2010. Animals lacking link protein have attenuated perineuronal nets and persistent plasticity. *Brain* **133**: 2331–2347.
- Chahrouh M, Jung SY, Shaw C, Zhou X, Wong STC, Qin J, Zoghbi HY. 2008. MeCP2, a Key Contributor to Neurological Disease, Activates and Represses Transcription. *Science* **320**: 1224–1229.

- Chattopadhyaya B, Di Cristo G, Wu CZ, Knott G, Kuhlman S, Fu Y, Palmiter RD, Huang ZJ. 2007. GAD67-mediated GABA Synthesis and Signaling Regulate Inhibitory Synaptic Innervation in the Visual Cortex. *Neuron* **54**: 889–903.
- Chen RZ, Akbarian S, Tudor M, Jaenisch R. 2001. Deficiency of methyl-CpG binding protein-2 in CNS neurons results in a Rett-like phenotype in mice. *Nat Genet* **27**: 327–331.
- Cheval H, Guy J, Merusi C, De Sousa D, Selfridge J, Bird A. 2012. Postnatal inactivation reveals enhanced requirement for MeCP2 at distinct age windows. *Hum Mol Genet* **21**: 3806–3814.
- Cisneros-Franco JM, de Villers-Sidani É. 2019. Reactivation of critical period plasticity in adult auditory cortex through chemogenetic silencing of parvalbumin-positive interneurons. *Proc Natl Acad Sci U S A* **116**: 26329–26331.
- Cohen L, Mizrahi A. 2015. Plasticity during Motherhood: Changes in Excitatory and Inhibitory Layer 2/3 Neurons in Auditory Cortex. *J Neurosci* **35**: 1806–1815.
- Cohen L, Rothschild G, Mizrahi A. 2011. Multisensory integration of natural odors and sounds in the auditory cortex. *Neuron* **72**: 357–369.
- Connors BW, Gutnick MJ. 1990. Intrinsic firing patterns of diverse neocortical neurons. *Trends Neurosci* **13**: 99–104.
- Corona A, Choe J, Muñoz-Castañeda R, Osten P, Shea SD. 2022. A circuit from the locus coeruleus to the anterior cingulate cortex modulates offspring interactions in mice. 2022.12.04.519053. <https://www.biorxiv.org/content/10.1101/2022.12.04.519053v1> (Accessed March 11, 2023).
- D'amour JA, Froemke RC. 2015. Inhibitory and excitatory spike-timing-dependent plasticity in the auditory cortex. *Neuron* **86**: 514–528.
- Dani VS, Chang Q, Maffei A, Turrigiano GG, Jaenisch R, Nelson SB. 2005. Reduced cortical activity due to a shift in the balance between excitation and inhibition in a mouse model of Rett syndrome. *Proc Natl Acad Sci USA* **102**: 12560–12565.
- Day AJ, Prestwich GD. 2002. Hyaluronan-binding proteins: tying up the giant. *J Biol Chem* **277**: 4585–4588.
- DeFelipe J. 1993. Neocortical neuronal diversity: chemical heterogeneity revealed by colocalization studies of classic neurotransmitters, neuropeptides, calcium-binding proteins, and cell surface molecules. *Cereb Cortex* **3**: 273–289.
- DeFelipe J. 1997. Types of neurons, synaptic connections and chemical characteristics of cells immunoreactive for calbindin-D28K, parvalbumin and calretinin in the neocortex. *J Chem Neuroanat* **14**: 1–19.

- DeFelipe J, López-Cruz PL, Benavides-Piccione R, Bielza C, Larrañaga P, Anderson S, Burkhalter A, Cauli B, Fairén A, Feldmeyer D, et al. 2013. New insights into the classification and nomenclature of cortical GABAergic interneurons. *Nat Rev Neurosci* **14**: 202–216.
- Deidda G, Parrini M, Naskar S, Bozarth IF, Contestabile A, Cancedda L. 2015. Reversing excitatory GABAAR signaling restores synaptic plasticity and memory in a mouse model of Down syndrome. *Nat Med* **21**: 318–326.
- Deleuze C, Bhumbra GS, Paziienti A, Lourenço J, Mailhes C, Aguirre A, Beato M, Bacci A. 2019. Strong preference for autaptic self-connectivity of neocortical PV interneurons facilitates their tuning to γ -oscillations. *PLoS Biol* **17**: e3000419.
- Demars MP, Morishita H. 2014. Cortical parvalbumin and somatostatin GABA neurons express distinct endogenous modulators of nicotinic acetylcholine receptors. *Mol Brain* **7**: 75.
- Devienne G, Picaud S, Cohen I, Piquet J, Tricoire L, Testa D, Nardo AAD, Rossier J, Cauli B, Lambolez B. 2021. Regulation of perineuronal nets in the adult cortex by the activity of the cortical network. *J Neurosci*.
<https://www.jneurosci.org/content/early/2021/05/25/JNEUROSCI.0434-21.2021>
(Accessed June 1, 2021).
- Di Cristo G, Chattopadhyaya B, Kuhlman SJ, Fu Y, Bélanger M-C, Wu CZ, Rutishauser U, Maffei L, Huang ZJ. 2007. Activity-dependent PSA expression regulates inhibitory maturation and onset of critical period plasticity. *Nat Neurosci* **10**: 1569–1577.
- Disteche CM, Berletch JB. 2015. X-chromosome inactivation and escape. *J Genet* **94**: 591–599.
- Dityatev A, Brückner G, Dityateva G, Grosche J, Kleene R, Schachner M. 2007. Activity-dependent formation and functions of chondroitin sulfate-rich extracellular matrix of perineuronal nets. *Dev Neurobiol* **67**: 570–588.
- Donato F, Rompani SB, Caroni P. 2013. Parvalbumin-expressing basket-cell network plasticity induced by experience regulates adult learning. *Nature* **504**: 272–276.
- Dvorkin R, Shea SD. 2022. Precise and Pervasive Phasic Bursting in Locus Coeruleus during Maternal Behavior in Mice. *J Neurosci* **42**: 2986–2999.
- Eales LA. 1987. Song learning in female-raised zebra finches: another look at the sensitive phase. *Animal Behaviour* **35**: 1356–1365.
- Ehret G. 2005. Infant rodent ultrasounds -- a gate to the understanding of sound communication. *Behav Genet* **35**: 19–29.
- Ehret G. 1987. Left hemisphere advantage in the mouse brain for recognizing ultrasonic communication calls. *Nature* **325**: 249–251.

- Elyada YM, Mizrahi A. 2015. Becoming a mother—circuit plasticity underlying maternal behavior. *Current Opinion in Neurobiology* **35**: 49–56.
- Erzurumlu RS, Gaspar P. 2012. Development and critical period plasticity of the barrel cortex. *Eur J Neurosci* **35**: 1540–1553.
- Etter G, van der Veldt S, Manseau F, Zarrinkoub I, Trillaud-Doppia E, Williams S. 2019. Optogenetic gamma stimulation rescues memory impairments in an Alzheimer’s disease mouse model. *Nat Commun* **10**: 5322.
- Everitt BJ, Robbins TW. 1997. Central cholinergic systems and cognition. *Annu Rev Psychol* **48**: 649–684.
- Fagiolini M, Fritschy J-M, Löw K, Möhler H, Rudolph U, Hensch TK. 2004. Specific GABAA circuits for visual cortical plasticity. *Science* **303**: 1681–1683.
- Fagiolini M, Hensch TK. 2000. Inhibitory threshold for critical-period activation in primary visual cortex. *Nature* **404**: 183–186.
- Fang Y-Y, Yamaguchi T, Song SC, Tritsch NX, Lin D. 2018. A Hypothalamic Midbrain Pathway Essential for Driving Maternal Behaviors. *Neuron* **98**: 192-207.e10.
- Favuzzi E, Marques-Smith A, Deogracias R, Winterflood CM, Sánchez-Aguilera A, Mantoan L, Maeso P, Fernandes C, Ewers H, Rico B. 2017. Activity-Dependent Gating of Parvalbumin Interneuron Function by the Perineuronal Net Protein Brevican. *Neuron* **95**: 639-655.e10.
- Francis NA, Winkowski DE, Sheikhattar A, Armengol K, Babadi B, Kanold PO. 2018. Small Networks Encode Decision-Making in Primary Auditory Cortex. *Neuron* **97**: 885-897.e6.
- Friard O, Gamba M. 2016. BORIS: a free, versatile open-source event-logging software for video/audio coding and live observations. *Methods in Ecology and Evolution* **7**: 1325–1330.
- Galarreta M, Hestrin S. 1999. A network of fast-spiking cells in the neocortex connected by electrical synapses. *Nature* **402**: 72–75.
- Galindo-Leon EE, Lin FG, Liu RC. 2009. Inhibitory Plasticity in a Lateral Band Improves Cortical Detection of Natural Vocalizations. *Neuron* **62**: 705–716.
- Geiger JR, Lübke J, Roth A, Frotscher M, Jonas P. 1997. Submillisecond AMPA receptor-mediated signaling at a principal neuron-interneuron synapse. *Neuron* **18**: 1009–1023.
- Geissler DB, Ehret G. 2004. Auditory perception vs. recognition: representation of complex communication sounds in the mouse auditory cortical fields. *European Journal of Neuroscience* **19**: 1027–1040.

- Ghazanfar AA, Schroeder CE. 2006. Is neocortex essentially multisensory? *Trends Cogn Sci* **10**: 278–285.
- Giamanco KA, Matthews RT. 2012. Deconstructing the perineuronal net: cellular contributions and molecular composition of the neuronal extracellular matrix. *Neuroscience* **218**: 367–384.
- Goard M, Dan Y. 2009. Basal forebrain activation enhances cortical coding of natural scenes. *Nat Neurosci* **12**: 1444–1449.
- Gogolla N, Caroni P, Lüthi A, Herry C. 2009. Perineuronal nets protect fear memories from erasure. *Science* **325**: 1258–1261.
- Gold WA, Krishnaraj R, Ellaway C, Christodoulou J. 2018. Rett Syndrome: A Genetic Update and Clinical Review Focusing on Comorbidities. *ACS Chem Neurosci* **9**: 167–176.
- Good KV, Vincent JB, Ausió J. 2021. MeCP2: The Genetic Driver of Rett Syndrome Epigenetics. *Front Genet* **12**: 620859.
- Guillem K, Bloem B, Poorthuis RB, Loos M, Smit AB, Maskos U, Spijker S, Mansvelder HD. 2011. Nicotinic acetylcholine receptor $\beta 2$ subunits in the medial prefrontal cortex control attention. *Science* **333**: 888–891.
- Gurevicius K, Gureviciene I, Valjakka A, Schachner M, Tanila H. 2004. Enhanced cortical and hippocampal neuronal excitability in mice deficient in the extracellular matrix glycoprotein tenascin-R. *Mol Cell Neurosci* **25**: 515–523.
- Guy J, Hendrich B, Holmes M, Martin JE, Bird A. 2001. A mouse *Mecp2*-null mutation causes neurological symptoms that mimic Rett syndrome. *Nat Genet* **27**: 322–326.
- Hackett TA, Schroeder CE. 2009. Multisensory integration in auditory and auditory-related areas of cortex. *Hear Res* **258**: 1–3.
- Hanover JL, Huang ZJ, Tonegawa S, Stryker MP. 1999. Brain-derived neurotrophic factor overexpression induces precocious critical period in mouse visual cortex. *J Neurosci* **19**: RC40.
- Happel MFK, Niekisch H, Castiblanco Rivera LL, Ohl FW, Deliano M, Frischknecht R. 2014. Enhanced cognitive flexibility in reversal learning induced by removal of the extracellular matrix in auditory cortex. *Proc Natl Acad Sci U S A* **111**: 2800–2805.
- Harauzov A, Spolidoro M, DiCristo G, De Pasquale R, Cancedda L, Pizzorusso T, Viegi A, Berardi N, Maffei L. 2010. Reducing intracortical inhibition in the adult visual cortex promotes ocular dominance plasticity. *J Neurosci* **30**: 361–371.
- Härtig W, Brauer K, Brückner G. 1992. Wisteria floribunda agglutinin-labelled nets surround parvalbumin-containing neurons. *Neuroreport* **3**: 869–872.

- Härtig W, Derouiche A, Welt K, Brauer K, Grosche J, Mäder M, Reichenbach A, Brückner G. 1999. Cortical neurons immunoreactive for the potassium channel Kv3.1b subunit are predominantly surrounded by perineuronal nets presumed as a buffering system for cations. *Brain Res* **842**: 15–29.
- He L, Liu N, Cheng T, Chen X, Li Y, Shu Y, Qiu Z, Zhang X. 2014. Conditional deletion of *MeCP2* in parvalbumin-expressing GABAergic cells results in the absence of critical period plasticity. *Nat Commun* **5**: 5036.
- Hensch TK. 2005. Critical period plasticity in local cortical circuits. *Nat Rev Neurosci* **6**: 877–888.
- Hensch TK, Fagiolini M, Mataga N, Stryker MP, Baekkeskov S, Kash SF. 1998. Local GABA circuit control of experience-dependent plasticity in developing visual cortex. *Science* **282**: 1504–1508.
- Hofer SB, Mrsic-Flogel TD, Bonhoeffer T, Hübener M. 2006. Prior experience enhances plasticity in adult visual cortex. *Nat Neurosci* **9**: 127–132.
- Horvath PM, Monteggia LM. 2018. MeCP2 as an Activator of Gene Expression. *Trends Neurosci* **41**: 72–74.
- House DR, Elstrott J, Koh E, Chung J, Feldman DE. 2011. Parallel regulation of feedforward inhibition and excitation during whisker map plasticity. *Neuron* **72**: 819–831.
- Huang ZJ, Kirkwood A, Pizzorusso T, Porciatti V, Morales B, Bear MF, Maffei L, Tonegawa S. 1999. BDNF regulates the maturation of inhibition and the critical period of plasticity in mouse visual cortex. *Cell* **98**: 739–755.
- Hubel DH, Henson CO, Rupert A, Galambos R. 1959. “Attention” Units in the Auditory Cortex. *Science* **129**: 1279–1280.
- Hubel DH, Wiesel TN. 1970. The period of susceptibility to the physiological effects of unilateral eye closure in kittens. *The Journal of Physiology* **206**: 419–436.
- Ibrahim A, Papin C, Mohideen-Abdul K, Le Gras S, Stoll I, Bronner C, Dimitrov S, Klaholz BP, Hamiche A. 2021. MeCP2 is a microsatellite binding protein that protects CA repeats from nucleosome invasion. *Science* **372**: eabd5581.
- Ito-Ishida A, Ure K, Chen H, Swann JW, Zoghbi HY. 2015. Loss of MeCP2 in Parvalbumin-and Somatostatin-Expressing Neurons in Mice Leads to Distinct Rett Syndrome-like Phenotypes. *Neuron* **88**: 651–658.
- Iwai Y, Fagiolini M, Obata K, Hensch TK. 2003. Rapid critical period induction by tonic inhibition in visual cortex. *J Neurosci* **23**: 6695–6702.

- Jing M, Li Y, Zeng J, Huang P, Skirzewski M, Kljakic O, Peng W, Qian T, Tan K, Zou J, et al. 2020. An optimized acetylcholine sensor for monitoring in vivo cholinergic activity. *Nat Methods* **17**: 1139–1146.
- Kamphuis W, Huisman E, Wadman WJ, Heizmann CW, Lopes da Silva FH. 1989. Kindling induced changes in parvalbumin immunoreactivity in rat hippocampus and its relation to long-term decrease in GABA-immunoreactivity. *Brain Res* **479**: 23–34.
- Karnani MM, Agetsuma M, Yuste R. 2014. A blanket of inhibition: functional inferences from dense inhibitory connectivity. *Curr Opin Neurobiol* **26**: 96–102.
- Kawaguchi Y, Kubota Y. 1997. GABAergic cell subtypes and their synaptic connections in rat frontal cortex. *Cereb Cortex* **7**: 476–486.
- Kawaguchi Y, Wilson CJ, Augood SJ, Emson PC. 1995. Striatal interneurons: chemical, physiological and morphological characterization. *Trends in Neurosciences* **18**: 527–535.
- Kepecs A, Fishell G. 2014. Interneuron cell types are fit to function. *Nature* **505**: 318–326.
- Kim H, Åhrlund-Richter S, Wang X, Deisseroth K, Carlén M. 2016. Prefrontal Parvalbumin Neurons in Control of Attention. *Cell* **164**: 208–218.
- Kim T, Thankachan S, McKenna JT, McNally JM, Yang C, Choi JH, Chen L, Kocsis B, Deisseroth K, Strecker RE, et al. 2015. Cortically projecting basal forebrain parvalbumin neurons regulate cortical gamma band oscillations. *Proc Natl Acad Sci U S A* **112**: 3535–3540.
- Kirby RS, Lane JB, Childers J, Skinner SA, Annese F, Barrish JO, Glaze DG, Macleod P, Percy AK. 2010. Longevity in Rett syndrome: analysis of the North American Database. *J Pediatr* **156**: 135-138.e1.
- Kishi N, Macklis JD. 2004. MECP2 is progressively expressed in post-migratory neurons and is involved in neuronal maturation rather than cell fate decisions. *Mol Cell Neurosci* **27**: 306–321.
- Knudsen EI. 2004. Sensitive Periods in the Development of the Brain and Behavior. *Journal of Cognitive Neuroscience* **16**: 1412–1425.
- Koch M, Ehret G. 1989. Estradiol and parental experience, but not prolactin are necessary for ultrasound recognition and pup-retrieving in the mouse. *Physiology & Behavior* **45**: 771–776.
- Krashes MJ, Koda S, Ye C, Rogan SC, Adams AC, Cusher DS, Maratos-Flier E, Roth BL, Lowell BB. 2011. Rapid, reversible activation of AgRP neurons drives feeding behavior in mice. *J Clin Invest* **121**: 1424–1428.
- Krishnan K, Lau BYB, Ewall G, Huang ZJ, Shea SD. 2017. MECP2 regulates cortical plasticity underlying a learned behaviour in adult female mice. *Nature Communications* **8**: 14077.

- Krishnan K, Wang B-S, Lu J, Wang L, Maffei A, Cang J, Huang ZJ. 2015. MeCP2 regulates the timing of critical period plasticity that shapes functional connectivity in primary visual cortex. *Proc Natl Acad Sci U S A* **112**: E4782–E4791.
- Kuchibhotla K, Bathellier B. 2018. Neural encoding of sensory and behavioral complexity in the auditory cortex. *Curr Opin Neurobiol* **52**: 65–71.
- Kuhlman SJ, Lu J, Lazarus MS, Huang ZJ. 2010. Maturation of GABAergic inhibition promotes strengthening of temporally coherent inputs among convergent pathways. *PLoS Comput Biol* **6**: e1000797.
- Kuramoto E, Tanaka YR, Hioki H, Goto T, Kaneko T. 2022. Local Connections of Pyramidal Neurons to Parvalbumin-Producing Interneurons in Motor-Associated Cortical Areas of Mice. *eNeuro* **9**. <https://www.eneuro.org/content/9/1/ENEURO.0567-20.2021> (Accessed February 9, 2023).
- Lakatos P, Chen C-M, O’Connell MN, Mills A, Schroeder CE. 2007. Neuronal oscillations and multisensory interaction in primary auditory cortex. *Neuron* **53**: 279–292.
- Lau BYB, Krishnan K, Huang ZJ, Shea SD. 2020. Maternal experience-dependent cortical plasticity in mice is circuit- and stimulus-specific and requires MECP2. *J Neurosci*. <https://www.jneurosci.org/content/early/2020/01/06/JNEUROSCI.1964-19.2019> (Accessed January 14, 2020).
- Lendvai B, Stern EA, Chen B, Svoboda K. 2000. Experience-dependent plasticity of dendritic spines in the developing rat barrel cortex in vivo. *Nature* **404**: 876–881.
- Lensjø KK, Lepperød ME, Dick G, Hafting T, Fyhn M. 2017. Removal of Perineuronal Nets Unlocks Juvenile Plasticity Through Network Mechanisms of Decreased Inhibition and Increased Gamma Activity. *J Neurosci* **37**: 1269–1283.
- Li Y, Wang H, Muffat J, Cheng AW, Orlando DA, Lovén J, Kwok S, Feldman DA, Bateup HS, Gao Q, et al. 2013. Global transcriptional and translational repression in human embryonic stem cells-derived Rett Syndrome neurons. *Cell Stem Cell* **13**: 446–458.
- Lin FG, Galindo-Leon EE, Ivanova TN, Mappus RC, Liu RC. 2013. A role for maternal physiological state in preserving auditory cortical plasticity for salient infant calls. *Neuroscience* **247**: 102–116.
- Lisi M, Bonato M, Zorzi M. 2015. Pupil dilation reveals top-down attentional load during spatial monitoring. *Biol Psychol* **112**: 39–45.
- Liu RC, Linden JF, Schreiner CE. 2006. Improved cortical entrainment to infant communication calls in mothers compared with virgin mice. *Eur J Neurosci* **23**: 3087–3097.
- Liu RC, Schreiner CE. 2007. Auditory Cortical Detection and Discrimination Correlates with Communicative Significance. *PLOS Biology* **5**: e173.

- Lu J, Li C, Zhao J-P, Poo M, Zhang X. 2007. Spike-Timing-Dependent Plasticity of Neocortical Excitatory Synapses on Inhibitory Interneurons Depends on Target Cell Type. *J Neurosci* **27**: 9711–9720.
- MacLaren DAA, Browne RW, Shaw JK, Krishnan Radhakrishnan S, Khare P, España RA, Clark SD. 2016. Clozapine N-Oxide Administration Produces Behavioral Effects in Long-Evans Rats: Implications for Designing DREADD Experiments. *eNeuro* **3**: ENEURO.0219-16.2016.
- Maffei A, Lambo ME, Turrigiano GG. 2010. Critical Period for Inhibitory Plasticity in Rodent Binocular V1. *J Neurosci* **30**: 3304–3309.
- Maffei A, Nataraj K, Nelson SB, Turrigiano GG. 2006. Potentiation of cortical inhibition by visual deprivation. *Nature* **443**: 81–84.
- Mahn M, Gibor L, Patil P, Malina KC-K, Oring S, Printz Y, Levy R, Lampl I, Yizhar O. 2018. High-efficiency optogenetic silencing with soma-targeted anion-conducting channelrhodopsins. *Nat Commun* **9**: 1–15.
- Markram H, Toledo-Rodriguez M, Wang Y, Gupta A, Silberberg G, Wu C. 2004. Interneurons of the neocortical inhibitory system. *Nature Reviews Neuroscience* **5**: 793–807.
- Marlin BJ, Mitre M, D’amour JA, Chao MV, Froemke RC. 2015. Oxytocin enables maternal behaviour by balancing cortical inhibition. *Nature* **520**: 499–504.
- Martín-Sánchez A, Valera-Marín G, Hernández-Martínez A, Lanuza E, Martínez-García F, Agustín-Pavón C. 2015. Wired for motherhood: induction of maternal care but not maternal aggression in virgin female CD1 mice. *Front Behav Neurosci* **9**: 197.
- Mathis A, Mamidanna P, Cury KM, Abe T, Murthy VN, Mathis MW, Bethge M. 2018. DeepLabCut: markerless pose estimation of user-defined body parts with deep learning. *Nat Neurosci* **21**: 1281–1289.
- McGinley MJ, David SV, McCormick DA. 2015. Cortical membrane potential signature of optimal states for sensory signal detection. *Neuron* **87**: 179–192.
- McGraw CM, Samaco RC, Zoghbi HY. 2011. Adult neural function requires MeCP2. *Science* **333**: 186.
- Metcalf BM, Mullaney BC, Johnston MV, Blue ME. 2006. Temporal shift in methyl-CpG binding protein 2 expression in a mouse model of Rett syndrome. *Neuroscience* **139**: 1449–1460.
- Miyata S, Kitagawa H. 2017. Formation and remodeling of the brain extracellular matrix in neural plasticity: Roles of chondroitin sulfate and hyaluronan. *Biochim Biophys Acta Gen Subj* **1861**: 2420–2434.

- Morello N, Schina R, Pilotto F, Phillips M, Melani R, Plicato O, Pizzorusso T, Pozzo-Miller L, Giustetto M. 2018. Loss of Mecp2 Causes Atypical Synaptic and Molecular Plasticity of Parvalbumin-Expressing Interneurons Reflecting Rett Syndrome–Like Sensorimotor Defects. *eNeuro* **5**: ENEURO.0086-18.2018.
- Morrison RG, Nottebohm F. 1993. Role of a telencephalic nucleus in the delayed song learning of socially isolated zebra finches. *Journal of Neurobiology* **24**: 1045–1064.
- Murase S, Lantz CL, Quinlan EM. 2017. Light reintroduction after dark exposure reactivates plasticity in adults via perisynaptic activation of MMP-9 ed. S.B. Nelson. *eLife* **6**: e27345.
- Musall S, Kaufman MT, Juavinett AL, Gluf S, Churchland AK. 2019. Single-trial neural dynamics are dominated by richly varied movements. *Nat Neurosci* **22**: 1677–1686.
- Myers MM, Ali N, Weller A, Brunelli SA, Tu AY, Hofer MA, Shair HN. 2004. Brief maternal interaction increases number, amplitude, and bout size of isolation-induced ultrasonic vocalizations in infant rats (*Rattus norvegicus*). *J Comp Psychol* **118**: 95–102.
- Na ES, Nelson ED, Kavalali ET, Monteggia LM. 2013. The Impact of MeCP2 Loss- or Gain-of-Function on Synaptic Plasticity. *Neuropsychopharmacology* **38**: 212–219.
- Nan X, Campoy FJ, Bird A. 1997. MeCP2 is a transcriptional repressor with abundant binding sites in genomic chromatin. *Cell* **88**: 471–481.
- Nan X, Ng HH, Johnson CA, Laherty CD, Turner BM, Eisenman RN, Bird A. 1998. Transcriptional repression by the methyl-CpG-binding protein MeCP2 involves a histone deacetylase complex. *Nature* **393**: 386–389.
- Neul JL, Kaufmann WE, Glaze DG, Christodoulou J, Clarke AJ, Bahi-Buisson N, Leonard H, Bailey MES, Schanen NC, Zappella M, et al. 2010. Rett syndrome: revised diagnostic criteria and nomenclature. *Ann Neurol* **68**: 944–950.
- Neul JL, Lane JB, Lee H-S, Geerts S, Barrish JO, Annese F, Baggett LM, Barnes K, Skinner SA, Motil KJ, et al. 2014. Developmental delay in Rett syndrome: data from the natural history study. *J Neurodev Disord* **6**: 20.
- Nguyen MVC, Du F, Felice CA, Shan X, Nigam A, Mandel G, Robinson JK, Ballas N. 2012. MeCP2 is critical for maintaining mature neuronal networks and global brain anatomy during late stages of postnatal brain development and in the mature adult brain. *J Neurosci* **32**: 10021–10034.
- Niwa M, Johnson JS, O’Connor KN, Sutter ML. 2012. Activity related to perceptual judgment and action in primary auditory cortex. *J Neurosci* **32**: 3193–3210.
- Nowlan AC, Kelahan C, Shea SD. 2022. Multisensory integration of social signals by a pathway from the basal amygdala to the auditory cortex in maternal mice. 2022.02.17.480854.

<https://www.biorxiv.org/content/10.1101/2022.02.17.480854v1> (Accessed March 11, 2023).

- Packer AM, Yuste R. 2011. Dense, Unspecific Connectivity of Neocortical Parvalbumin-Positive Interneurons: A Canonical Microcircuit for Inhibition? *J Neurosci* **31**: 13260–13271.
- Pakan JM, Lowe SC, Dylida E, Keemink SW, Currie SP, Coutts CA, Rochefort NL. 2016. Behavioral-state modulation of inhibition is context-dependent and cell type specific in mouse visual cortex. *Elife* **5**: e14985.
- Patrizi A, Awad PN, Chattopadhyaya B, Li C, Di Cristo G, Fagiolini M. 2020. Accelerated Hyper-Maturation of Parvalbumin Circuits in the Absence of MeCP2. *Cerebral Cortex* **30**: 256–268.
- Patz S, Grabert J, Gorba T, Wirth MJ, Wahle P. 2004. Parvalbumin expression in visual cortical interneurons depends on neuronal activity and TrkB ligands during an Early period of postnatal development. *Cereb Cortex* **14**: 342–351.
- Percy AK. 2011. Rett syndrome: exploring the autism link. *Arch Neurol* **68**: 985–989.
- Percy AK, Lane JB, Childers J, Skinner S, Annese F, Barrish J, Caeg E, Glaze DG, MacLeod P. 2007. Rett syndrome: North American database. *J Child Neurol* **22**: 1338–1341.
- Percy AK, Zoghbi HY, Lewis KR, Jankovic J. 1988. Rett syndrome: qualitative and quantitative differentiation from autism. *J Child Neurol* **3 Suppl**: S65-67.
- Pereira G, Dória S. 2021. X-chromosome inactivation: implications in human disease. *J Genet* **100**: 63.
- Petersen CCH, Crochet S. 2013. Synaptic computation and sensory processing in neocortical layer 2/3. *Neuron* **78**: 28–48.
- Petilla Interneuron Nomenclature Group, Ascoli GA, Alonso-Nanclares L, Anderson SA, Barrionuevo G, Benavides-Piccione R, Burkhalter A, Buzsáki G, Cauli B, Defelipe J, et al. 2008. Petilla terminology: nomenclature of features of GABAergic interneurons of the cerebral cortex. *Nat Rev Neurosci* **9**: 557–568.
- Pini G, Bigoni S, Congiu L, Romanelli AM, Scusa MF, Di Marco P, Benincasa A, Morescalchi P, Ferlini A, Bianchi F, et al. 2016. Rett syndrome: a wide clinical and autonomic picture. *Orphanet J Rare Dis* **11**: 132.
- Pizzorusso T, Medini P, Berardi N, Chierzi S, Fawcett JW, Maffei L. 2002. Reactivation of Ocular Dominance Plasticity in the Adult Visual Cortex. *Science* **298**: 1248–1251.
- Poulet JFA. 2014. Keeping an eye on cortical states. *Neuron* **84**: 246–248.
- Privitera CM, Renninger LW, Carney T, Klein S, Aguilar M. 2010. Pupil dilation during visual target detection. *J Vis* **10**: 3.

- Reh RK, Dias BG, Nelson CA, Kaufer D, Werker JF, Kolb B, Levine JD, Hensch TK. 2020. Critical period regulation across multiple timescales. *Proc Natl Acad Sci U S A* **117**: 23242–23251.
- Reimer J, Froudarakis E, Cadwell CR, Yatsenko D, Denfield GH, Tolias AS. 2014. Pupil Fluctuations Track Fast Switching of Cortical States during Quiet Wakefulness. *Neuron* **84**: 355–362.
- Reimer J, McGinley MJ, Liu Y, Rodenkirch C, Wang Q, McCormick DA, Tolias AS. 2016. Pupil fluctuations track rapid changes in adrenergic and cholinergic activity in cortex. *Nat Commun* **7**: 13289.
- Reimers S, Hartlage-Rübsamen M, Brückner G, Rossner S. 2007. Formation of perineuronal nets in organotypic mouse brain slice cultures is independent of neuronal glutamatergic activity. *Eur J Neurosci* **25**: 2640–2648.
- Rosenblatt JS. 1967. Nonhormonal Basis of Maternal Behavior in the Rat. *Science* **156**: 1512–1513.
- Rossier J, Bernard A, Cabungcal J-H, Perrenoud Q, Savoye A, Gallopin T, Hawrylycz M, Cuénod M, Do K, Urban A, et al. 2015. Cortical fast-spiking parvalbumin interneurons enwrapped in the perineuronal net express the metalloproteinases Adamts8, Adamts15 and Neprilysin. *Mol Psychiatry* **20**: 154–161.
- Roth BL. 2016. DREADDs for Neuroscientists. *Neuron* **89**: 683–694.
- Rothschild G, Cohen L, Mizrahi A, Nelken I. 2013. Elevated correlations in neuronal ensembles of mouse auditory cortex following parturition. *J Neurosci* **33**: 12851–12861.
- Rowlands D, Lensjø KK, Dinh T, Yang S, Andrews MR, Hafting T, Fyhn M, Fawcett JW, Dick G. 2018. AggreCAN Directs Extracellular Matrix-Mediated Neuronal Plasticity. *J Neurosci* **38**: 10102–10113.
- Rudy B, Fishell G, Lee S, Hjerling-Leffler J. 2011. Three groups of interneurons account for nearly 100% of neocortical GABAergic neurons. *Dev Neurobiol* **71**: 45–61.
- Rudy B, McBain CJ. 2001. Kv3 channels: voltage-gated K⁺ channels designed for high-frequency repetitive firing. *Trends Neurosci* **24**: 517–526.
- Rupert DD, Pagliaro A, Choe J, Shea SD. 2023. Selective deletion of Methyl CpG binding protein 2 from parvalbumin interneurons in the auditory cortex delays the onset of maternal retrieval in mice. 2023.01.30.526321. <https://www.biorxiv.org/content/10.1101/2023.01.30.526321v1> (Accessed February 19, 2023).
- Rupert DD, Shea SD. 2022. Parvalbumin-Positive Interneurons Regulate Cortical Sensory Plasticity in Adulthood and Development Through Shared Mechanisms. *Front Neural Circuits* **16**: 886629.

- Samaco RC, McGraw CM, Ward CS, Sun Y, Neul JL, Zoghbi HY. 2013. Female *Mecp2*^{+/-} mice display robust behavioral deficits on two different genetic backgrounds providing a framework for pre-clinical studies. *Hum Mol Genet* **22**: 96–109.
- Sattler NJ, Wehr M. 2021. A Head-Mounted Multi-Camera System for Electrophysiology and Behavior in Freely-Moving Mice. *Frontiers in Neuroscience* **14**.
<https://www.frontiersin.org/articles/10.3389/fnins.2020.592417> (Accessed March 10, 2023).
- Schiavo JK, Valtcheva S, Bair-Marshall CJ, Song SC, Martin KA, Froemke RC. 2020. Innate and plastic mechanisms for maternal behaviour in auditory cortex. *Nature* **587**: 426–431.
- Schindelin J, Arganda-Carreras I, Frise E, Kaynig V, Longair M, Pietzsch T, Preibisch S, Rueden C, Saalfeld S, Schmid B, et al. 2012. Fiji: an open-source platform for biological-image analysis. *Nat Methods* **9**: 676–682.
- Schliebs R, Arendt T. 2011. The cholinergic system in aging and neuronal degeneration. *Behav Brain Res* **221**: 555–563.
- Schneider DM, Mooney R. 2018. How Movement Modulates Hearing. *Annu Rev Neurosci* **41**: 553–572.
- Seip KM, Morrell JI. 2008. Exposure to pups influences the strength of maternal motivation in virgin female rats. *Physiol Behav* **95**: 599–608.
- Sewell GD. 1970. Ultrasonic Communication in Rodents. *Nature* **227**: 410–410.
- Shepard KN, Chong KK, Liu RC. 2016. Contrast Enhancement without Transient Map Expansion for Species-Specific Vocalizations in Core Auditory Cortex during Learning. *eNeuro* **3**. <https://www.eneuro.org/content/3/6/ENEURO.0318-16.2016> (Accessed June 5, 2020).
- Shepard KN, Lin FG, Zhao CL, Chong KK, Liu RC. 2015. Behavioral Relevance Helps Untangle Natural Vocal Categories in a Specific Subset of Core Auditory Cortical Pyramidal Neurons. *J Neurosci* **35**: 2636–2645.
- Shoykhet M, Land PW, Simons DJ. 2005. Whisker trimming begun at birth or on postnatal day 12 affects excitatory and inhibitory receptive fields of layer IV barrel neurons. *J Neurophysiol* **94**: 3987–3995.
- Sigal YM, Bae H, Bogart LJ, Hensch TK, Zhuang X. 2019. Structural maturation of cortical perineuronal nets and their perforating synapses revealed by superresolution imaging. *PNAS* **116**: 7071–7076.
- Sirianni N, Naidu S, Pereira J, Pillotto RF, Hoffman EP. 1998. Rett syndrome: confirmation of X-linked dominant inheritance, and localization of the gene to Xq28. *Am J Hum Genet* **63**: 1552–1558.

- Sohal VS, Zhang F, Yizhar O, Deisseroth K. 2009. Parvalbumin neurons and gamma rhythms enhance cortical circuit performance. *Nature* **459**: 698–702.
- Sorg BA, Berretta S, Blacktop JM, Fawcett JW, Kitagawa H, Kwok JCF, Miquel M. 2016. Casting a Wide Net: Role of Perineuronal Nets in Neural Plasticity. *J Neurosci* **36**: 11459–11468.
- Southwell DG, Froemke RC, Alvarez-Buylla A, Stryker MP, Gandhi SP. 2010. Cortical plasticity induced by inhibitory neuron transplantation. *Science* **327**: 1145–1148.
- Steinhauer SR, Siegle GJ, Condray R, Pless M. 2004. Sympathetic and parasympathetic innervation of pupillary dilation during sustained processing. *Int J Psychophysiol* **52**: 77–86.
- Sternson SM, Roth BL. 2014. Chemogenetic tools to interrogate brain functions. *Annu Rev Neurosci* **37**: 387–407.
- Stiebler I, Neulist R, Fichtel I, Ehret G. 1997. The auditory cortex of the house mouse: left-right differences, tonotopic organization and quantitative analysis of frequency representation. *J Comp Physiol A* **181**: 559–571.
- Stolzenberg DS, Champagne FA. 2016. Hormonal and non-hormonal bases of maternal behavior: The role of experience and epigenetic mechanisms. *Horm Behav* **77**: 204–210.
- Szegedi V, Paizs M, Baka J, Barzó P, Molnár G, Tamas G, Lamsa K. 2020. Robust perisomatic GABAergic self-innervation inhibits basket cells in the human and mouse supragranular neocortex. *Elife* **9**: e51691.
- Takesian AE, Hensch TK. 2013. Balancing plasticity/stability across brain development. *Prog Brain Res* **207**: 3–34.
- Tamamaki N, Yanagawa Y, Tomioka R, Miyazaki J-I, Obata K, Kaneko T. 2003. Green fluorescent protein expression and colocalization with calretinin, parvalbumin, and somatostatin in the GAD67-GFP knock-in mouse. *J Comp Neurol* **467**: 60–79.
- Taneja P, Ogier M, Brooks-Harris G, Schmid DA, Katz DM, Nelson SB. 2009. Pathophysiology of locus ceruleus neurons in a mouse model of Rett syndrome. *J Neurosci* **29**: 12187–12195.
- Tasaka G, Guenther CJ, Shalev A, Gilday O, Luo L, Mizrahi A. 2018. Genetic tagging of active neurons in auditory cortex reveals maternal plasticity of coding ultrasonic vocalizations. *Nat Commun* **9**: 1–14.
- Tewari BP, Sontheimer H. 2019. Protocol to quantitatively assess the structural integrity of Perineuronal Nets ex vivo. *Bio Protoc* **9**: e3234.
- Tremblay R, Lee S, Rudy B. 2016. GABAergic interneurons in the neocortex: From cellular properties to circuits. *Neuron* **91**: 260–292.

- Tsunada J, Liu ASK, Gold JJ, Cohen YE. 2016. Causal contribution of primate auditory cortex to auditory perceptual decision-making. *Nat Neurosci* **19**: 135–142.
- Tursky B, Shapiro D, Crider A, Kahneman D. 1969. Pupillary, heart rate, and skin resistance changes during a mental task. *J Exp Psychol* **79**: 164–167.
- Vinck M, Batista-Brito R, Knoblich U, Cardin JA. 2015. Arousal and locomotion make distinct contributions to cortical activity patterns and visual encoding. *Neuron* **86**: 740–754.
- Vogels TP, Sprekeler H, Zenke F, Clopath C, Gerstner W. 2011. Inhibitory plasticity balances excitation and inhibition in sensory pathways and memory networks. *Science* **334**: 1569–1573.
- Voss P. 2013. Sensitive and critical periods in visual sensory deprivation. *Frontiers in Psychology* **4**. <https://www.frontiersin.org/articles/10.3389/fpsyg.2013.00664> (Accessed February 6, 2023).
- Wang J, Xiao Y, Liu C, Huang Y, Petersen RB, Zheng L, Huang K. 2021. Emerging physiological and pathological roles of MeCP2 in non-neurological systems. *Arch Biochem Biophys* **700**: 108768.
- Werner-Reiss U, Kelly KA, Trause AS, Underhill AM, Groh JM. 2003. Eye position affects activity in primary auditory cortex of primates. *Curr Biol* **13**: 554–562.
- Wiesel TN, Hubel DH. 1963. SINGLE-CELL RESPONSES IN STRIATE CORTEX OF KITTENS DEPRIVED OF VISION IN ONE EYE. *J Neurophysiol* **26**: 1003–1017.
- Wingert JC, Sorg BA. 2021. Impact of Perineuronal Nets on Electrophysiology of Parvalbumin Interneurons, Principal Neurons, and Brain Oscillations: A Review. *Frontiers in Synaptic Neuroscience* **13**. <https://www.frontiersin.org/articles/10.3389/fnsyn.2021.673210> (Accessed March 12, 2023).
- Winn MB, Edwards JR, Litovsky RY. 2015. The Impact of Auditory Spectral Resolution on Listening Effort Revealed by Pupil Dilation. *Ear Hear* **36**: e153-165.
- Xie Y, Huang L, Corona A, Pagliaro AH, Shea SD. 2023. A dopaminergic reward prediction error signal shapes maternal behavior in mice. *Neuron* **111**: 557-570.e7.
- Xue M, Atallah BV, Scanziani M. 2014. Equalizing excitation-inhibition ratios across visual cortical neurons. *Nature* **511**: 596–600.
- Yamada J, Ohgomori T, Jinno S. 2015. Perineuronal nets affect parvalbumin expression in GABAergic neurons of the mouse hippocampus. *Eur J Neurosci* **41**: 368–378.
- Yasui DH, Peddada S, Bieda MC, Vallero RO, Hogart A, Nagarajan RP, Thatcher KN, Farnham PJ, Lasalle JM. 2007. Integrated epigenomic analyses of neuronal MeCP2 reveal a role for long-range interaction with active genes. *Proc Natl Acad Sci U S A* **104**: 19416–19421.

- Yavorska I, Wehr M. 2021. Effects of Locomotion in Auditory Cortex Are Not Mediated by the VIP Network. *Front Neural Circuits* **15**: 618881.
- Yizhar O, Fenno LE, Prigge M, Schneider F, Davidson TJ, O’Shea DJ, Sohal VS, Goshen I, Finkelstein J, Paz JT, et al. 2011. Neocortical excitation/inhibition balance in information processing and social dysfunction. *Nature* **477**: 171–178.
- Zatorre RJ, Chen JL, Penhune VB. 2007. When the brain plays music: auditory-motor interactions in music perception and production. *Nat Rev Neurosci* **8**: 547–558.
- Zekveld AA, Koelewijn T, Kramer SE. 2018. The Pupil Dilation Response to Auditory Stimuli: Current State of Knowledge. *Trends Hear* **22**: 2331216518777174.
- Zekveld AA, Kramer SE, Festen JM. 2010. Pupil response as an indication of effortful listening: the influence of sentence intelligibility. *Ear Hear* **31**: 480–490.
- Zhan J, Komal R, Keenan WT, Hattar S, Fernandez DC. 2019. Non-invasive Strategies for Chronic Manipulation of DREADD-controlled Neuronal Activity. *J Vis Exp* 10.3791/59439.
- Zhao S, Bury G, Milne A, Chait M. 2019. Pupillometry as an Objective Measure of Sustained Attention in Young and Older Listeners. *Trends Hear* **23**: 2331216519887815.
- Znamenskiy P, Zador AM. 2013. Corticostriatal neurons in auditory cortex drive decisions during auditory discrimination. *Nature* **497**: 482–485.
- Zoghbi HY. 2003. Postnatal neurodevelopmental disorders: meeting at the synapse? *Science* **302**: 826–830.